



Proyecto Final de Carrera

Study of Multipactor Effect in Communications Satellites considering RF Signals Digitally Modulated.

Alumno: M^a Pilar Belloch Rodríguez

Directores:

Benito Gimeno Martínez. Departamento Física Aplicada y Electromagnetismo- ICMUV UVEG
Jose Luis Hueso Pagoaga. Departamanto de Matemática Aplicada- IMM UPV

October 2012.

El proyecto final de carrera de la alumna M^a Pilar Belloch, estudiante de la Escuela Técnica Superior de Ingenieros de Telecomunicación de la Universitat Politècnica de València ha sido dirigido por dos profesores de diferentes escuelas. En primer lugar por Benito Gimeno Martínez, perteneciente al Dpto. de Física Aplicada y Electromagnetismo – ICMUV de la Universitat de València (UVEG). En segundo lugar, José Luis Hueso Pagoaga, perteneciente al Dpto. de Matemática Aplicada – IMM de la Universitat Politècnica de València (UPV).



VNIVERSITAT
DE VALÈNCIA



UNIVERSIDAD
POLITECNICA
DE VALENCIA

A mis co-directores, a Vicente E. Boria, David Raboso, y en especial a Òscar Monerris agradecerles toda su ayuda durante estos meses. Todo trabajo tiene su recompensa.

A mi familia y amigos, gracias.

INDEX

1	INTRODUCTION	4
2	OBJECTIVES	5
3	MULTIPLIER EFFECT IN SINGLE CARRIER	6
3.1	Multipactor Theory	6
3.1.1	Multipactor Description.....	6
3.1.2	Multipactor Analysis	6
3.1.3	SEY theory.....	9
	Secondary electrons model.....	9
3.2	Multipactor Software	12
3.2.1	Theoretical Model.....	12
	Probabilistic Description	14
3.2.2	Software Development.....	15
	Runge-Kutta.....	15
	Ode45	16
	Velocity-Verlet.....	16
	Example	17
	Parameters Influence.....	19
	Summary	22
4	MULTIPLIER EFFECT IN MODULATED SIGNALS	24
4.1	Modulated Signals Theory	25
4.1.1	Introduction	25
4.1.2	BPSK	25
	Phase Modulation Equals Amplitude Modulation.....	26
4.1.3	QPSK.....	27
	Modulating a Quadrature Carrier.....	28
4.1.4	Polar Display and IQ Formats.....	28
4.1.5	Constellation Diagram	30
4.1.6	Transition Diagram.....	31
4.1.7	Signal Envelope	32
4.2	Digital Communication System Metrics	33
4.2.1	EVM.....	33
4.2.2	BER.....	33
4.2.3	Bandwidth Efficiency	34
4.2.4	PAPR.....	34
4.2.5	CCDF	35
4.3	Multipactor Software for modulated signals	37
4.3.1	Objectives.....	37
4.3.2	Software Development.....	37
4.3.3	Results	39
	Example 1	39
	Example 2	42
	Example 3	44
	Symbol Period in MP Breakdown.....	46
	Pulse Shaping, PAPR and CCDF in the software. Theory.....	53
	Multipactor Software. Modulation Filtering.....	58

	Example 4	60
	Comparison modulated and non-modulated signal with any filter.	60
	Example 5	62
	Comparison BPSK modulated signal with square and SRRC filter.....	62
	Example 6.....	65
	BPSK modulated signal with different roll-off in SRRC filter.....	65
	Conclusion.....	66
 5	PRESENT RESULTS.....	67
	Convergence Study	67
5.1	Non-Modulated Signal.....	69
5.2	BPSK-Modulated Signal with RECTPULSE FILTER.....	70
5.3	BPSK-Modulated Signal with SRRC FILTER	73
 6	FUTURE WORK.....	78
6.1	Experimental setup	82
	Hardware	82
	Software.....	82
	Planning Tests.....	82
 7	CONCLUSIONS	83
 8	REFERENCES.....	84

|1 INTRODUCTION

Multipactor is a non-linear effect caused in vacuum systems due to secondary electron emission from solid surfaces bombarded by energetic free electrons being accelerated by the RF field. It presents a severe problem in many modern microwave systems such as, e.g., high power microwaves generators, RF accelerators, and spaceborn communication where the RF field intensity is high enough to provide electrons with oscillations energies above several tens of eV.

New generation telecommunication satellites are designed to cater for a constantly increasing number of users, requiring higher and higher bit rates. The high bit rates is nowadays combined with the use of more and more efficient modulation schemes and most links used in satellite telecommunication are employing systems based on modulation schemes.

The increasing number of users implies increasing power levels in the RF equipment downstream from the power amplifiers, so an avalanche of electrons produced by the RF electric field could possibly initiate a Multipactor discharge.

In order to predict and control under which situations multipactor breakdown can occur, it is important to consider that telecommunication satellites are usually based on multicarrier operation and modulated carriers in order to use efficiently the limited frequency band available. A typical multicarrier signal is composed of several modulated carriers with small frequency separation and their mix produces a modulated RF signal with a time varying periodic envelope. The study of multipactor in multicarrier operation is much more complex than in the single-carrier case. In view of this, it becomes an important issue to analyse multipactor initiation in modulated signals, where the main characteristic of the modulation is that the signal envelope stays or not constant depending on the modulation type. As well, the influence of modulations like PSK where the envelope is constant but the phase switches with regular intervals are very considered in this study. [1]-[2]-[3]

Multipactor discharges have a number of undesirable consequences that tend to degrade signal transmission quality and system performance, e.g., RF noise, change of the device impedance, and heating of the device walls, which may even permanently damage hardware components in the device. Therefore, it is very important to study the behaviour of a RF single carrier wave during the initiation of multipactor breakdown prior launching the satellite. Finally and in order to predict under which conditions multipactor will appear a Multipactor simulator software has been developed to simulate the electron movement within a parallel plate scenario in terms of the applied RF signal. Also, it will be feasible to study the influence of different modulation schemes in the theoretical threshold permitting a better understanding of the modulations.

|2 OBJECTIVES

Traditionally, multipactor has been studied for single carrier signals. The single carrier prediction techniques are usually based on the multipactor theory.

The first place on this proposal shall focus in the increase of the electron density that occurs due to secondary electron emission, when electrons, accelerated by the RF electric field, hit the wall of the microwave device. Multipactor simulator considers a particular scenario inside a parallel plate waveguide where an electric field exists creating an electric potential difference and producing the electron movement. Detailed numerical simulations have been carried out, taking into account the influence of several parameters.

Nevertheless, using this general purpose Multipactor simulator in which the RF field can be defined as needed (not necessarily as a simple non-modulated sinusoidal wave), a set of different pass-band modulated signals will be analysed by the algorithm. A modulation of the signal amplitude may significantly modify the conditions for the development of the multipactor breakdown and causes uncertainty about the multipactor threshold in modulated operations.

The main objective of the analysis is to understand how the growth rate of the electron avalanche depends on the type of modulation applied and the understanding of the effect of modulated signals in the RF breakdown values to define a theoretical prediction for the multipactor breakdown. In view of this, it becomes an important issue to analyse multipactor initiation using signals with these characteristics.

All these aspects have been considered with a new perspective using Matlab. Matlab is a numerical computing environment developed by MathWorks and allows to prototype custom modulation schemes using together with other instruments. With Matlab is possible to illustrate and simulate a prototype communications system and is one of the best tools to study the different signals behaviours. Multipactor software is a new simulation tool that has been developed during the present project using Matlab. This software tool simulates the multipactor effect considering a basic scenario composed by two parallel plates and a harmonic excitation between them will be used for this objective. The software will be able to provide important conclusions before any testing.

Thus, the purpose of the work consists in the study of the variation in the multipactor threshold for a set of digitally modulated signals. Additionally, and in order to complete all the investigation to validate this new platform simulation several tests will be provided in a near future to verify the behaviour of modulated signals in real testing. The investigations will take place at the Joint High Power RF laboratory established between ESA and Val Space Consortium in Valencia, Spain.

|3 MULTIPACTOR EFFECT IN SINGLE CARRIER

3.1 Multipactor Theory

3.1.1 *Multipactor Description*

Multipactor, also known as multipactoring or multipaction, is an electron avalanche-like discharge occurring in microwave devices operating at high power levels and in vacuum or near vacuum condition. When initially discovered, it was studied as a beneficial effect for signal amplification in cold-cathode tube for TV applications by Farnsworth (1934), who originally coined the name “multipactor.” Today, multipactor is considered as a dangerous collateral effect in high power vacuum applications, which must be avoided.

The phenomenon occurs when initial free electrons (primary) are accelerated by the RF fields, and impact against the device walls with enough energy to extract more electrons (secondary) from the surface. If the resulting electronic bunch enters in resonance with the field, this process repeats itself until the electron density reaches a certain level to produce noticeable disturbance of the signal, such as distortion, additive noise, or reflection, and ultimately produces a destructive discharge that can even damage the device. In operation, primary electrons come from different sources such as field emission or electron cascades produced by cosmic rays.

Under some circumstances, that are not considered in this study, multipactor can occur on a single surface. Multipactor can be greatly modified – either enhanced or suppressed- by electric or magnetic fields, but it does not basically require the presence of either. It can also occur in other conditions when there is the combination of high vacuum, RF fields, and half-cycle transit times between secondary-emitting surfaces. Multipactor may appear in many types of components, such as passive or active high-power devices in guided or microstrip technologies and antennas. Thus, it affects different industry sectors such as satellite communications or particle accelerators.

The biggest effort of the multipactor research lines is devoted to the study and characterization of the phenomenon in order to predict under which conditions it will appear, and designing multipactor-free components.

3.1.2 *Multipactor Analysis*

The simplest case of multipactor is the discharge between two plane-parallel surfaces, separated by a distance d , driven by a peak RF voltage V_{RF} for a given frequency ω . It is assumed that the surfaces have identical secondary emission characteristics, and that secondary emission velocity v_o can be treated as a single-valued constant over the range of impact voltages for which the secondary emission ratio δ is greater than unity. The

equations of motion for the plane-parallel multipactor have been given many times but they are repeated here simply for convenience of having a consistent set on hand as a basis for the present study.

In order to determinate the movement of an electron in a uniform and harmonic variation field, it is considered a one-dimensional model waveguide (plane-parallel plates) with vacuum conditions between walls. The electric field is represented in Fig. 1.

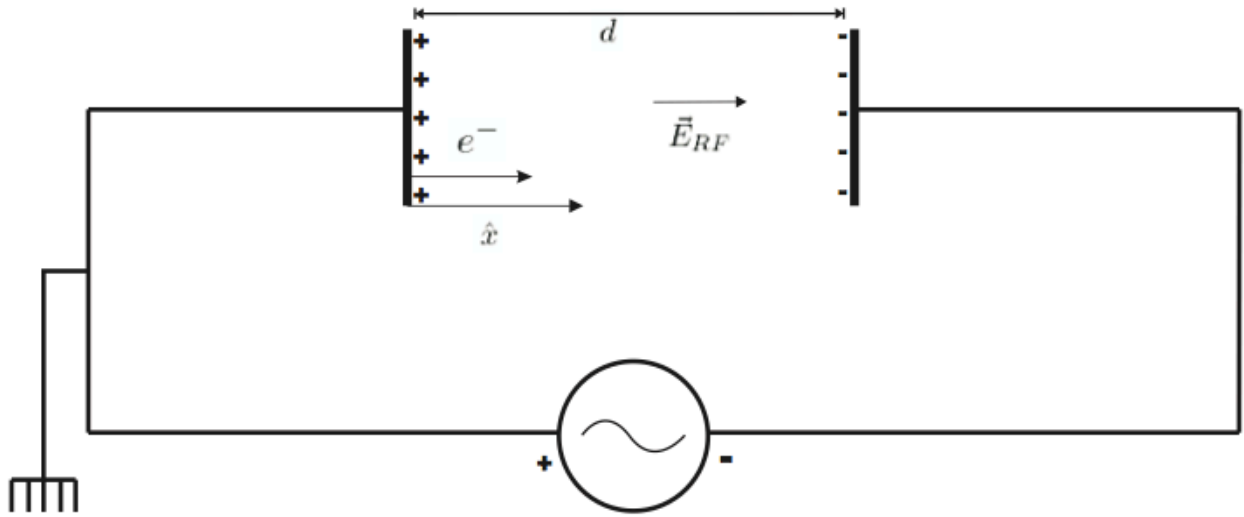


Fig.1 Plate capacitor with plane-parallel and electric field \vec{E}_{RF}

$$\vec{E}_{RF} = E_{RF} \hat{x} = \frac{V_{RF}}{d} \hat{x} \quad (1)$$

$$\vec{E}_{RF} = \frac{V_{RF}}{d} = \frac{V}{d} \cdot \cos(\omega \cdot t + \theta) \quad (2)$$

Between these two plates, it exists an electric field (Eq. 1 and 2) with an electric potential difference V_{RF} (Eq. 3) which produces the electron movement.

$$V_{RF} = V_{RF}(t) = V \cos(\omega t + \theta) \quad (3)$$

Electrons motion is governed by Lorentz force equation. Applying the Newton equations (Eq. 4) to this environment, it is possible to solve the differential equation (Eq. 5) and find out the position and the speed of the particle at any time.

$$\vec{F} = m \cdot \vec{a} = -e \cdot \vec{E}_{RF} \quad (4)$$

$$m \cdot \vec{a} = -e \cdot \frac{V}{d} \cdot \cos(\omega \cdot t + \theta) \quad (5)$$

The expression above expressed (Eq.5) can be numerically solved using numerical methods like Runge-Kutta or Velocity-Verlet. The key idea is to determine the impact time for the electron subject to the field given by equation 2. The initial conditions to solve equation (5) are:

$$\begin{aligned} \alpha &= \omega \cdot t_\alpha \\ \dot{x}(t_\alpha) &= v_0 \\ x(t_\alpha) &= x_0 \end{aligned} \quad (6)$$

where t_α is the instant in which the electron begins its interaction with the electric field and starts being accelerated by it. α represents the phase of the electric field t_α .

Solving the differential equation using the above initial conditions (Eq. 6), it is possible to obtain the exact equation for the speed (Eq. 7) and the trajectory of an electron (Eq. 8).

$$v = v_0 + \frac{eV}{m\omega d} \sin(\alpha) + \frac{-eV}{m\omega d} \sin(\omega t) \quad (7)$$

$$x = x_0 + \frac{v_0}{\omega} (\omega t - \alpha) + \frac{eV}{m\omega^2 d} (\cos(\omega t) - \cos(\alpha) + (\omega t - \alpha) \sin(\alpha)) \quad (8)$$

Legend:

V (Field Amplitude, Volts)

d (distance between plates, mm)

ω (frequency, rad)

e (electron charge, 1.602176×10^{-19} coulombs)

m (electron mass, 9.109×10^{-31} kilograms)

θ (electric field phase)

The electric field amplitude, frequency and distance between plates play also an important role in the development of the multipactor discharge. One of the main objectives of our Multipactor software is to determine and draw the electron trajectory at every time instant checking if the electron has impacted with the wall at every time step.

3.1.3 SEY theory

Secondary emission is a phenomenon where additional electrons, called secondary electrons, are emitted from the surface of a material when an incident particle (often, charged particle such as electron or ion) impacts the material with sufficient energy. In this case, the number of secondary electrons emitted per incident particle is called **Secondary Emission Yield (SEY)**. The SEY (also called secondary electron emission coefficient, SEEC) is defined as follows

$$SEY(\delta) = \frac{\text{probability of emission of } \delta \text{ electrons}}{1 \text{ incident free electron}} \quad (9)$$

The search for reliable low-secondary-electron-emission coatings is considered as one of the main research lines to reduce the multipactor effect in high-power RF devices in spacecraft and in other important technological fields as high-energy particle accelerators.

Secondary-electron-emission processes under electron bombardment play an essential role in vacuum electronic devices. The materials used in the devices may need to be judiciously selected in some cases to enhance the secondary-electron emission and in other cases to suppress the emission. In microwave and millimetre wave power tubes, low secondary-electron-emission materials are desirable for depressed collectors in order to ensure a high efficiency in the energy conversion. Low-emission materials are also sought for coating the grids and the tube walls to prevent RF vacuum breakdown, which is the area of our interest.

Secondary electrons model

The electric field can eventually drive an electron to the waveguide walls and when this happens, this electron can be absorbed, reflected or can extract secondary electrons from the surface. It is well known that the multipactor effect characteristics strongly depend on the surface properties. This is basically material dependent and is quantitatively considered by means of the secondary electron emission coefficient (SEEC). The typical curve aspect of this coefficient as a function of the impacting electron kinetic energy is shown in Fig. 2 for the low energy range. One of the most commonly used models for the SEEC was formulated by Vaughan [4]. The Vaughan's formula is:

$$\begin{aligned}\delta(E, \theta) &= \delta_{max}(\theta) \cdot (\gamma e^{1-\gamma})^k \quad \text{for } \gamma \leq 3.6 \\ \delta(E, \theta) &= \delta_{max} \cdot 1.125/\gamma^{0.35} \quad \text{for } \gamma > 3.6\end{aligned}\quad (10)$$

$$\gamma = \frac{E - E_0}{E_{max}(\theta) - E_0}$$

$$k = 0.56 \quad \text{for } \gamma < 1,$$

$$k = 0.25 \quad \text{for } 1 < \gamma \leq 3.6$$

$$\delta_{max}(\theta) = \delta_{max} \cdot (1 + k_E \theta^2/2\pi)$$

$$E_{max}(\theta) = E_{max} \cdot (1 + k_\theta \theta^2/2\pi)$$

$\delta(E, \theta)$ being the SEEC value for an impacting electron energy E and incident angle θ respect to the surface normal, $E_0 = 12.5 \text{ eV}$, k_E and k_θ parameters dependent on the roughness of the surface (normally taken equal to 1), E_{max} the impact energy at which the SEEC is maximum and δ_{max} the maximum SEEC at this energy.

As seen in equation 10, the Vaughan curve mainly depends on two parameters: δ_{max} and E_{max} . This leads to two basic problems:

- 1) At very low energies (below E_0), $\delta(E, \theta)$ is not defined.
- 2) The first crossover energy at which the SEEC equals to 1 (E_1) is not fitted in the curve.

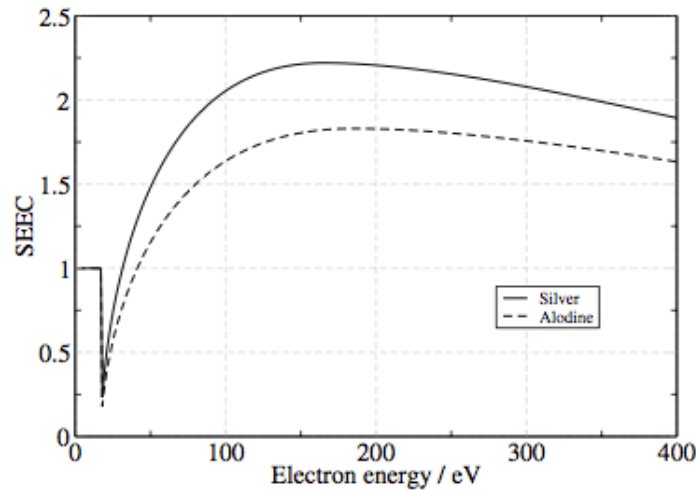


Fig. 2 Modified secondary emission curves for silver and alodine.

In order to overcome such problems, a modified version of the Vaughan's formula has been employed [5]. It is based on adding one more fitting parameter in order to force the SEEC curve to have the first crossover at E_1 . To do this, the arbitrarily defined parameter E_0 has been varied until the SEEC curve indeed passes by E_1 . Additionally, since at very low energies almost all the electrons are reflected, it has been assumed that the SEEC below E_0 is equal to 1. Thus, for instance, using the ECSS standard [6] values for the SEEC parameters of silver plated ($E_{max} = 165$ eV, $\delta_{max} = 2.22$, $E_1 = 30$ eV) and alodine ($E_{max} = 180$ eV, $\delta_{max} = 1.83$, $E_1 = 41$ eV) surfaces , curves like those shown in Fig. 2 are obtained.

At each electron impact the average number of electrons generated is given by the SEEC value for the energy and angle of the colliding electron. A well-known approach to model multipactor is to use effective electrons in such a way that the real number of electrons to be tracked remains constant throughout the calculation but each electron represents a larger (or smaller) number of electrons depending on the accumulated SEEC values at each impact. Despite the fact that this approach is extremely useful in many cases and provides reliable results in many geometries, it can not be universally employed.

Its main drawback comes from the fact that if the length of the device geometry where multipactor is investigated is about the order of the gap height, many electrons can escape from the gap. This makes the effective electron approach unstable since, as time goes by, less and less electrons remain in the region of interest and finally, there are a few electrons in order to have enough statistics. One can argue that just using more electrons in the simulation can solve this. However, this does not improve the whole picture since the multipactor breakdown criterion is normally based on the increase of the electron population respect to its initial value and hence, to reach the multipactor breakdown condition would again mean that few electrons (compared to the number of primaries) are representing the whole electron sample.

In the developed Multipactor software a secondary emission function will be created allowing to predict the effect of secondary emission and conductivity of surface coatings on multipactor and RF-performance. It is taking into account that the main parameters of SEY influencing multipactor are the maximum value δ_{max} of SEY coefficient and the first crossover primary energy E_1 ($\delta = 1$). These values are considered at normal incidence. Figure 3 represents the limits E_1 and E_2 described above including the multipactor region where the effect occurs.

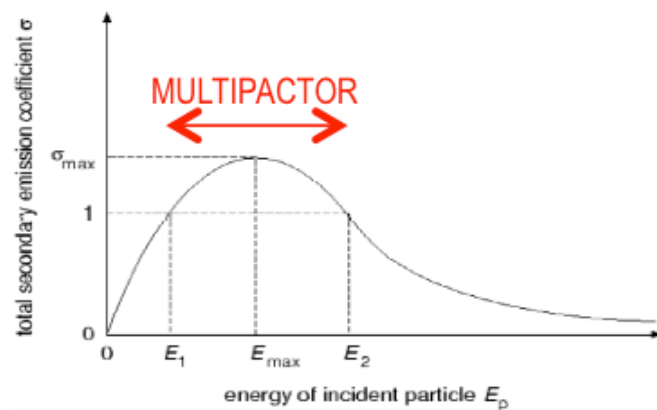


Fig 3. Multipactor Region

3.2 Multipactor Software

The multipactor phenomenon takes place because free electrons within the device are leaded by the RF field to a metallic wall, where they release secondary electrons. Under resonance conditions these generated electrons are re-emitted in reverse electric field sense, reaching the opposite metallic wall in, approximately, a multiple of the half-cycle time, colliding again into the wall, and releasing more electrons. If this process is continuously repeated an electron avalanche occurs. When the electron population becomes high enough, the return losses of the particular component increases which typically distorts the electric response of the component. Moreover, if the multipacting conditions are maintained, the outgassing from the metallic walls can lead to the increase of the inner pressure, which could destroy the device.

As a consequence, it is extremely important to take into account the multipactor effect in the design process of RF components for satellite systems. The specifications imposed by the space agencies are usually very restrictive and any component must be multipactor tested. Thus, it is very welcome to have a software tool for predicting the multipactor onset with enough accuracy.

The main goal of this section is to define a theoretical prediction for the multipactor breakdown. Multipactor simulator provides a first approximation to the testing of many materials in different situations, allowing the elimination of the least promising ones and reducing the cost of the real experiments. In this section it is explained how this software tool has been carried out, how it should be used and finally is presented an analysis about the obtained results.

3.2.1 *Theoretical Model*

In this system, it is considered infinite parallel plates in the xy plane, with the RF electric field unidirectional in the z coordinate. Border effects are not considered. The approximation corresponds to a narrow gap (relative to the other dimensions). Electrons are modelled individually, assuming that their trajectories are only modified by the electric field and are not affected by other electrons in the system. That is, effects due to space charge are not taken into account.

The collision of the electron with a plate can rip zero or more electrons from the wall following a probabilistic model that is described in next section. The newly created electrons are again individually tracked. Given the parameters of a certain material, the SEY depends only on the primary energy (E_p) and its incidence angle. Following the energy conservation principle, the total output kinetic energy should be equal or less than the

input electron kinetic energy. For the initial conditions, a certain number of free electrons (created during the first period of the electric field) are assigned a normally distributed energy and start at plate “ $x = 0$ ”.

As mentioned above, a minimum set of four parameters seem to be necessary, plus at least one more for taking into account the dependence on incident angle (in its simpler factorizable expression). When an electron collides with one of the plates, it can be absorbed, backscattered, or a number of true *secondary electrons* may be generated. The three kind of electrons emitted provide their own contributions to the SEY curve, which is represented as a function of the impacting energy and the incidence electron angle. The addition of the three contributions results in the total SEY. Figure 4 shows a typical SEY curve for a given angle [7].

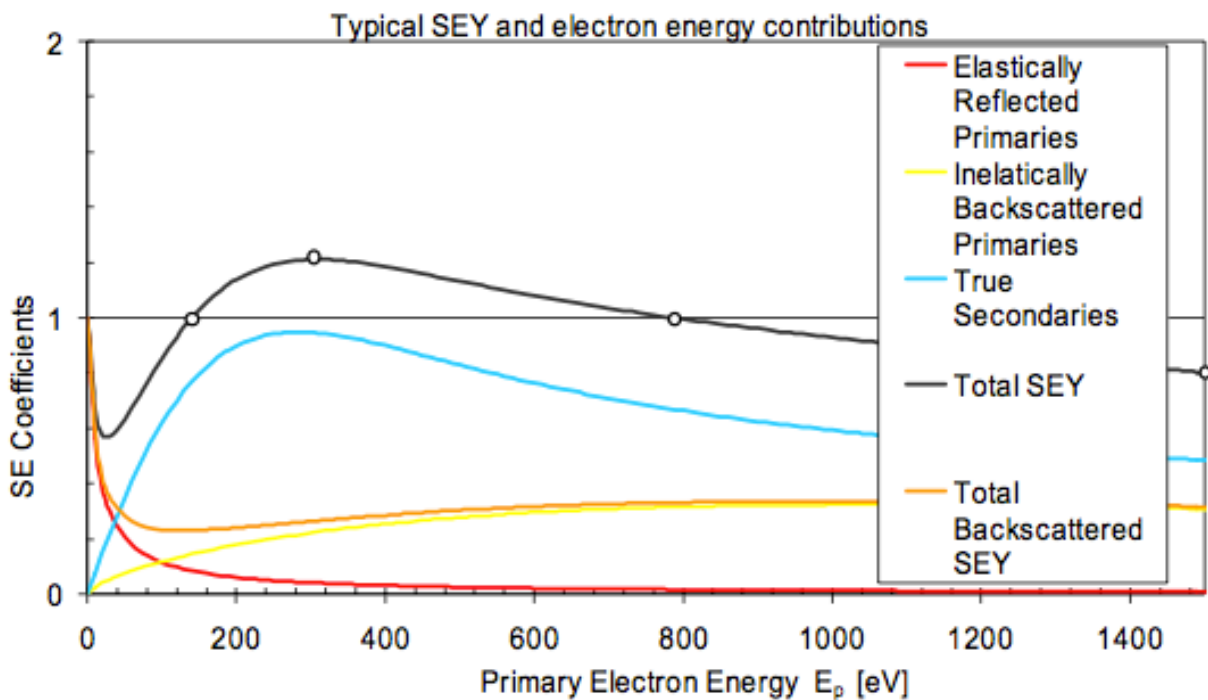


Fig. 4 Typical SEY curve with the Dependence of Different SEY Coefficients.

They could represent those of clean Cu after electron conditioning and for normal incidence. Zero limit of elastic electrons coefficient might be less than 1, difficult to measure. Definition of backscattered coefficient is usually arbitrary. Here is based on fitting energy distribution curves or spectra of secondaries. Some impacting primary electrons are backscattered with some energy loss after very few collisions.

Probabilistic Description

Now it is provided a microscopic, i.e., event-by-event, description of the secondary emission process, where an “event” is a single electron-surface collision. This process is quantum mechanical hence probabilistic in nature; thus an electron with kinetic energy E_0 striking a surface at an angle θ_0 will yield n secondary electrons with a probability $P_n(E_0, \theta_0)$, $n = 1, \dots, \infty$ as sketched in Fig. 5 [8] (it is adopted the convention that θ_0 is measured relative to the normal to the surface at the point of impact). The P_n 's obviously satisfy

$$\sum_{n=0}^{\infty} P_n = 1, \quad P_n \geq 0 \quad (11)$$

where P_0 is the probability that the incident electron is absorbed without emission. In terms of the P_n 's, the SEY defined is simply the average electron multiplicity in the collision.

$$\delta = \langle n \rangle = \sum_{n=1}^{\infty} n P_n \quad (12)$$

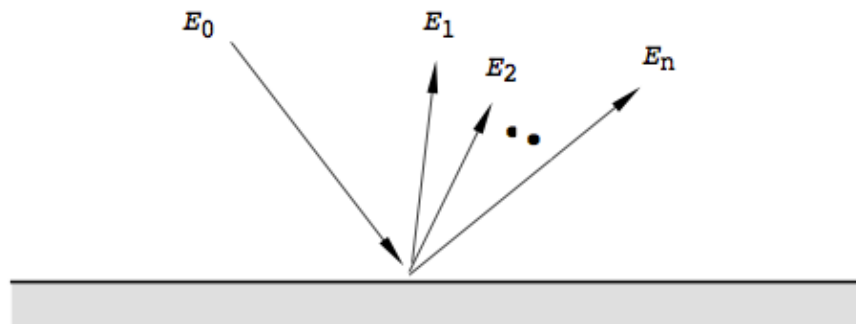


Fig. 5 A single electron with energy E_0 strikes a yielding n secondary electrons with the energies E_1, E_2, \dots, E_n

3.2.2 *Software Development*

A software tool that simulates the multipactor effect considering a basic scenario composed by two parallel plates and a harmonic excitation between them will be used for this objective. The software will be able to provide important conclusions before testing.

All these aspects have been considered with a new perspective using Matlab. Matlab is a numerical computing environment developed by MathWorks and allows to prototype custom modulation schemes using together with other instruments. With Matlab is possible to illustrate and simulate a prototype communications system and is one of the best tools to study the different signals behaviours.

To solve equations of motion for particles by taking a small step in time, approximate numerical methods are used to predict the new particle positions and velocities at the end of the step.

In this first section, it is just considered the existence of an electric field (a sinusoidal wave) between the plates. However, the equation of the electric field will be easily replaced by a modulated signal. Applying the Newton equations to this environment, it is possible to find out the position and the velocity of the particle at any given moment. As previously was explained, the main equations modelling this movement are:

$$\overrightarrow{E}_{RF} = \frac{V_{RF}}{d} = \frac{V}{d} \cdot \cos(\omega \cdot t + \theta) \quad (2)$$

$$\vec{F} = m \cdot \vec{a} = -e \cdot \overrightarrow{E}_{RF} \quad (4)$$

Differential equation (4) can be numerically solved using several algorithms like Runge-kutta, Ode45 or Velocity-Verlet. It is included a small description about the main performance of each one.

Runge-Kutta

The Runge-Kutta algorithm is an iterative method for the approximation of solutions of ordinary differential equations. It is known to be very accurate and well-behaved for a wide range of problems like initial value ones (Eq.13). The Runge-Kutta method is a fourth-order method (RK4) given by the following equations (Eq.14).

$$\dot{y} = f(t, y), \quad y(t_0) = y_0 \quad (13)$$

This means that the rate at which y changes is a function of y itself and of t (time).

$$y_{n+1} = y_n + \frac{1}{6} (k_1 + 2k_2 + 2k_3 + k_4) \quad (14)$$

$$t_{n+1} = t_n + h$$

where y_{n+1} is the RK4 approximation of $y(t_{n+1})$, and

$$k_1 = h f(t_n, y_n),$$

$$k_2 = h f\left(t_n + \frac{1}{2}h, y_n + \frac{1}{2}k_1\right),$$

$$k_3 = h f\left(t_n + \frac{1}{2}h, y_n + \frac{1}{2}k_2\right),$$

$$k_4 = h f(t_n + h, y_n + k_3)$$

Ode45

Matlab provides methods of several orders of accuracy to solve ODE's (Ordinary Differential Equations). All of them are used in the same way. This function solves initial value problems for ordinary differential equations. Ode45 is one of these functions that provides the most usual (medium order) to resolve an ED. This algorithm is the faster than RK4, but their solutions may be a bit different because the times values in which the function is evaluated are not exactly the same if the user does not control its maximum time step.

Velocity-Verlet

The Verlet integrator offers greater stability, as well as other properties that are important in physical systems such as time-reversibility and preservation of the simplistic form on phase space, without significant additional cost over other methods. Verlet integration was used to compute the trajectories of particles moving in a magnetic field.

A related, and more commonly used, algorithm is the Velocity Verlet algorithm, and the main characteristic is that the velocity and position are calculated at the same value of the time variable, and for this reason may be regarded as the most complete form of Verlet algorithm (Eq. 15). The global error of this method is of order two.

$$\vec{x}(t + \Delta t) = \vec{x}(t) + \vec{v}(t)\Delta t + \frac{1}{2} \vec{a}(t)\Delta t^2 \quad (15)$$

$$\vec{v}(t + \Delta t) = \vec{v}(t) + \frac{\vec{a}(t) + \vec{a}(t + \Delta t)}{2} \Delta t$$

It is not unusual for certain values of initial phase (in the electron) to get different results due to the sensitivity to initial conditions. It is possible that in critical cases, ode45 refines the solution or not depending on the number of points evaluated in a period of time (also controlled by the user). Thus, the approach chosen and the spacing in the vector of time (Δt) are an important factor to consider using numerical methods to solve the equation described.

It is considered that the events are the collisions of the electrons with the plates. The collision time can be efficiently calculated, because in the case of parallel plates geometry is also possible to calculate solutions of the electron trajectories analytically. Nevertheless, we are going to use numerical methods to calculate the necessary parameters.

As stated before, each electron is modelled individually and to perform a simulation, the next explained steps are followed in the software. The main idea is to control the impact of one electron in a wall, calculating the exact time (t), position (x) and velocity (v) in which the electron reaches the plate (interpolating between two time values just before and after the impact). Moreover knowing the velocity v , it is possible to calculate the energy value lost by the electron in the impact (E_p) with the next equation (16).

$$E_p = \frac{1}{2} m v^2 \quad (16)$$

Consequently, it is immediately known the δ_p using the SEY curve for the material used in the simulation. It should be noted that the SEY material curve has been programmed using Matlab too. The equations explained in “SEY Theory” section (Eq. 10) are implemented directly as the next example shows:

Example

Material between plates: A_{g3A}

$$E_1 = 30 \text{ eV}$$

$$E_2 = 5000 \text{ eV}$$

$$E_{max} = 165 \text{ eV}$$

$$\delta_{max} = 2.22$$

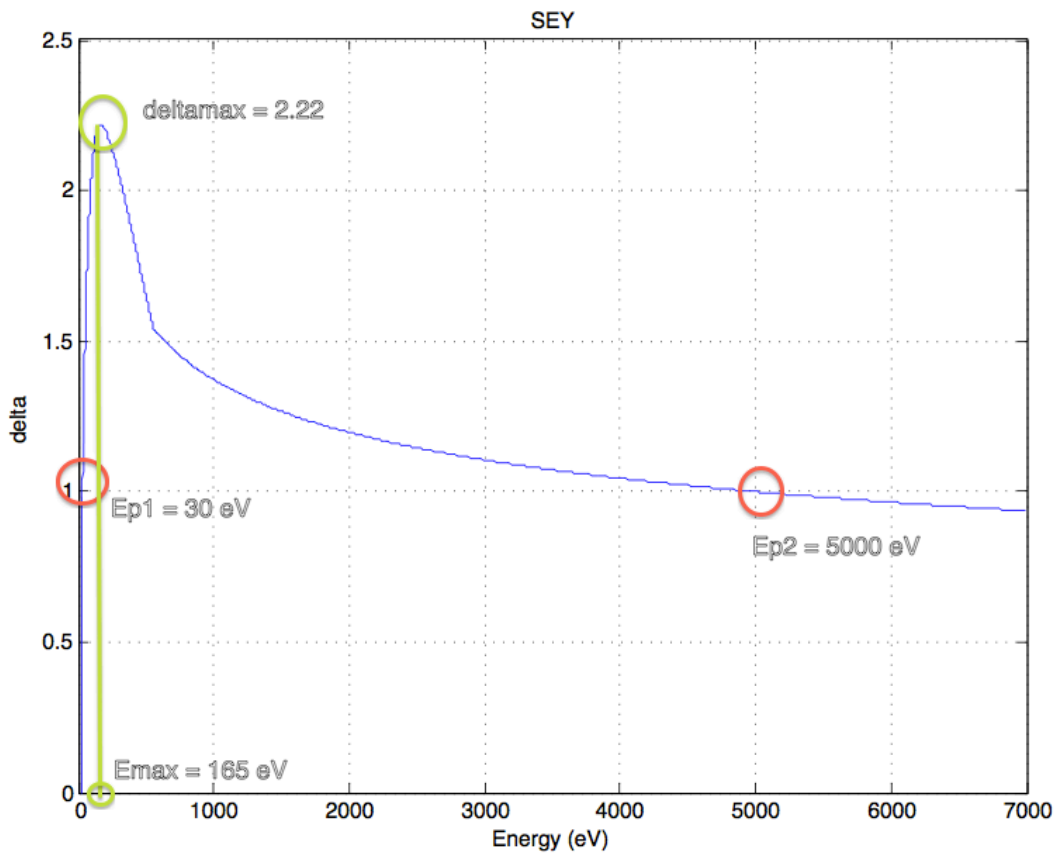


Fig. 6 SEY curve for $A_{g_3}A$ with Matlab

The most interesting region in Figure 6 is the left-down one, so if we take a zoom from this zone, it is clearly that the minimum energy value for this material is about 16 eV. The electron which impacts with an energy value below the minimum energy (E_{min}) in the SEY material curve is considered absorbed by the plate and this electron can not initiate any type of multipactor.

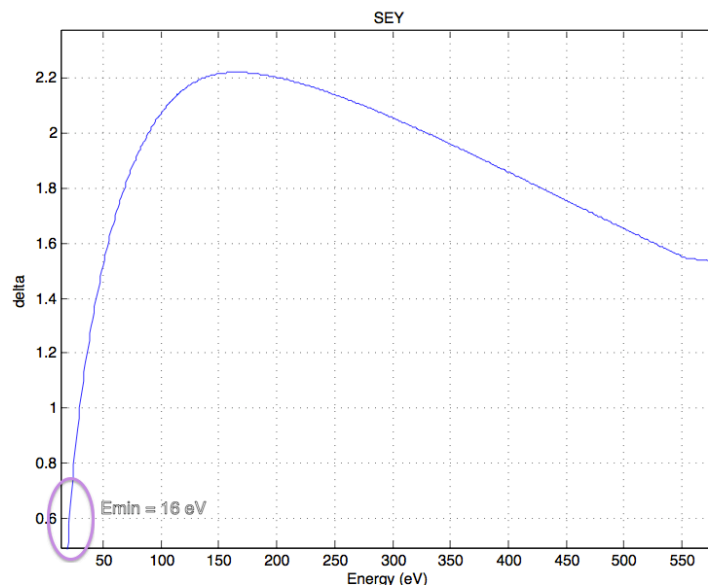


Fig. 6.1 Zoom Sey Curve for $A_{g_3}A$ with Matlab

Parameters Influence

These are the basic parameters that will be taken into account and the output data that will be provided.

Input data:

1. Electric Power/Amplitude of the field (*Volts*)
2. Frequency range (*GHz*)
3. Distance between plates (*mm*)
4. Electron initial velocity, v_0 (*eV*)
5. Electron initial phase, α ($^\circ$)
6. Material Properties for SEY ($E_1, E_2, E_{max}, \delta_{max}$)
7. Number of initial electrons introduced (initial electron seeding)

Output data:

1. Presence or absence of Multipactor
2. Total number of impacts (optional)
3. δ_m value in every impact (optional)

However, if the objective is to study the trajectory of one electron for a particular case, it is feasible to draw the trajectory followed by the electron between the plates. Parameters like electric field amplitude, initial phase of the electron, frequency and distance (gap) play an important role in the development of the multipactor discharge. For completeness, the following examples are proposed to check the main influence of the input parameters in the multipactor presence or absence.

Simulation 1: NO MULTIPACTOR DISCHARGE (Figure 7.1)

The objective is to detect the influence of applying different α (initial phase of the electron) and Voltage.

Electric Field Amplitude = 30 Volts

$$f \times d = 1 \text{ GHzmm}, d = 1 \text{ mm}, f = 1 \text{ GHz}$$

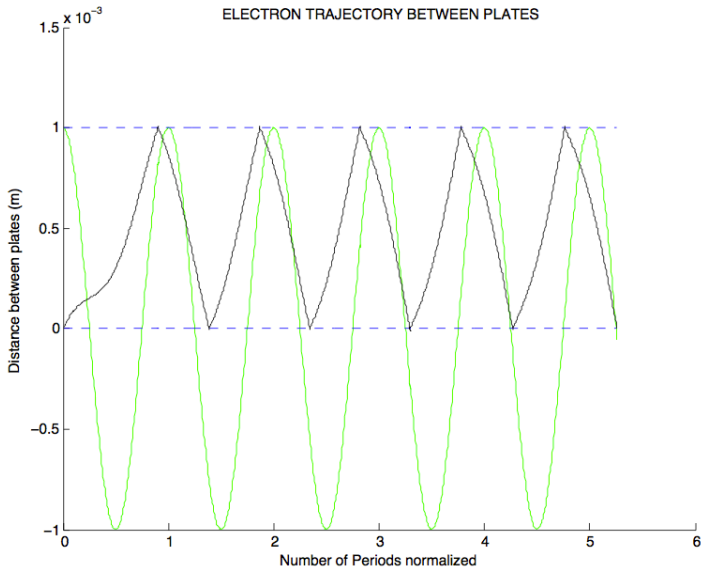
Simulation 2: MULTIPACTOR DISCHARGE (Figure 7.2)

The objective is to detect the influence of applying different α (initial phase of the electron) and Voltage.

Electric Field Amplitude = 100 Volts

$$f \times d = 1 \text{ GHzmm}, d = 1 \text{ mm}, f = 1 \text{ GHz}$$

$$\alpha = 0^\circ$$



$$\alpha = 300^\circ$$

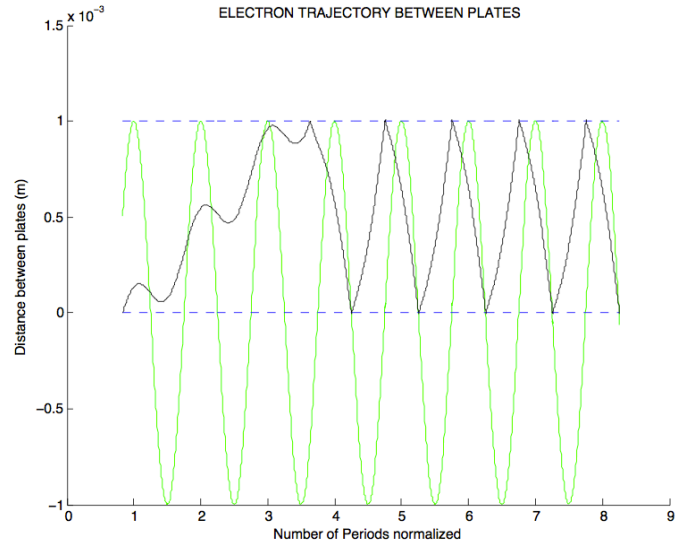
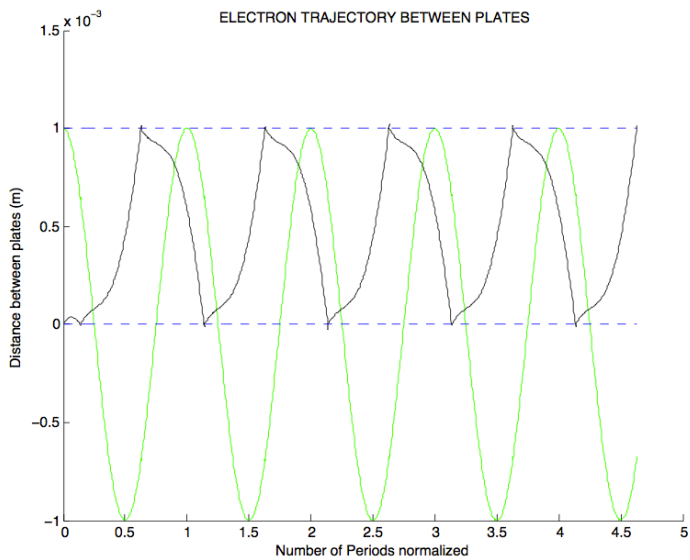


Fig. 7.1 Simulation for different α and Amplitude = 30 Volts

$$\alpha = 0^\circ$$



$$\alpha = 300^\circ$$

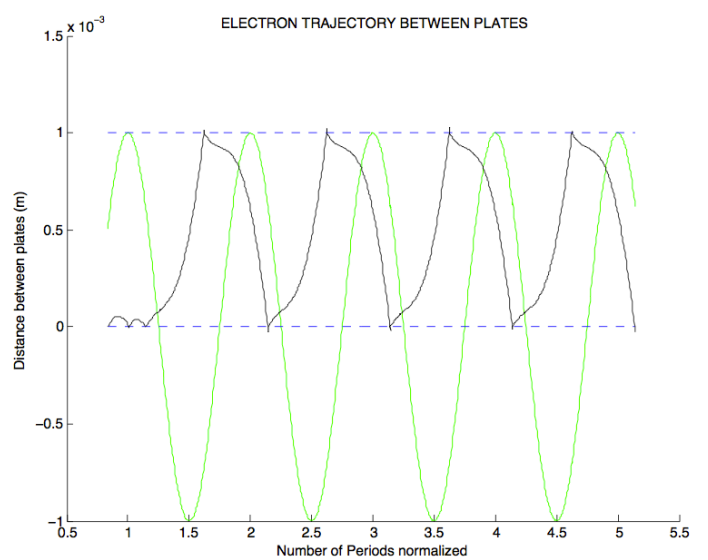


Fig. 7.2 Simulation for different α and Amplitude = 100 Volts

Simulations 1 and 2 (Fig. 7.1 and 7.2) show clearly the difference in the trajectory of the electron when the initial phase is different. If α is higher, the time the electron takes to interact with the electric field ($t\alpha = \alpha / \omega$) is also greater. The exact time in which the electron becomes influenced by the harmonic excitation is different in both simulations and this implies that the phase of the field is in a different point, so obviously, the electron can not have the same behaviour because the initial conditions are not equal.

On the other hand, we point out that the amplitude value (potential generated between plates) of the electric field is different in every simulation and therefore each simulation results are also different. In the first case multipactor does not occur because applying a potential of 30 Volts the electron does not impact the wall with enough power to cause the appearance of new electrons. However, if the electric field has an amplitude about 100 Volts as in simulation 2, this time the electron impacts with enough energy to generate new electrons producing a multipactor discharge.

Simulation 3: (Figure 8)

The objective is to detect the influence of applying different d (distance between plates)

Electric Field Amplitude = 100 Volts

$\alpha = 120^\circ$

$f \times d = 2 \text{ GHzmm}, d = 2\text{mm}, f = 1\text{GHz}$

$f \times d = 1\text{GHzmm}$

$f \times d = 2\text{GHzmm}$

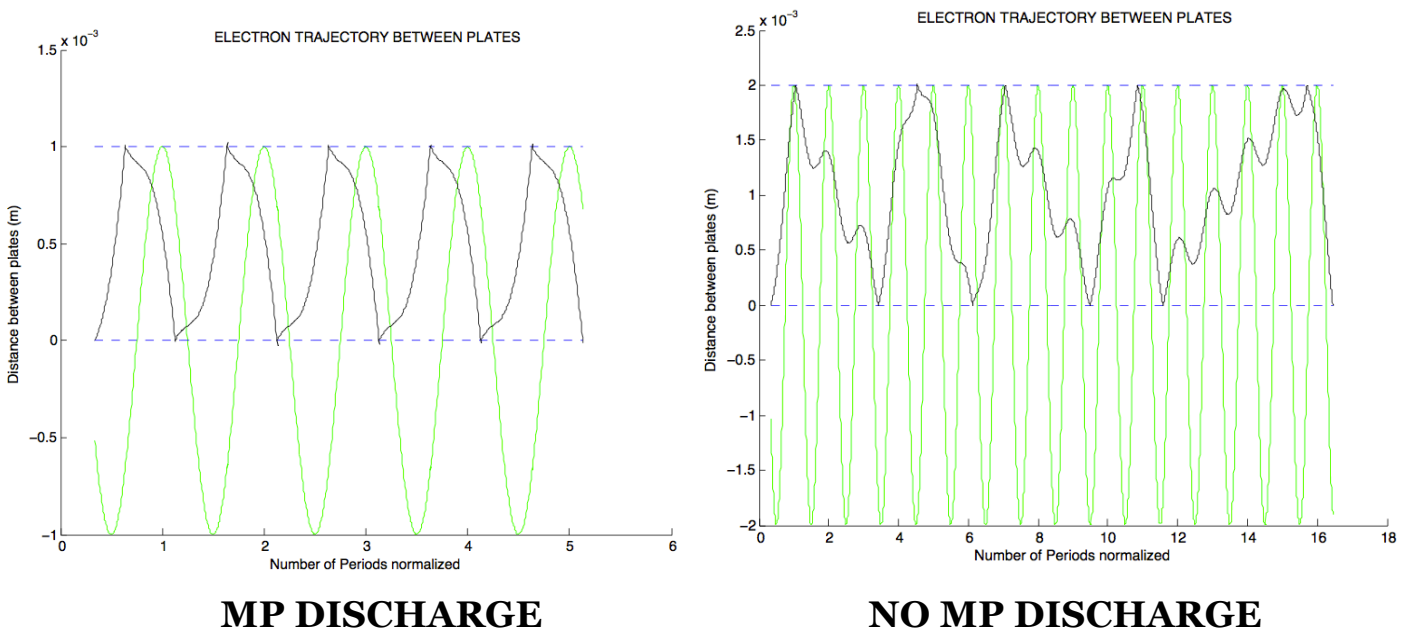


Fig. 8 Simulation for different d

In the case of the third simulation we pretend to analyse the influence of using a different gap ($f \times d$). The gap parameter is also one of the most important parameters to consider. In real testing the geometry and dimensions of the device must be controlled as precisely as possible to detect the multipactor discharge. Figure 8 shows clearly that if the distance between plates is, for this case, twice, the electron does not reach the wall with enough energy to extract more electrons from the surface. In both graphs the same amplitude and the same electron initial phase.

Summary

SEY of various potential coatings for reduced multipactor thresholds applications have been studied. The first crossover E_1 and the maximum δ_{max} are the SEY properties most influencing on multipactor initiation.

The results of the simulations in Multipactor software can be represented in a graphic, as the previous examples show, where the y-axis shows the distance between plates (d in m) and the x-axis the time normalized by the period of the electric field ($T = T_{rf} = 1/f$). Nevertheless, it is very important to note that the graphs only show the path followed by an electron accelerated by the signal applied between the plates. Just visualizing the paths is not currently possible to determine whether there has occurred the discharge. To predict if the multipactor effect is present or not depending on the initial conditions applied to the problem at the beginning of the simulation, we must study the value of the secondary emission coefficient. As defined in section 3.1.3, "Secondary electrons model", if this coefficient (δ) is greater than one, the number of secondary released electrons is greater than the incident in the considered plates structure and it means that new electrons have appeared as a consequence of one of the impacts.

In the examples above shown using the Multipactor software, it is possible to specify intervals for the gap distance trying that the difference between the estimate solution and the exact one does not exist. Nevertheless, depending on the approximation chosen in the integration algorithms the solution could be quite different. Thus, it is very important to control this type of issues because small variations in the software can provide us different solutions for a same case.

Also, we have been working in a calibration method in which the error between the results calculated using numerical integration methods (to solve the differential equation 4) and the results using the analytical solution (Eq. 7 and 8) are the minimum. The error between their solutions must be below a specified tolerance. In next figure, (Fig. 9), are represented the function to compare the solutions obtained using numerical methods (in this case ode45) and the analytical results using the exact equations.

The process followed is the next one. The graph represented on the top is performed using numerical methods to approximate the solution and then compared with the exact solution (bottom graph). The results are completely valid and in improved versions of the software will provide security in solving the problem using different numerical methods.

Figure 9 shows the trajectory followed by five different electrons with different initial phases. The path of each electron is shown with different colours in both graphs. It is possible to observe that the approximate solutions using analytical and numerical methods are almost identical.

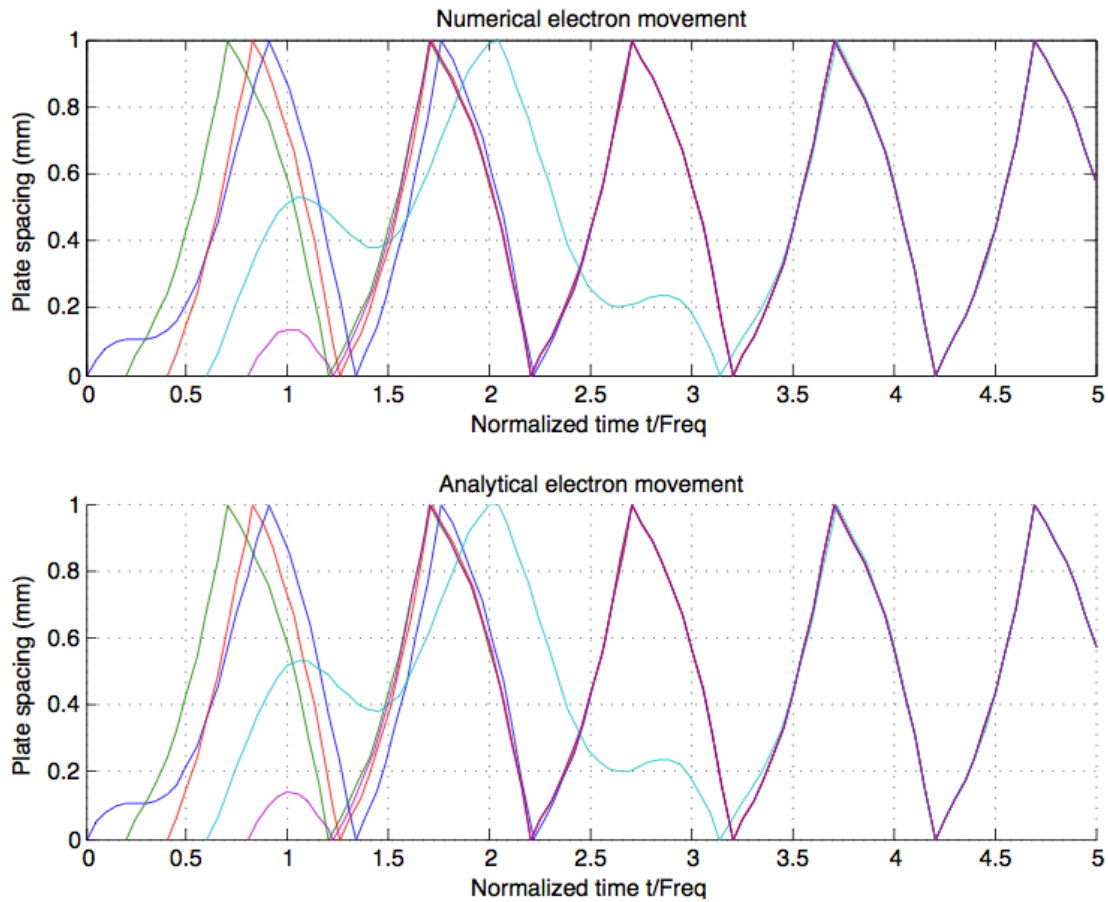


Fig. 9 Numerical vs Analytical results.

The simulation algorithm for the numerical solution of the electron motion chosen for this problem is ode45 (an specific function of Matlab which implements the Runge-kutta method). After doing several simulations, it is concluded that employing a MaxStep option (included in the own ode45) function with values about 10^{-11} or 10^{-12} the ode45 algorithm has the same behaviour as in the case of using its default time step in the intervals where the equation is solved.

Finally, one of the most representative aspects of this software is to display the trajectory followed by the electron between the plates because then, when the electric field signal is replaced by a modulated signal will be possible to detect the particular instant at which a phase or an amplitude switch occurs and may possibly play an important role in the trajectory of the electron and in the growth of the electron avalanche. It is a very simple and representative way to observe and predict how the electron behaves under the influence of different signals.

In conclusion, given some input parameters, such as the frequency of operation, device dimensions, and material secondary emission yield (SEY) properties, these single carrier prediction methods provide the threshold for the multipactor breakdown power. The predicted thresholds are used by the industry to design and assess the margins of operated power in the device to be multipactor free. Our software results are validated with the ECCS Multipactor Tool, a software tool based on the European Cooperation for Space Standardization. The main objective is to perform reliable and consistent multipactor analysis at the components.

|4 MULTIPACTOR EFFECT IN MODULATED SIGNALS

Power is a critical issue in telecommunications and narrow-band communication systems require the use of tightly band limited signalling formats. This analysis has a major importance in case of using high amplitude signals due to the ever-growing demand in high spectral efficiency telecommunications systems implying multi-dimensional waveform considerations (in frequency, time, space, etc.) where parameters like PAPR (Peak Power to Average) are of major concern. Traditional modulation and coding schemes have been designed from the standpoint of minimizing average power but it is also important to look into modulation formats to minimize peak power and retain high spectral efficiency.

In this section, the focus is done in single carrier modulations. The main objective of the analysis is to understand the effect of modulated signals in the RF breakdown values. Also it is presented an analysis of different performance parameters such as EVM (Error Vector Magnitude), Bandwidth Efficiency and BER (Bit Error Rate) of modulated signals in transmission systems, which are considered to be useful system metrics for any digital communication system. The purpose consists in the study of the variation in the multipactor threshold for a set of digitally modulated signals and the Multipactor simulator tool is improved to validate a set of different pass-band modulated signals.

At the present, the study has been focused mainly in BPSK and QPSK modulation schemes. The reason is that the most links used in satellite telecommunication are employing modulation by means of quadrature phase-shift keying (QPSK). However, to analyse multipactor initiation in QPSK-modulated signals, firstly a digital phase modulation study is included making a review of the fundamentals of binary phase shift keying (BPSK) which is the simplest form of digital phase modulation. The main characteristic of this type of modulation is that the signal envelope stays constant, but the phase switches with regular intervals. It is an important issue to consider that any jump in the RF phase can be treated as a considerable perturbation of the multipactor resonance. The aim of this section is to study the influence of such phase switches on the initiation and dynamics of the multipactor discharge. Finally, one of the purposes is to predict important parameters as the Symbol Period (T_s) we must use to prevent and avoid the growth of the electron avalanche.

4.1 Modulated Signals Theory

4.1.1 Introduction

The fundamental concept of digital communication is to move digital information from one point to another over an analog channel. More specifically, pass-band digital communication involves modulating the amplitude, phase or frequency of an analog carrier signal with a baseband information-bearing signal. By definition, frequency is the time derivative of phase; therefore, we may generalize phase modulation to include frequency modulation. Ordinarily, the carrier frequency is much greater than the symbol rate of the modulation, though this is not always so. Given a sinusoidal carrier with frequency f_c , digitally-modulated pass-band signal, $S(t)$, is defined as:

$$S(t) = A(t) \cos(2\pi f_c t + \theta(t)), \quad (17)$$

where $A(t)$ is a time-varying amplitude modulation and $\theta(t)$ is a time-varying phase modulation. For digital phase modulation, we only modulate the phase of the carrier, $\theta(t)$, leaving the amplitude, $A(t)$, constant.

Digital phase modulation need not be limited to the simple binary case. By grouping bits together and choosing the phase modulation accordingly, we obtain M -ary PSK. BPSK is the result when $M = 2$. For $M = 4$, we group the bits into pairs, and the resulting signal is known as quadrature phase shift keying (QPSK).

4.1.2 BPSK

Binary phase shift keying (BPSK) is the most simple modulation case where only two phase-switching events can affect the trajectory of the electron. Furthermore, this is the worst case because if we consider only two values of phase (0 and π), the jump between the phases is the greatest one and it may affect more directly the trajectory of the electron inside the device.

For BPSK, each symbol consists of a single bit. Accordingly, we must choose two distinct values of $\theta(t)$, one to represent 0 , and one to represent 1 . Since there are 2π radians per cycle of carrier, and since our symbols can only take on two distinct values, we can choose $\theta(t)$ as follows. Let $\theta_1(t)$, the value of $\theta(t)$ that represents a one, be 0 , and let $\theta_0(t)$, the value of $\theta(t)$ that represents a zero, be π . Doing so, we obtain:

$$S_0(t) = \sqrt{E_s} \cos(2\pi f_c t + \pi), \quad (18)$$

$$S_1(t) = \sqrt{E_s} \cos(2\pi f_c t + 0),$$

where $\sqrt{E_s}$ is the peak amplitude of the modulated sinusoidal carrier, $S_0(t)$ is the BPSK signal that represents a zero, and $S_1(t)$ is the BPSK signal that represents a one.

Phase Modulation Equals Amplitude Modulation

The expressions for $S(t)$ given in (18) clearly show BPSK as a form of phase modulation. However, since: $\cos(\theta + \pi) = -\cos(\theta)$, we can rewrite $S_0(t)$ and $S_1(t)$ as:

$$S_0(t) = -\sqrt{E_s} \cos(2\pi f_c t), \quad (19)$$

$$S_1(t) = \sqrt{E_s} \cos(2\pi f_c t),$$

These expressions for $S(t)$ show BPSK as a form of amplitude modulation, where $A_0(t) = -1$ and $A_1(t) = +1$. So, BPSK can be considered a phase modulation or an amplitude modulation, since the two are equivalent, as demonstrated by the trigonometric identity we used to convert between the two forms.

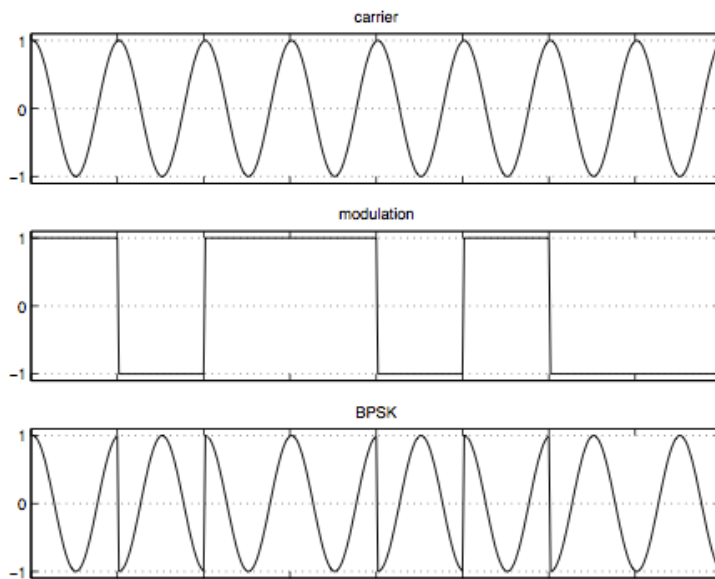


Fig. 10 BPSK Modulation

The modulation process is probably easier to understand when viewed from the perspective of amplitude modulation. For the above expressions, the carrier signal is $\sqrt{E_s} \cos(2\pi f_c t)$, and the amplitude modulation is a square wave that has an amplitude of ± 1 and a period of T_s , the duration of one symbol. Figure 10 illustrates how we create BPSK by multiplying a sinusoidal carrier by rectangular bit pulses. In the example, the duration of each symbol, T_s , is exactly one carrier cycle.

4.1.3 QPSK

In QPSK, Quadrature Phase Shift Keying, we have four symbols, each representing a particular value. Therefore, we must select four values for $\theta(t)$, the time-varying phase modulation of our digital pass-band signal. Suppose we use the map listed in Table 1 to assign phase modulation to each of the four possible symbols.

Bits	$\theta(t)$
00	$+\frac{3\pi}{4}$
01	$-\frac{3\pi}{4}$
10	$+\frac{\pi}{4}$
11	$-\frac{\pi}{4}$

Table 1: QPSK Symbol Map

The mapping shown in Table 1 results in the following expressions for the QPSK signal, $S(t)$:

(20)

$$S_{00}(t) = \sqrt{E_s} \cos\left(2\pi f_c t + \frac{3\pi}{4}\right),$$

$$S_{01}(t) = \sqrt{E_s} \cos\left(2\pi f_c t - \frac{3\pi}{4}\right),$$

$$S_{10}(t) = \sqrt{E_s} \cos\left(2\pi f_c t + \frac{\pi}{4}\right),$$

$$S_{11}(t) = \sqrt{E_s} \cos\left(2\pi f_c t - \frac{\pi}{4}\right).$$

Using the identity: $\cos(a + b) = \cos(a)\cos(b) - \sin(a)\sin(b)$, we can rewrite (20) in a more intuitive form as in (21).

In this form (Eq. 21), we have expressed QPSK in terms of an amplitude modulated quadrature carrier. A quadrature carrier may be thought of as either a complex exponential, $e^{+j\omega_c t}$, or the equivalent sum of sinusoids in phase quadrature, $\cos(\omega_c t) + j\sin(\omega_c t)$.

(21)

$$S_{00}(t) = -\frac{\sqrt{2E_s}}{2}\cos(2\pi f_c t) - \frac{\sqrt{2E_s}}{2}\sin(2\pi f_c t),$$

$$S_{01}(t) = -\frac{\sqrt{2E_s}}{2}\cos(2\pi f_c t) + \frac{\sqrt{2E_s}}{2}\sin(2\pi f_c t),$$

$$S_{10}(t) = +\frac{\sqrt{2E_s}}{2}\cos(2\pi f_c t) - \frac{\sqrt{2E_s}}{2}\sin(2\pi f_c t),$$

$$S_{11}(t) = +\frac{\sqrt{2E_s}}{2}\cos(2\pi f_c t) + \frac{\sqrt{2E_s}}{2}\sin(2\pi f_c t).$$

Modulating a Quadrature Carrier

Expressing $S(t)$ as an amplitude modulated quadrature carrier allows us to conceptualize QPSK as the sum of two BPSK signals, which are in phase quadrature with each other. The carrier signals are $\frac{\sqrt{2E_s}}{2}\cos(2\pi f_c t)$ and $\frac{\sqrt{2E_s}}{2}\sin(2\pi f_c t)$, and the signals that amplitude modulate these carriers are square waves that have amplitudes of ± 1 and periods of one symbol, T .

Figure 11 illustrates a QPSK modulation created by summing two sinusoidal carriers that have been amplitude modulated with rectangular bit pulses. The top three graphs show the in-phase (real) channel, and the next three graphs show the quadrature (imaginary) channel. The bottom graph shows the QPSK signal resulting from the sum of the in-phase and quadrature BPSK signals.

4.1.4 Polar Display and IQ Formats

Typically to transmit digital signals we use the polar form of the signal. In general, a simple way to view amplitude and phase is with the polar diagram. The carrier becomes a frequency and phase reference and the signal is interpreted relative to the carrier. The phase is relative to a reference signal (usually the carrier in most communication systems). Magnitude is represented as the distance from the centre and phase is represented as the angle. In phase modulations only the phase of the signal changes while in amplitude modulations changes only the magnitude of the signal. (Figures 12, 13 and 14)

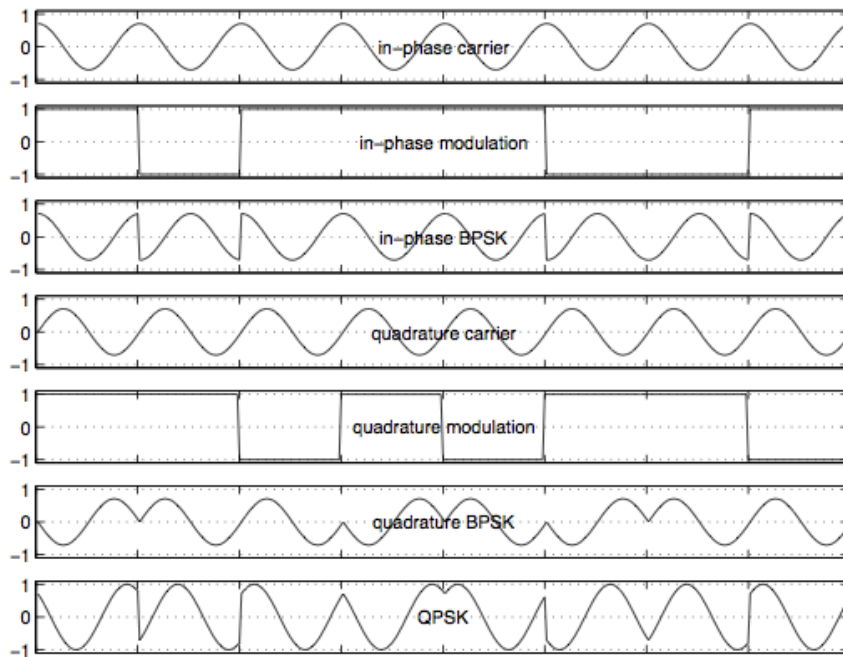


Fig. 11 QPSK Modulation

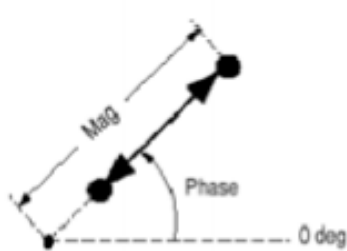


Fig. 12 Amplitude Change

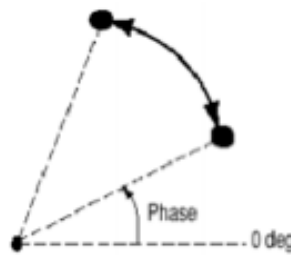


Fig. 13 Phase Change

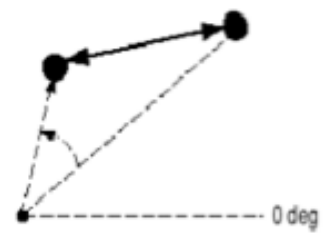


Fig. 14 Amplitude and Phase Change

In digital communications, modulation is often expressed in terms of I and Q. This is a rectangular representation of the polar diagram. On a polar diagram, the I axis lies on the zero degree phase reference, and the Q axis is rotated by 90 degrees. The signal vector's projection onto I axis is its "I" component and the projection onto the Q axis is its "Q" component.

I/Q diagrams are useful since they mirror the way in which digital communication signals are created using an I/Q modulator. In digital modulation is easy to accomplish with I/Q modulators. In fact, the most modulators map data onto a number of discrete points on the I-Q plane. These points are known as constellation points and when the signal moves from one point to another, simultaneous amplitude and phase modulation usually takes place

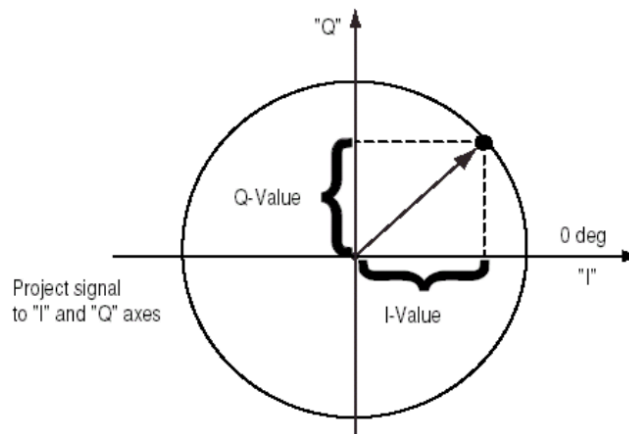


Fig. 15 Polar to rectangular Conversion

A composite signal described by its envelope and phase form can be decomposed to an equivalent quadrature-carrier (IQ) as:

$$A(t) \sin[2\pi ft + \phi(t)] = I(t) \sin(2\pi ft) + Q(t) \sin\left(2\pi ft + \frac{\pi}{2}\right)$$

where f represents the carrier frequency, and:

$$\begin{aligned} I(t) &= A(t) \cos[\phi(t)] \\ Q(t) &= A(t) \sin[\phi(t)] \end{aligned}$$

$A(t)$ and $\phi(t)$ represent the possible modulation of a pure carrier wave ($\sin(2\pi ft)$). The modulation alters the original “sin” component of the carrier and creates a new “cos” component, as shown above. The component that is in phase with the original carrier is referred to as the *direct or in-phase component*. The other component, which is 90° out of phase, is referred to as the *quadrature component*.

4.1.5 Constellation Diagram

A constellation diagram shows the symbol locations in complex signal space. The horizontal axis is the real or in-phase component, which is also the amplitude of the cosine portion of the quadrature carrier. The vertical axis is the imaginary or quadrature component, which is also the amplitude of the sine portion of the quadrature carrier. The instantaneous energy, or amplitude, of a symbol is its distance from the origin. The phase angle of a symbol is its angular displacement from the positive horizontal axis.

In the BPSK signal constellation does not particularly matter exactly where the constellation points are positioned, in Fig. 16 they are shown on the real axis, at 0° and 180° . As we explained above, this modulation is the most robust of all the PSKs since it takes the highest level of noise or distortion to make the demodulator reach an incorrect decision.

The QPSK signal constellation resulting from the symbol map of Table 1 is shown in Fig 17. The four symbols are represented by gray circles, and are labelled according to the mapping of Table 1. The dashed circle represents a locus of constant signal energy, meaning any point on this circle requires the same amount of transmitter power.

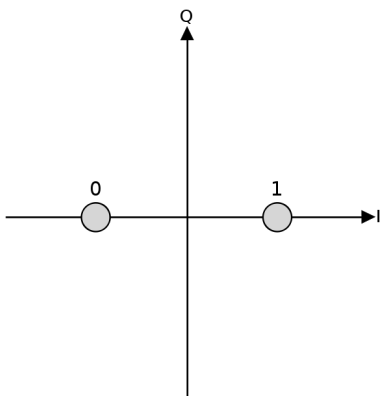


Fig. 16 BPSK Signal Constellation

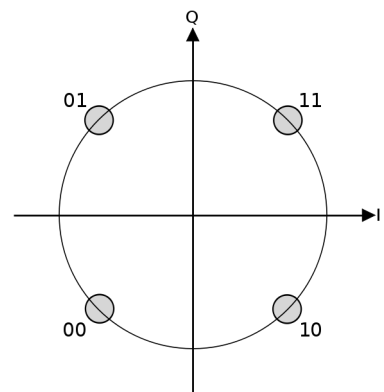


Fig. 17 QPSK Signal Constellation

4.1.6 Transition Diagram

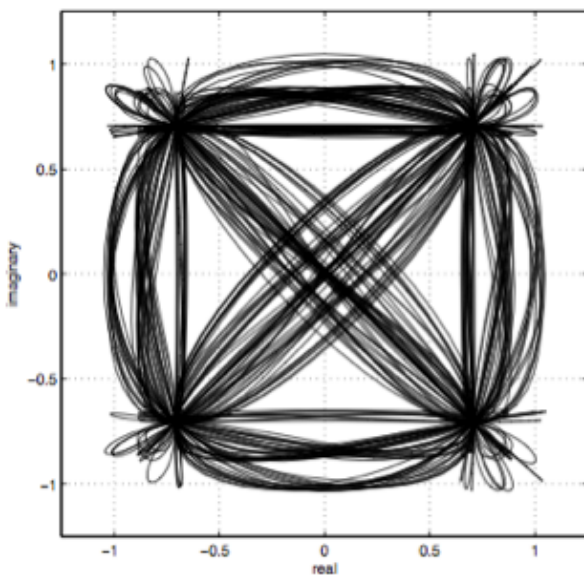


Fig. 18 QPSK Transition Diagram

The transition diagram is similar to the constellation diagram, in that they both show the QPSK signal in complex signal space. However, the transition diagram shows the signal transitions between symbols, whereas the constellation diagram does not. Fig. 18 shows a QPSK transition diagram.

At the centre of each symbol, the signal will be located at one of the four corners of the constellation. At all other times, the signal will be transitioning between symbols. The exact shape of the transition diagram is determined by the filter roll-off factor as well as the number of samples per symbol.

4.1.7 Signal Envelope

We generally regard PSK as a form of constant-envelope modulation, since we are modulating the phase instead of the amplitude of the carrier signal. However, since:

$$\sqrt{E_s} \cos(\omega_c t + \theta(t)) = \sqrt{E_s} \cos(\omega_c t) \cos(\theta(t)) - \sqrt{E_s} \sin(\omega_c t) \sin(\theta(t)),$$

phase modulation of a sinusoidal carrier is equivalent to amplitude modulation of a quadrature carrier. This leads us to wonder whether or not PSK is truly constant-envelope modulation. The answer can be found in the transition diagram. The transition diagram shows the signal in complex signal space, plotted over some period of time. At any instant, the signal amplitude is simply the distance from the origin to a specific point on the transition diagram. In order to have a constant envelope, the signal must always be equally distant from the origin.

For unfiltered QPSK, the symbols are simply rectangular pulses, and the transitions between symbols are instantaneous. In this case, the transition diagram is a square. Although it has straight lines between all four symbols, these transitions occur in zero time. Therefore, the signal must be at one of the four corners of the square at all times, resulting in a constant envelope signal. However, when we apply a pulse shaping filter to the symbols, the envelope is no longer constant. This is clearly evident in the transition diagram shown in Fig. 18. Since the symbols have been filtered, the transitions are no longer instantaneous, and the signal can take on any value shown in the transition diagram.

Fig. 19 shows a typical QPSK signal (thin lines) and its envelope (thick lines). Clearly, the envelope is not constant, since it becomes zero for brief instants whenever there is a π radian phase transition, which occurs when the next symbol is diagonally opposite of the present symbol.

The signal envelope is important on channels which suffer from amplitude distortion, especially channels which are hard limited. If a signal does not have a nearly- constant envelope, it will be severely distorted on such a channel. This can result in bandwidth expansion, intersymbol interference, and quadrature channel crosstalk. If the distortion is severe, it may not be possible for the receiver to recover the modulation.

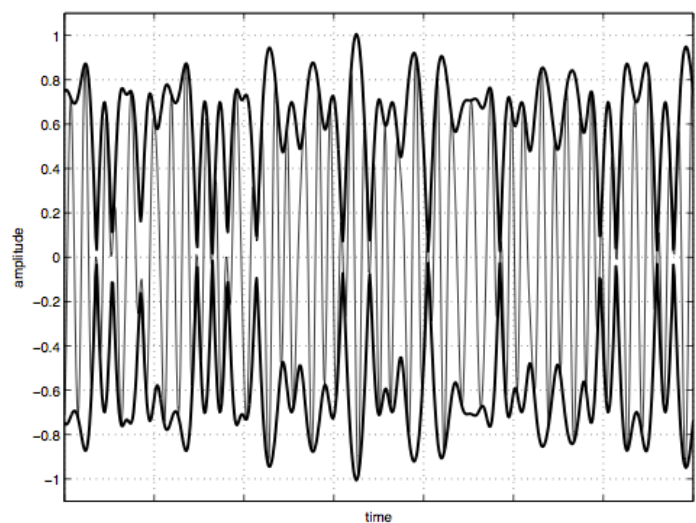


Fig. 19 QPSK Signal and Envelope

4.2 Digital Communication System Metrics

It is necessary to review the performance of some communication system metrics such as Error Vector Magnitude (EVM), Magnitude Error, Phase Error, Bit Error Rate (BER), Peak to Average Power (PAPR) or Complementary Cumulative Distribution Function (CCDF) to understand their importance and influence in the digital communication systems and consequently in our study.

4.2.1 EVM

EVM is a common figure of merit for system linearity in digital wireless communication standards where a maximum level of EVM is specified. By definition, EVM is a measure of the departure of signal constellation from its ideal reference because of non-linearity, signal impairments and distortion. I- Q Magnitude Error shows the magnitude difference between the actual and the ideal signals, where as I-Q Phase Error measures the instantaneous angle difference between the measured signal and the ideal reference signal. Magnitude Error and Phase Error are the indicators of the quality of the amplitude and phase component of the modulated signal. Fig. 20 clearly defines the EVM, Magnitude Error and Phase Error in case of I-Q modulation.

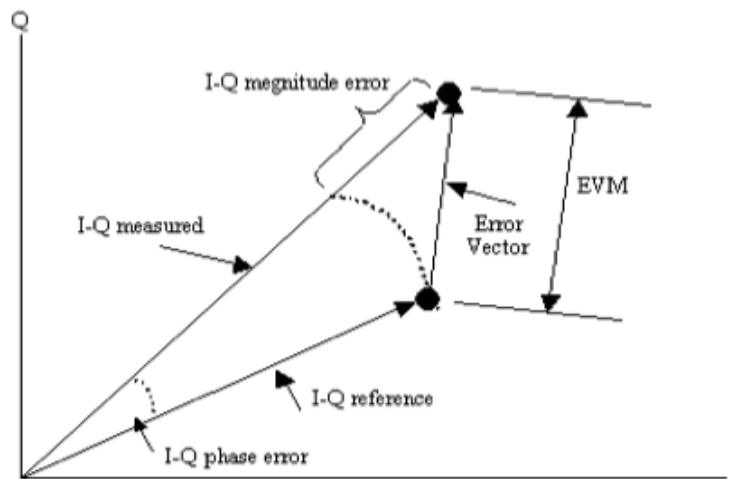


Fig. 20 EVM and related quantities.

4.2.2 BER

The *Bit Error Rate (BER)* is defined as the ratio of number of erroneous bits detected to the number of transmitted bits.

4.2.3 Bandwidth Efficiency

Bandwidth Efficiency describes the ability of a modulation scheme to accommodate data within a limited bandwidth and is defined as the ratio of the throughput data rate per Hertz in a given bandwidth.

4.2.4 PAPR

Realistic satellite communication systems combine more than one channel in a single output, what is called a multicarrier signal. The multicarrier signal combines the transmission power of the individual channels. Its amplitude is time varying and depends on the relative amplitudes and phases of the channel carriers, so its behaviour could be very similar as in the case of modulated signals. Therefore, in the multicarrier path of the spacecraft, extremely high peak power levels may be attained, thus increasing the risk of a multipactor discharge.

The *Peak to Average Power Ratio (PAPR)* is currently viewed as an important implementation issue in communication systems. PAPR is considered extensively for multicarrier systems, however although PAPR effects are less important in single carrier (SC) modulated signals it takes a significant value when the roll-off factor in Square Root Raised Cosine (SRRC) filter tends to zero. Thus, PAPR issue must be considered for single carrier as well.

PAPR is the ratio of the instantaneous power to the mean power for a particular signal. The PAPR definition is rather used when radio frequency signals are considered whereas Peak to Mean Envelop Power Ratio (PMEPR) definition refers to base band signals. The PAPR and PMEPR are defined as (Eq. 22):

$$PAPR = \frac{\max\{|x(t)|^2\}}{E[|x(t)|^2]} = \frac{|x|_{peak}^2}{x_{rms}^2} \quad (22)$$

$$PMEPR |_{dB} = PAPR |_{dB} - 3 \text{ dB}$$

PAPR depends on the bandwidth efficiency regardless of the modulation structure. Typically pulse shapes filters such as raised-cosine or root-raised-cosine cause a substantial increase in the peak power of traditional linear modulation formats such as M-ary phase shift keying (M-PSK) and M-ary quadrature amplitude modulation (M-QAM). This is one of the issues we will consider in next sections. In conclusion, there is a need to produce spectrally efficient modulation formats to have a low PAPR.

4.2.5 CCDF

The *power Complementary Cumulative Distribution Function (CCDF)* curves characterize the higher-level power statistics of a digitally modulated signal. Many digitally modulated signals look noise-like in the time and frequency domain. This means that statistical measurements of the signals can be a useful characterization. The curves can be useful in determining design parameters for digital communications systems. Perhaps the most important application of power CCDF curves is to specify completely and without ambiguity the power characteristics of the signals that will be mixed, amplified, and decoded in communication systems.

A CCDF curve is defined by how much time the waveform spends at or above a given power level. The per cent of time the signal spends at or above the level defines the probability for that particular power level. The power level is expressed in dB relative to the average power. For example, each of the lines across the waveform shown in Figure 21 represents a specific power level above the average. The percentage of time the signal spends at or above each line defines the probability for that particular power level. A CCDF curve is a plot of relative power levels versus probability.

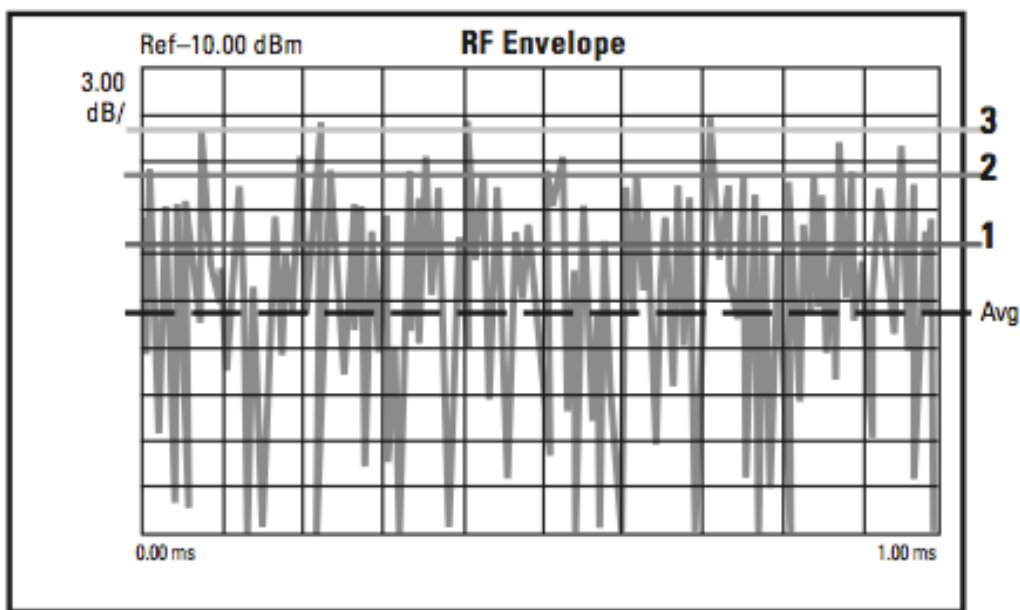


Fig. 21 Construction of a CCDF curve

The figure showed above (Fig.21) represents the power versus time. This plot represents the instantaneous envelope power defined by the equation:

$$Power = I^2 + Q^2$$

where I and Q are the in-phase and quadrature components of the waveform.

Unfortunately, the signal in the form shown in Figure 21 is difficult to quantify because of its inherent randomness and inconsistencies. In order to extract useful information from this noise-like signal, we need a statistical description of the power levels in this signal, and a CCDF curve gives just that.

This is the case in next figure (Fig 21.1) which displays a typical CCDF curve. Here, the x-axis is scaled to dB above the average signal power, which means we are actually measuring the peak-to-average ratios as opposed to absolute power levels. The y-axis is the percent of time the signal spends at or above the power level specified by the x-axis. For example, at $t = 1\%$ on the y-axis, the corresponding peak-to-average ratio is 7.5 dB on the x-axis. This means the signal power exceeds the average by at least 7.5 dB for 1 percent of the time. The position of the CCDF curve indicates the degree of peak-to-average deviation, with more stressful signals further to the right.

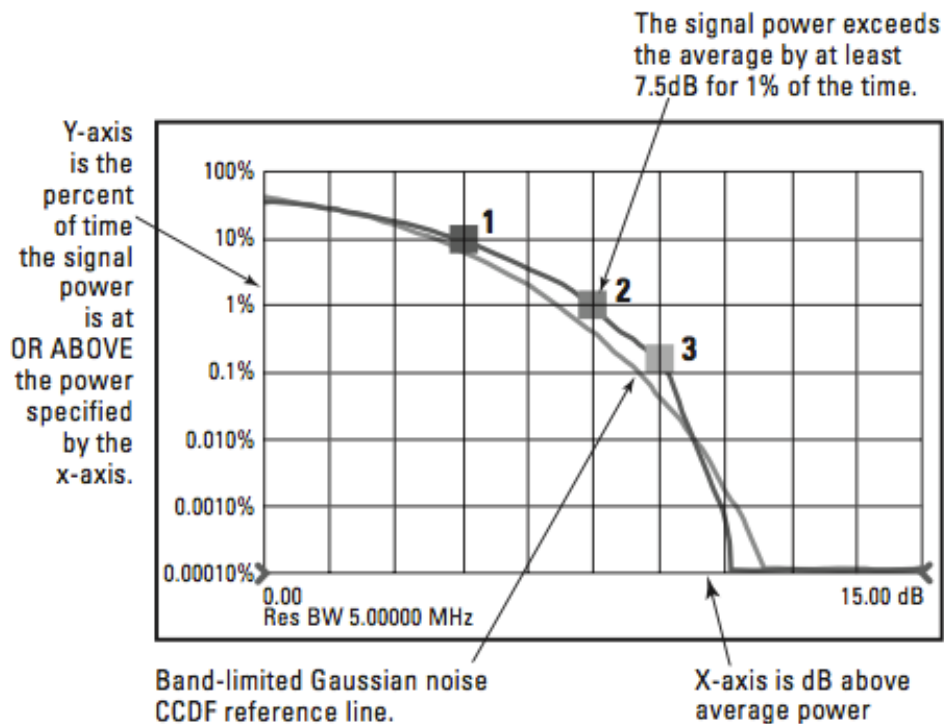


Fig. 21.1 Typical CCDF curve

Evidently, the modulation format of a signal affects its power characteristics. Using CCDF curves, we can fully characterize the power statistics of different modulation formats, and compare the results of choosing one modulation format over another.

4.3 Multipactor Software for modulated signals

4.3.1 Objectives

The next software to simulate single carrier modulated signals is an improved version from the above explained. In this one, it is possible to choose the type of the modulation and some characteristic parameters to simulate the signal. It is clear that in real-world modulated signals the ideal case is to use symbol periods (T_s) much bigger than the period of the RF signal (T). Nevertheless, currently there are significant limitations to implement this theory.

Obviously, the trajectory of the electron will be affected applying a modulated signal. This software takes into account theoretical cases where it is possible to simulate T_s values as small as the user desires. For example, it is possible to simulate a BPSK or QPSK signals with a given frequency, separation between plates and different T_s values.

To get some insight into what can be obtained using this software, different aspects will be used to compare the properties between a modulated signal with a non-modulated one. Typically, the simulations does not use any type of filter but currently it is possible to introduce a pulse shaping filter or a rectpulse filter in the software studying their influences in the transmitted signal. It is very important to consider that filtering parameters for a particular modulation format can significantly affect the characteristics of the signal. A comparison between filters using the PAPR and the CCDF aspects of the signal will be presented.

Finally, the objective is to simulate different scenarios and observe the results in order to study what is the shortest symbol period (T_s) to prevent multipactor discharge. In other hand, other significant purpose is to analyse the influence of applying different types of filter to the modulated signal and study their effects on the development of a multipactor electron avalanche.

4.3.2 Software Development

In order to explain the whole study with Matlab about the modulation format of a signal, its power characteristics and the analysis to predict the multipactor initiation in modulated signals in next sections an extensive effort has been made to show all the theoretical situations under which multipactor breakdown can occur. This implies that different and several simulations have been carried out, taking into account several papers that have become on the basis for much simulations trying to confirm some aspects which until now were only theories.

Following the same procedure as above, these are the basic parameters that will be taken into account and the output data that will be provided.

Input data:

- 1 Electric Power/Amplitude of the field (*Volts*)
- 2 Frequency range (*GHz*)
- 3 Distance between plates (*mm*)
- 4 Electron initial velocity, v_0 (*eV*)
- 5 Electron initial phase, α ($^\circ$)
- 6 Material Properties for SEY ($E_1, E_2, E_{max}, \delta_{max}$)
- 7 Number of initial electrons introduced (initial electron seeding)
- 8 Number of Symbols (Nsym)
- 9 Symbol Period ($T_s = n \times T$) T_s is multiple of T ($T = 1/f$)

Output data:

- 10 Presence or absence of Multipactor
- 11 Total number of impacts (optional)
- 12 δ_m value in every impact (optional)

In order to study what is the minimum symbol period trying to avoid the multipactor discharge, in our Matlab's function we can choose how many RF periods must take one symbol. For each simulation we can determinate this value, that will be an integer number of RF periods. It is an intuitive way to check how many RF periods must take one symbol to produce multipactor.

The dependence of the multipactor behaviour on the moment of the phase switches is being studied by varying the phase of the RF electric field when the phase jump was applied.

As it has been developed in previous sections BPSK is the most simple case where only two phase-switching events affect to the electron trajectory. So, the best way to explain the performance of the simulation software is through some examples shown in next section "Results".

Another important factor to take into account is the sequence choice to modulate the signal. In next examples is used a general sequence composed by [1 0 1 0 1 0 1...]. It is easy to understand that this is the worst sequence case because every symbol period the phase suffers an abrupt change from one phase to another (0 to π and vice versa, evidently considering a BPSK modulated signal).

4.3.3 Results

Example 1

In the above sections the electric field equation (Eq. 5) was applied between the device plates to simulate the harmonic excitation with a cosine function (Figure 22). Now a BPSK signal is considered (Figure 23):

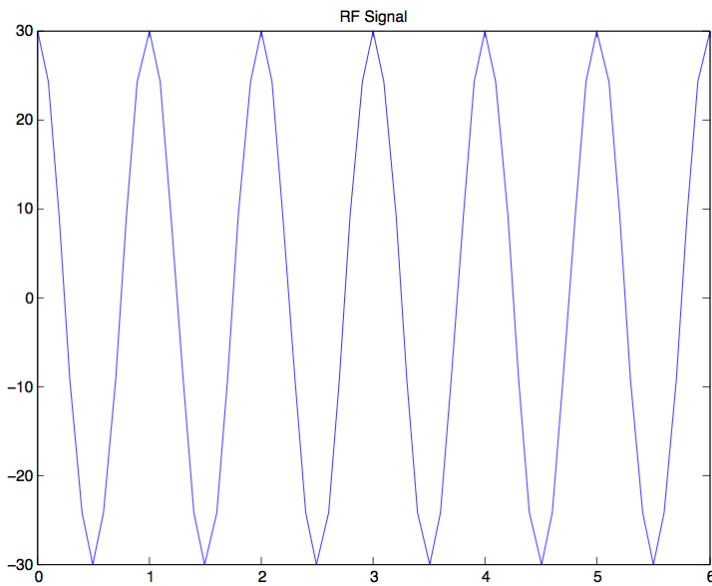


Fig. 22 RF signal. Cosine Function

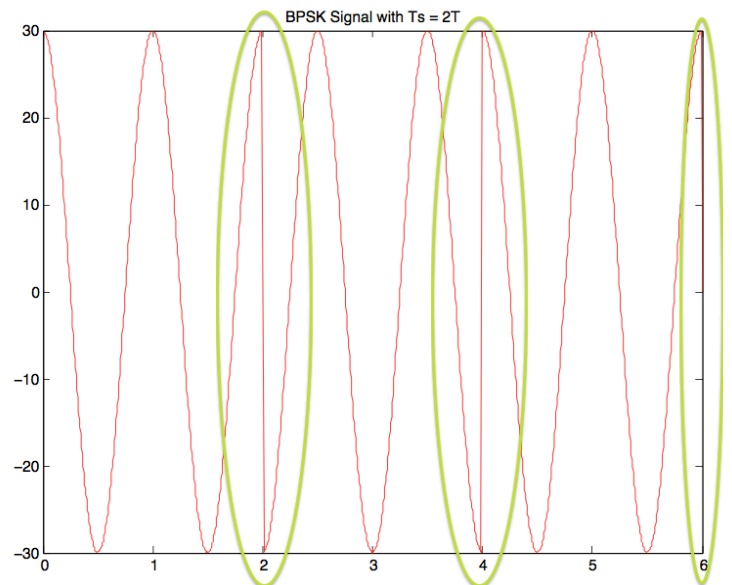


Fig. 23 BPSK Modulated Signal

Figure 23 shows the same signal as Figure 22 modulated with a BPSK scheme. In this case, one symbol takes two RF periods and after that a phase jump is observed. Because a BPSK signal is simulated, every symbol is composed by only one bit (1 or 0).

BPSK Modulation with the next input values:

Amplitude of the field, Amp = 30 Volts

Frequency, f = 1 GHz

Distance between plates, d = 1 mm

Electron initial velocity, $v_0 = 3.68$ eV

Material between plates: A_{g3A} ($E_1 = 30$ eV, $E_2 = 5000$ eV, $E_{max} = 165$ eV, $\delta_{max} = 2.22$)

Number of initial electrons introduced = 1 -> Electron initial phase, $\alpha = 0^\circ$

Number of Symbols, $N_{sym} = 3$

Symbol Period ($T_s = n \times T$) -> $n = 2$

Fig. 24 shows the trajectory followed by an electron excited with a cosine function. However, Fig. 25 illustrates just the same case applying a BPSK modulation with the above mentioned characteristics.

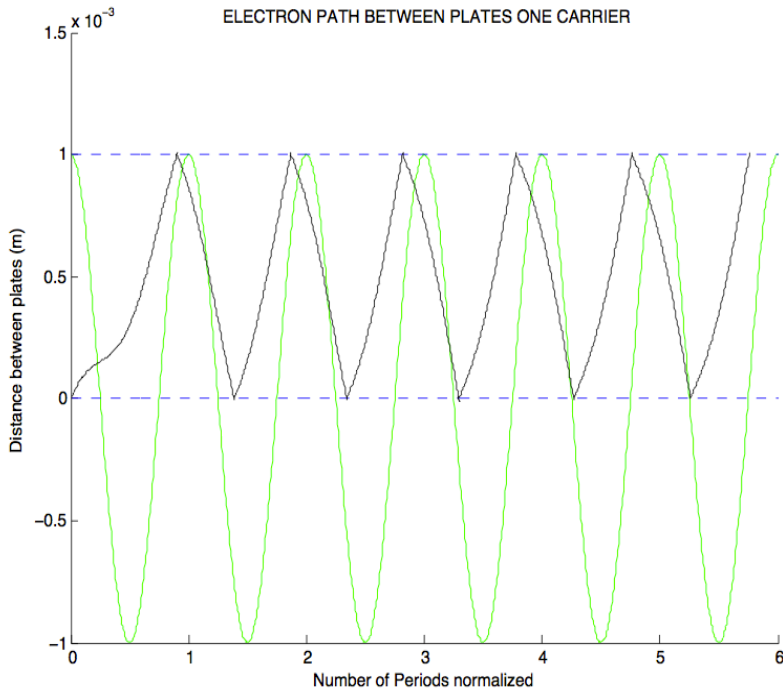


Fig. 24 Electron Trajectory with a RF signal

Table 2. Results Simulation (1)

N° impacts	Impact Energy (eV)	δ_{impact}
1	7.5050	1.0000
2	13.4588	1.0000
3	15.1756	1.0000
4	17.2694	0.2757
5	19.3424	0.4689
6	20.9431	0.5796
7	21.8651	0.6354
8	22.2912	0.6596
9	22.4482	0.6683
10	22.5050	0.6714
11	22.5239	0.6725

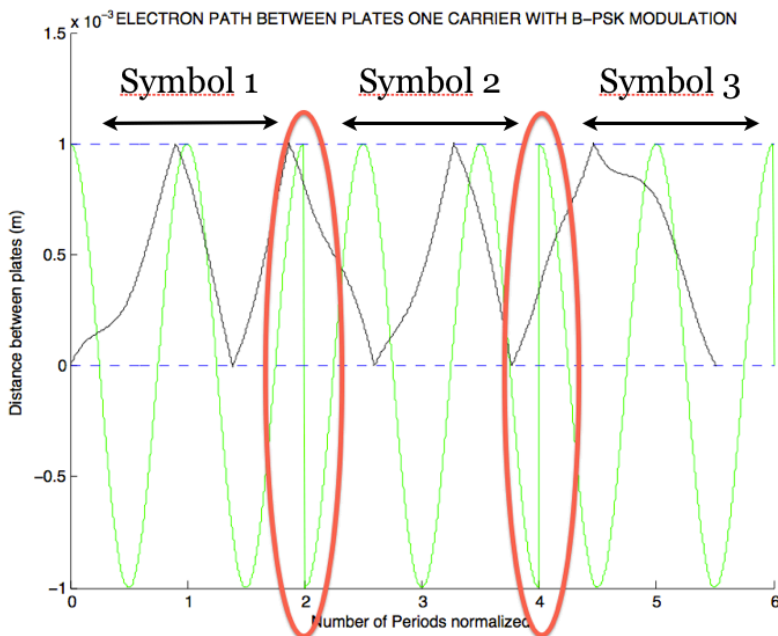


Fig. 25 Electron Trajectory with a BPSK modulated signal

Table 3. Results Simulation (2)

N° impacts	Impact Energy (eV)	δ_{impact}
1	7.5282	1.0000
2	13.4653	1.0000
3	15.1889	1.0000
4	14.3035	1.0000
5	17.0430	0.2474
6	22.3851	0.6648
7	9.1877	1.0000
8	2.5392	1.0000

Tables 2 and 3 show the number of times the electron impacts between the theoretical device walls. As well, both tables represent the energy with which the electron reaches the plate and the δ value according to the SEY graph for the simulated material (in this case A_{g3A}). Note that in the case that the energy of the impact is less than the minimum energy for the material (remember $E_{min} = 16 \text{ eV}$) the δ is considered equal to one. Once all the δ_{impact} are calculated the next step is to make the product of them.

$$\delta_{MP} = \delta_1 \cdot \delta_2 \cdot \dots \delta_i, \quad i = \text{number of impacts} \quad (23)$$

Finally, the last and most important conclusion,

$$\delta_{MP} \leq 1 \quad \text{NO MULTIPACTOR DISCHARGE} \quad (24)$$

$$\delta_{MP} > 1 \quad \text{MULTIPACTOR DISCHARGE}$$

The most part of the cases simulated with the software do not only consider one electron between the plates. In the case of simulating more than one electron, for example 360 (every one with a different initial phase value between 0 and 360°) the final condition to predict the multipactor breakdown is next one:

$$\alpha = 0 \rightarrow \delta_0 \quad (25)$$

.

.

.

$$\alpha = 360 \rightarrow \delta_{360}$$

$$\delta_{MP} = \frac{\sum_{\alpha=0}^{\alpha=360} \delta_{\alpha}}{\text{number of incident electrons (360)}}$$

Evidently, if $\delta_{MP} > 1$ means that the number of electrons leaving the plates is greater than the number of electrons introduced initially. Therefore, at least one of the electrons has initiated the catastrophic multipactor discharge.

Note that the figures 24 and 25 only show the trajectory of an electron that leaves with a certain initial phase value. It is not possible to predict or not multipactor just displaying the graphs.

Nevertheless, and although the procedure to detect multipactor is the same in modulated and non-modulated signals, it is clearly showed that the trajectory followed by the electron between the plates is different and in fact, the number of impacts is also different. In this particular example in which it is considered a BPSK modulation (only phase changes and constant envelope) simulating only 3 symbols with a $T_s = 2T$ ($T = 1/f$) multipactor does not occur. Thus, the final conclusion is that for these initial conditions the absence of multipactor is the same considering a RF signal or a modulated one.

Example 2

According to all the procedure followed in Example 1 and in order to show the software developed some simulations will be done:

Input Parameters:

Amplitude of the field, **Amp = 30 Volts**

Frequency, $f = 1$ GHz

Distance between plates, $d = 1$ mm

Electron initial velocity, $v_0 = 3.68$ eV

Material between plates: A_{g3A} ($E_1 = 30$ eV, $E_2 = 5000$ eV, $E_{\max} = 165$ eV, $\delta_{\max} = 2.22$)

Number of initial electrons introduced = 1 -> Electron initial phase, $\alpha = 0^\circ$

Number of Symbols, Nsym = 6

Symbol Period ($T_s = n \times T$) -> $n = 3$

Non-Modulated Signal:

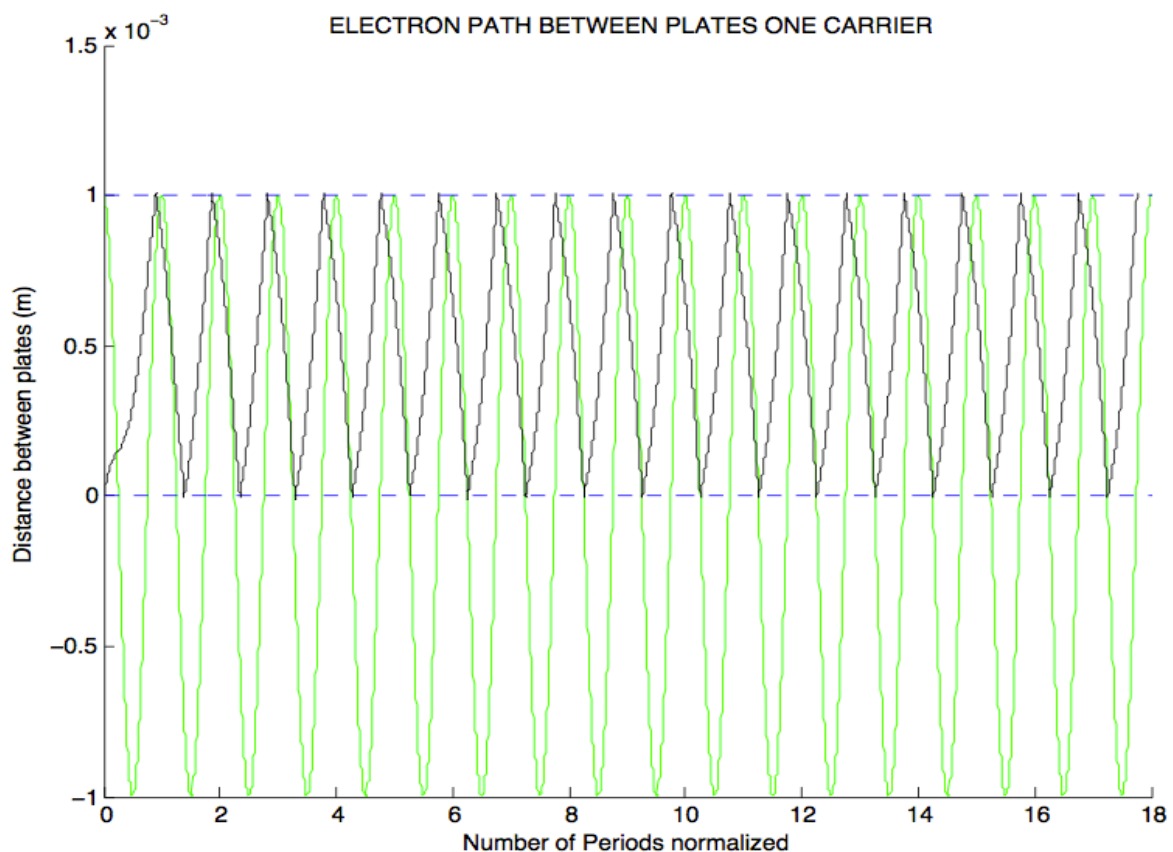


Fig. 26 Electron Trajectory with a RF signal. Amp = 30Volts

NO MULTIPACTOR DISCHARGE

To carry out this simulation in Matlab, data about modulation are ignored. Only the signal frequency, the distance between plates and the applied voltage are the main parameters in a RF single simulation. In the algorithm the user must enter the number of cycles of the RF signal he wants to simulate. In this example 18 periods of the signal have been simulated in order to compare with the modulated signal. If in the next BPSK modulated signal are simulated six symbols and each one takes three periods of the signal, the final number of periods is $6 \times 3 = 18$. In both simulations the numerical method to solve the equation and calculate the results is Runge-kutta algorithm taking an approximation of 1000 points per period.

BPSK Modulated Signal:

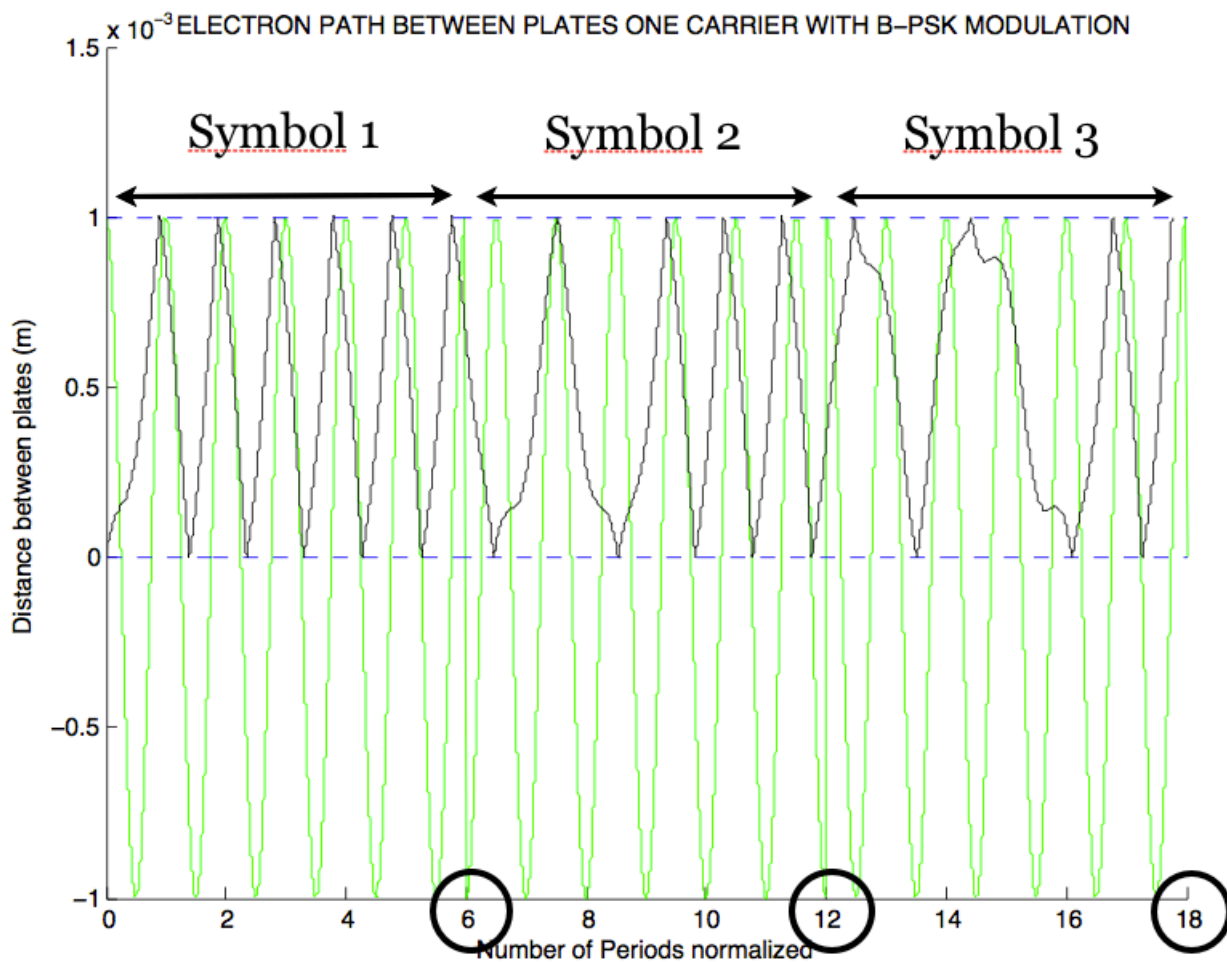


Fig. 27 Electron Trajectory with a BPSK modulated signal. Amp = 30 Volts

NO MULTIFACTOR DISCHARGE.

Example 3

Input Parameters:

Amplitude of the field, **Amp = 100 Volts**

Frequency, $f = 1 \text{ GHz}$

Distance between plates, $d = 1 \text{ mm}$

Electron initial velocity, $v_0 = 3.68 \text{ eV}$

Material between plates: $A_{g3}A$ ($E_1 = 30 \text{ eV}$, $E_2 = 5000 \text{ eV}$, $E_{\max} = 165 \text{ eV}$, $\delta_{\max} = 2.22$)

Number of initial electrons introduced = 1 \rightarrow Electron initial phase, $\alpha = 0^\circ$

Number of Symbols, Nsym = 6

Symbol Period ($T_s = n \times T$) $\rightarrow n = 3$

Non-Modulated Signal:

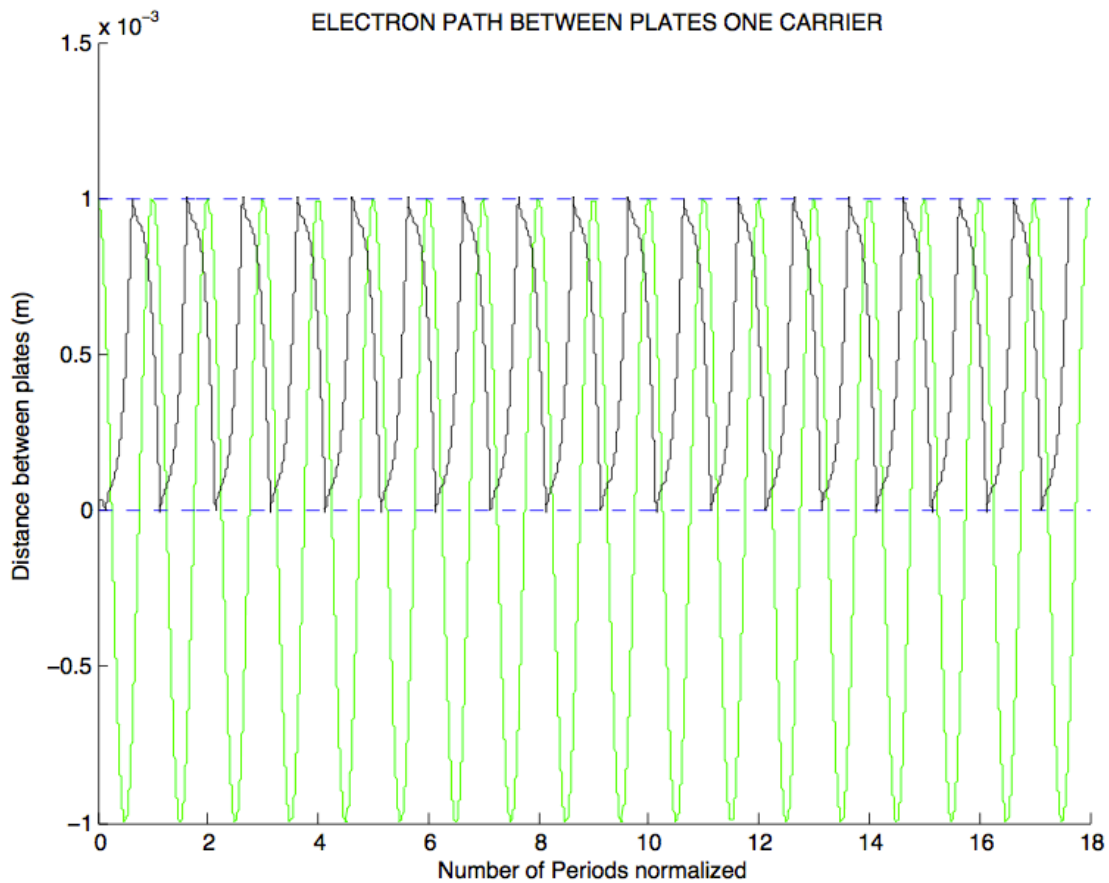


Fig. 28 Electron Trajectory with a RF signal. Amp = 100Volts

MULTIPACTOR DISCHARGE

BPSK Modulated Signal:

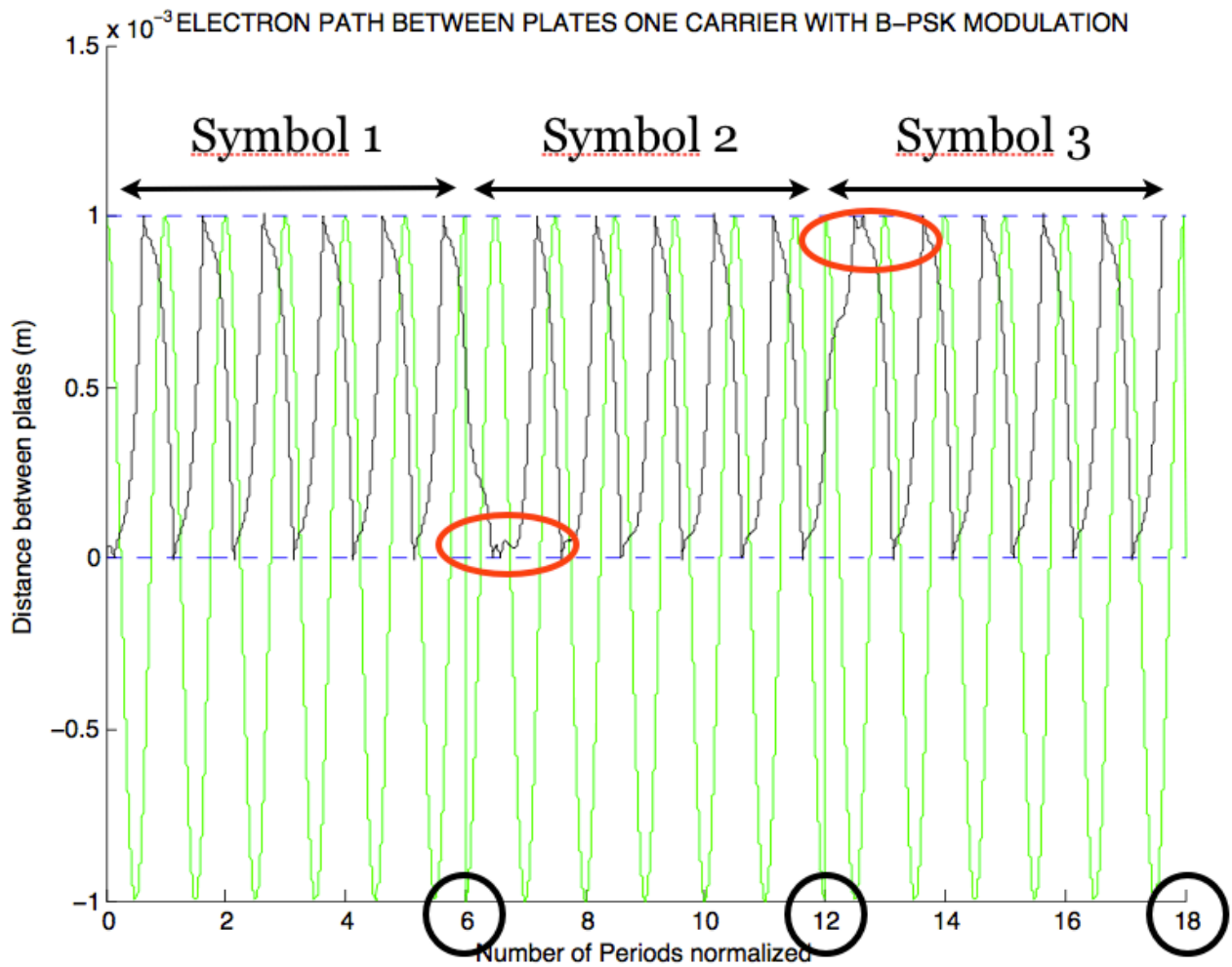


Fig. 29 Electron Trajectory with a BPSK modulated signal. Amp = 100 Volts

MULTIPACTOR DISCHARGE.

For such examples the only difference is the voltage applied between the plates. In both examples the presence or absence of multipactor does not depend whether the signal is modulated or not. Again, it is evident that the trajectory followed by the electron is different but the energy levels which ones the electron impacts the walls are similar. In the case of applying an amplitude of 100 Volts, as discussed in Section 3.2.2 the electron impacts with enough energy to start new electrons. However, it is found that for an amplitude of 30 volts any discharge occurs.

With the purpose to find a new multipactor threshold for modulated signals, in next point is considered the influence of the symbol period (T_s) to predict the multipactor discharge.

Symbol Period in MP Breakdown

Motivated by Ref [1] this section is totally based in much of the theory developed on it. The authors define that the interval between successive phase switches must be short enough in order to have a suppressing effect on the multipactor avalanche growth. Exactly, their theory says that if the symbol period (T_s) is less than ten times the RF signal period (T) the phase switches could play an important role avoiding even the multipactor discharge. Nevertheless, if $T_s > 10 \times T$ the electrons's avalanche grow and not significative changes are produced with respect the case where no one modulation is applied.

The above described section explains the Multipactor software performance when a modulated signal is applied between the plates. A general signal model has been programmed introducing the number of symbols and their symbols period. As a result, much of the previous work can be used to simulate the theory described in [1]. Multipactor simulator tries to prove that the phase modulation could have a suppressing effect on the multipactor development only if the interval between the successive phase switches is less than ten times the RF signal period. Then, the new objective is to simulate different scenarios and observe the results in order to study what is the shortest symbol period to prevent multipactor discharge depending on the signal's amplitude.

In the examples shown below different cases for a particular product $f \times d = 1 \text{ GHzmm}$ have been simulated using the software developed with Matlab. This section presents several simulations to study the multipactor initiation considering different amplitude values and symbol periods (T_s). The third column in the tables is one of the most important to consider because it determines how many RF periods takes one symbol in the applied modulation (in the first row, $T_s = T$, in the second, $T_s = 2 \times T$ and in the last one $T_s = 10 \times T$). The fourth column indicates whether multipactor exists or not (0 means NOT, and 1 means YES). Finally, the last column calculates the average value of impacts between plates using the specific conditions.

The objective is to compare the initiation of multipactor considering both cases, a BPSK modulated signal and the same signal without any type of modulation. The purpose is to study the effect considering different symbol periods in the modulated case and compare the number of impacts and the results with the non-modulated one.

All the results are calculated taking the same number of RF cycles (two hundred RF periods) and once again, the material simulated between plates is $A_{g3}A$. The number of electrons introduced is 72, all of them with different initial phase from 0 to 360° in increments of 5 degrees.

Simulations considering $f_{xd} = 1$ GHzmm and a non-modulated signal

Freq (GHz)	Amplitude (Volts)	MP	mean (n°impacts)
1	30	0	396

Table 4.1

Freq (GHz)	Amplitude (Volts)	MP	mean (n°impacts)
1	40	1	397

Table 4.2

Freq (GHz)	Amplitude (Volts)	MP	mean (n°impacts)
1	50	1	398

Table 4.3

Freq (GHz)	Amplitude (Volts)	MP	mean (n°impacts)
1	100	1	398

Table 4.4

Simulations considering $f_{xd} = 1$ GHzmm and a BPSK modulated signal

Freq (GHz)	Amplitude (Volts)	$T_s = n * T$ (n)	MP	mean (n°impacts)
1	30	1	0	200
1	30	2	0	299
1	30	3	0	265
1	30	4	0	276
1	30	5	0	308
1	30	7	0	341
1	30	10	0	339

Table 5.1

Freq (GHz)	Amplitude (Volts)	Ts= n*T (n)	MP	mean (n°impacts)
1	40	1	0	229
1	40	2	1	396
1	40	3	1	394
1	40	4	1	399
1	40	5	1	391
1	40	7	1	399
1	40	10	1	399

Table 5.2

Freq (GHz)	Amplitude (Volts)	Ts= n*T (n)	MP	mean (n°impacts)
1	50	1	0	398
1	50	2	1	398
1	50	3	1	395
1	50	4	1	399
1	50	5	1	391
1	50	7	1	399
1	50	10	1	399

Table 5.3

Freq (GHz)	Amplitude (Volts)	Ts= n*T (n)	MP	mean (n°impacts)
1	100	1	0	438
1	100	2	1	497
1	100	3	1	459
1	100	4	1	436
1	100	5	1	397
1	100	7	1	403
1	100	10	1	402

Table 5.4

This simulations takes a gap of $f \times d = 1 \text{ GHzmm}$ and the minimum value for the energy to take into account is $E_{min} = 16 \text{ eV}$. For the energy values that are below the minimum it is considered that the electron is absorbed. The method to solve the equation has been Runge-Kutta taking an approximation of 500 points per period.

Conclusions:

To compare the results between the modulated signal and the non-modulated the total number of impacts is a parameter to take into account. In most cases the final number of impacts are quite similar except in the case of applying an amplitude of 30 Volts. For this particular case to apply a BPSK modulation reduces the number of impacts on the device walls. This is probably due to phase change affects more the trajectory of the electron. Also, a curious aspect to consider is that independently the rest of conditions, if $T_s = T$ multipactor discharge does not occur. In the most part of cases, this fast phase change affects the electron changing its trajectory and therefore it does not time to impact against the plates with sufficient energy to generate new electrons. This last case is showed in Figure 30 (in red circles the electron has not acquired enough energy). The main issue is that in real cases are significant limitations to implement symbol periods as minimum as these ones.

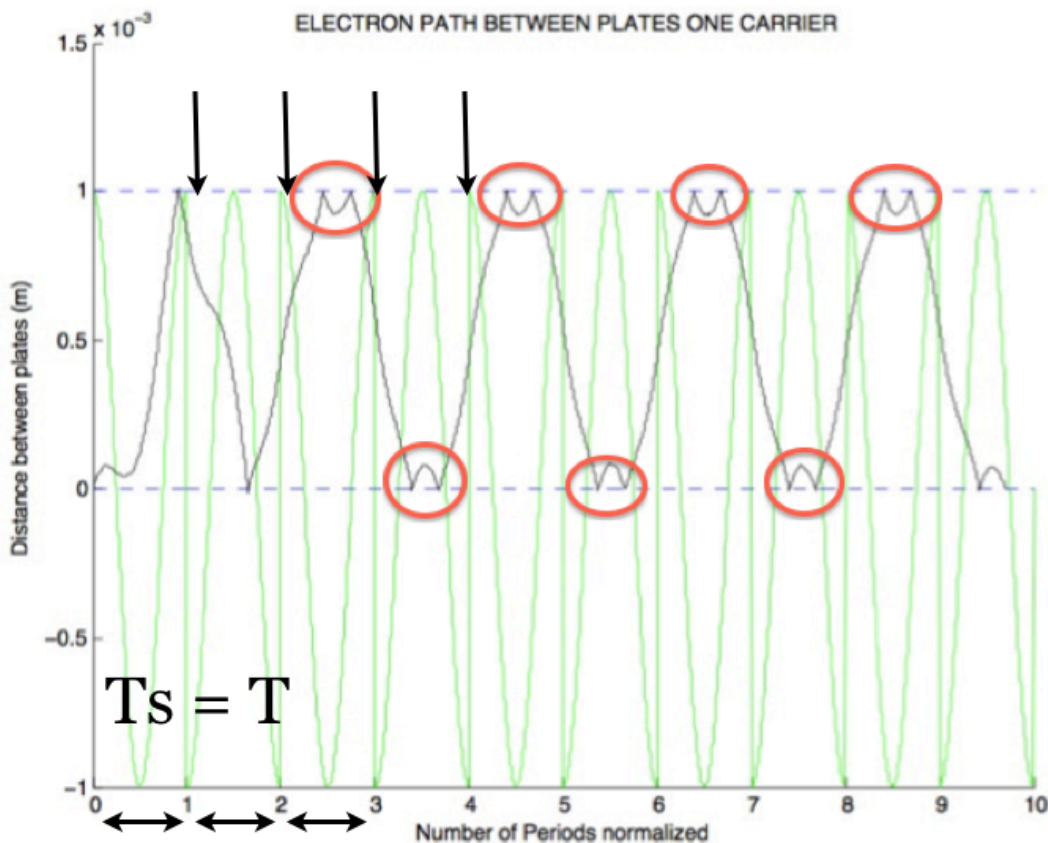


Fig 30. BPSK modulated signal with $T_s = T$

Simulations considering $f_{xd} = 0.859$ GHzmm and a non-modulated signal

Considering the possibility of a test-bed to 435 MHz (P-Band), the following tables show theoretically the presence or absence of multipactor. In this case, the material between plates is cooper (with SEY characteristics, Figure 31: $E_1 = 19.5$ eV, $E_{max} = 219.7$ eV, $\delta_{max} = 2.61$). It is clearly that the results will be completely different applying a SEY curve or another. In this case, the minimum energy value to consider is $E_{min} = 4.78$ so multipactor threshold is lower than in the case of using the SEY curve of the silver (A_{g3A}).

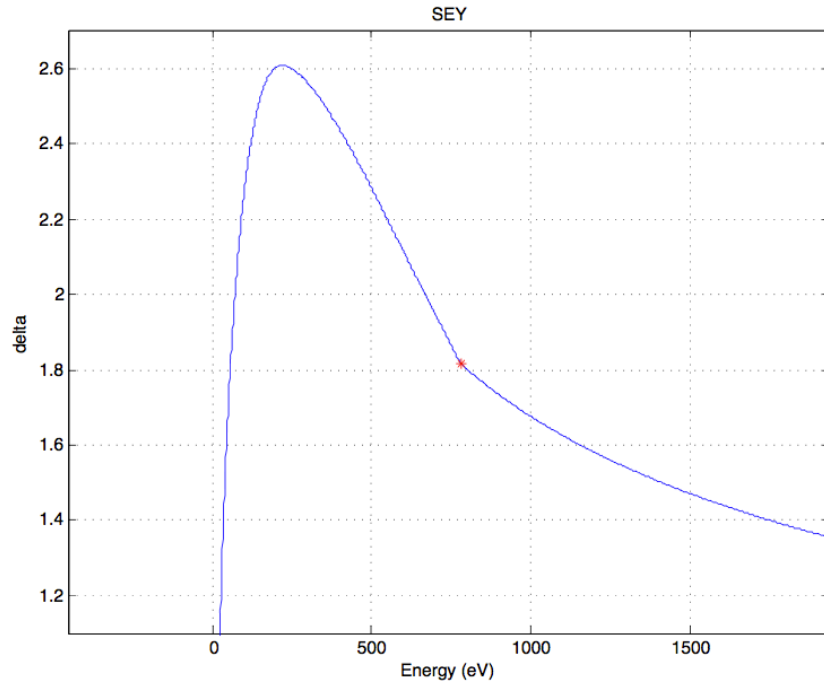


Fig. 31 Cooper SEY Curve

Freq (MHz)	Amplitude (Volts)	MP	n°impacts
435	30	1	399

Table 6.1

Freq (MHz)	Amplitude (Volts)	MP	n°impacts
435	40	1	398

Table 6.2

Freq (MHz)	Amplitude (Volts)	MP	n°impacts
435	50	1	399

Table 6.3

Freq (MHz)	Amplitude (Volts)	MP	n°impacts
435	100	1	794

Table 6.4

Simulations considering fxd = 0.859 GHzmm and a BPSK modulated signal

Simulation with Cooper SEY:

Freq (MHz)	Amplitude (Volts)	Ts= n*T (n)	MP	mean (n°impacts)
435	30	1	0	246
435	30	2	1	398
435	30	3	1	395
435	30	5	1	399
435	30	7	1	391
435	30	10	1	399

Table 7.1a)

Simulation with A_{g3A} SEY:

Freq (MHz)	Amplitude (Volts)	Ts= n*T (n)	MP	mean (n°impacts)
435	30	1	0	246
435	30	2	0	398
435	30	3	0	395
435	30	5	0	399
435	30	7	0	391
435	30	10	0	399

Table 7.1b)

The main objective to do this both simulations (Table 7.1a and Table 7.1b) using different material between plates is to confirm how the multipactor threshold using copper is less than using silver. The difference is produced by the delta value (due to different SEY curve). For this simulation using copper and an amplitude of 30 Volts, multipactor discharge has occurred, so for greater amplitude values multipactor effect will also be present in all the cases except when $T_s = T$ for the above explanation.

Freq (MHz)	Amplitude (Volts)	Ts= n*T (n)	MP	mean (n°impacts)
435	40	1	0	399
435	40	2	1	398
435	40	3	1	394
435	40	5	1	398
435	40	7	1	390
435	40	10	1	398

Table 7.2

Freq (MHz)	Amplitude (Volts)	Ts= n*T (n)	MP	mean (n°impacts)
435	50	1	0	399
435	50	2	1	399
435	50	3	1	395
435	50	5	1	399
435	50	7	1	391
435	50	10	1	399

Table 7.3

Freq (MHz)	Amplitude (Volts)	Ts= n*T (n)	MP	mean (n°impacts)
435	100	1	0	460
435	100	2	1	597
435	100	3	1	655
435	100	5	1	713
435	100	7	1	721
435	100	10	1	753

Table 7.4

Pulse Shaping, PAPR and CCDF in the software. Theory

In all previous examples, the baseband symbols are represented with any type of filter. Now, it is time to consider the influence of applying square pulses with amplitudes of ± 1 and widths of T . It is very common to think the baseband symbols as weighted impulses to which we apply a pulse shape. The top graph of Fig. 31 shows a baseband information sequence consisting of weighted impulses. The middle graph shows this same signal after applying a rectangular pulse shape to the impulses. The bottom graph in the figure shows the signal if we filter the impulses with a raised-cosine pulse shaping filter.

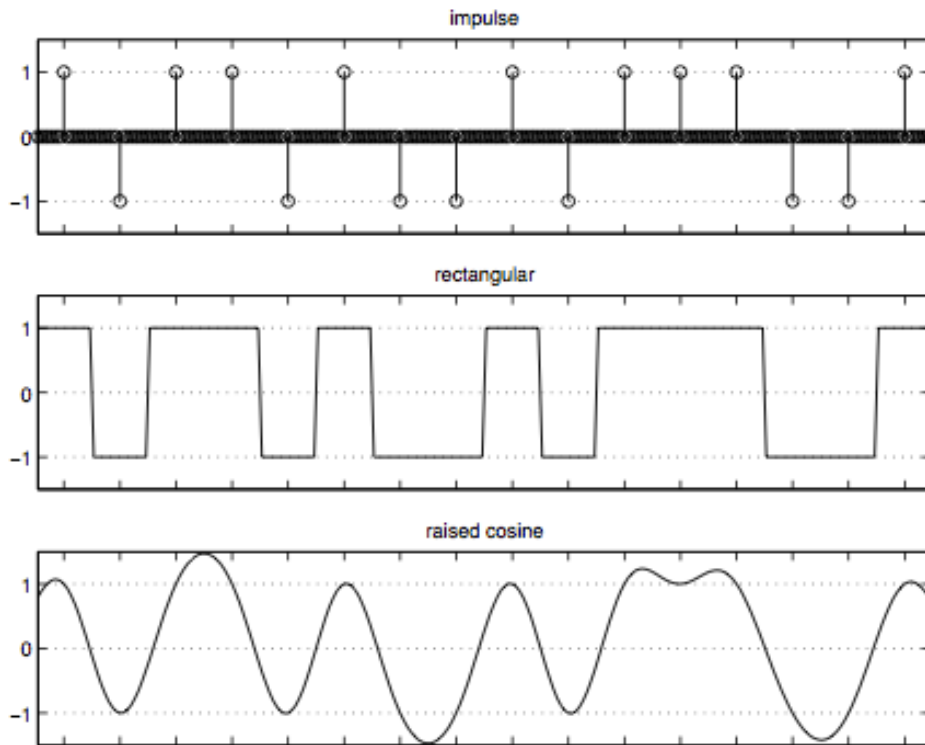


Figure 31. Baseband Pulse Shaping

The difference between the rectangular and raised-cosine pulse shapes is very easy to see in these time domain signals. The smoother transitions of the raised-cosine pulse result in a signal that uses less bandwidth than those of the rectangular pulse. The trace near the top of Figure 32 is the spectrum of the rectangular pulses, while the solid trace in the bottom is the spectrum of the raised-cosine shaped pulses.

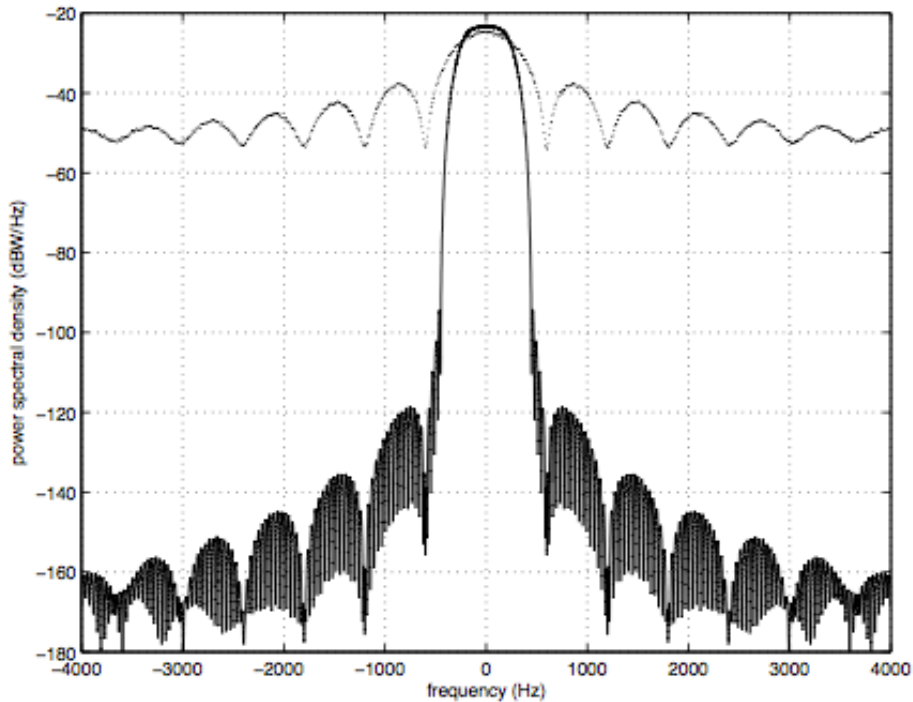


Fig 32 Comparison between spectrums

In digital communication systems is very common to use root-raised-cosine filter (RRC). In addition, in signal processing square-root-raised-cosine filter (SRRC) is further used in the transmission and reception in digital communication systems to perform matched filtering. It obtains its name from the fact that its frequency response is the square root of the frequency response of the raised-cosine filter. SRRC is a filter frequently used for pulse-shaping in digital modulation due to its ability to minimise intersymbol interference (ISI). The root-raised-cosine filter allows us to choose the amount of ‘excess’ bandwidth as one of our design parameters. The excess bandwidth, also known as the ‘roll-off’ factor, controls the smoothness of the pulse shape and determines the signal bandwidth. For a PSK signal:

$$B = f_{sym} \cdot (1 + \alpha)$$

f_{sym} is the symbol rate, and α (sometimes called β) is the filter roll-off factor.

In the improved version of Multipactor Software we consider the possibility of applying different types of filter to the modulated signal. We want to study the their effects (advantages and disadvantages) in the transmission of digital signals. The most common filters considered are squared filter and pulse shaping filters (commonly used SRRC).

To make the bandwith as small as possible, it is necessary to take a roll-off value as small as possible. As the amount of lowpass filtering applied to the signal increases, the symbol transistions become so smooth that they are impossible to identify (reasonable filter roll-off factors are from 0.25 to 0.5).

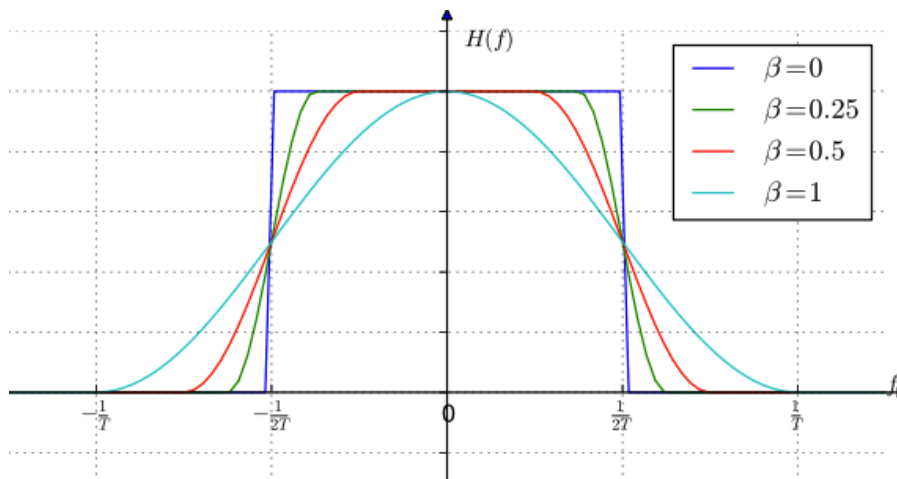


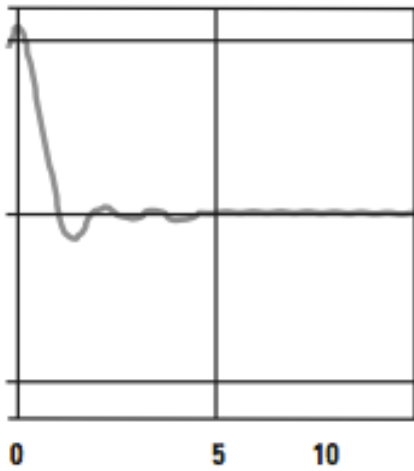
Fig. 33 Frequency response of raised-cosine filter with roll-off factors.

For example, for unfiltered signals the symbols are rectangular pulses, and the transitions between symbols are instantaneous. However, when a pulse shaping filter is applied to the symbols, the envelope is no longer constant. Since it was explained in Section 4.1 (Fig. 18) when the symbols have been filtered, the transitions are no longer instantaneous, and the signal can take on any value shown in the transition diagram. Note that the exact shape of the transition between symbols is determined by the roll-off factor as well as the number of samples per symbol (important parameters to take into account). Remember that in Figure 19 the envelope of the signal were not constant, because it illustrates the phase transitions between symbols. Taking into account all these theoretical aspects is easy to understand because PAPR value is nonzero when a pulse shaping filter is applied to the signal.

Also, it is quickly verified that certain types of modulation are capable of transmitting more bits per state than others for a given symbol rate (for example the bit rate of a 16QAM signal is twice that of a QPSK signal for a given symbol rate) and it also produces greater peak-to-average ratios than does QPSK.

The filtering parameters for a particular modulation format can significantly affect the PAPR of the signal. Although low-alpha (low α) filters require less bandwidth than high-alpha filters, they have a longer response time and more severe ringing (Figure 34). This time-domain ringing results in the addition of more symbols, which causes higher peak-power events.

High-alpha root-raised-cosine filter



Low-alpha root-raised-cosine filter

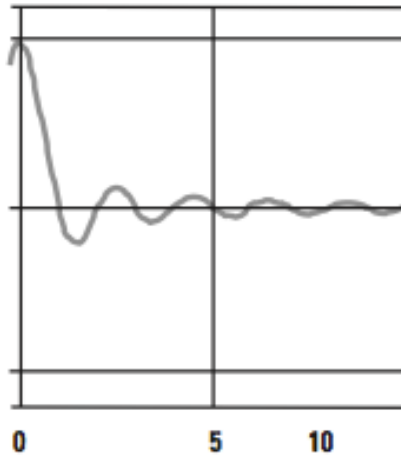


Fig. 34 Impulse response of a high-alpha and low-alpha filter

Reference [9] shows that PAPR depends on the bandwidth efficiency regardless of the modulation structure. In addition, it makes a definition for “bandwidth efficiency” and explains when roll-off factor decreases the bandwidth efficiency increases. They consider that roll-off factor plays just the role of “mediator” between the PAPR and the bandwidth efficiency because when the bandwidth efficiency increases the PAPR also increases.

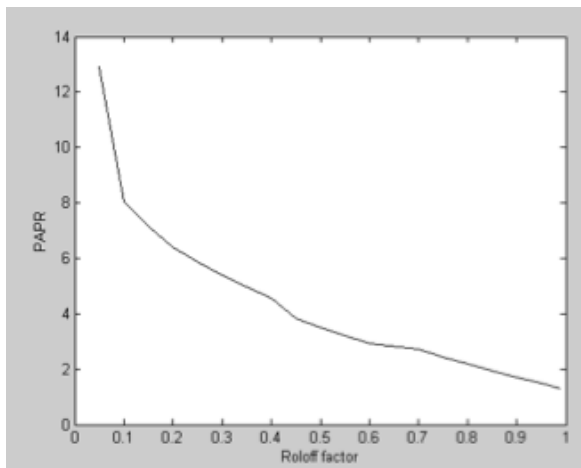


Fig. 35 PAPR as a function of roll-off factor in SC

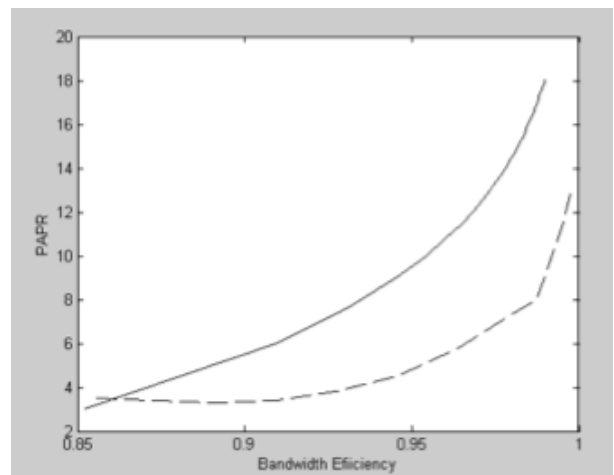


Fig. 36 PAPR as a function of bandwidth efficiency

In the same context, Figure 37c shows the CCDF plots of QPSK signals with different filtering factors. Also shown (Figures 37a and 37b) are the vector diagrams of the two signals. The magnitude of the time-trace vector plot squared would represent the power of the signals. Signal A clearly looks more spread out in the vector plot due to the lower filter

alpha. The CCDF plot confirms that the low-alpha filter produces higher peak-power events than the high-alpha filter. However, as mentioned above, high-alpha filters also require a larger bandwidth.

The CCDF curve can be used to troubleshoot signals. Higher or lower CCDF curves give an indication of the filtering present on the signal. An incorrect curve could identify incorrectly coded baseband signals.

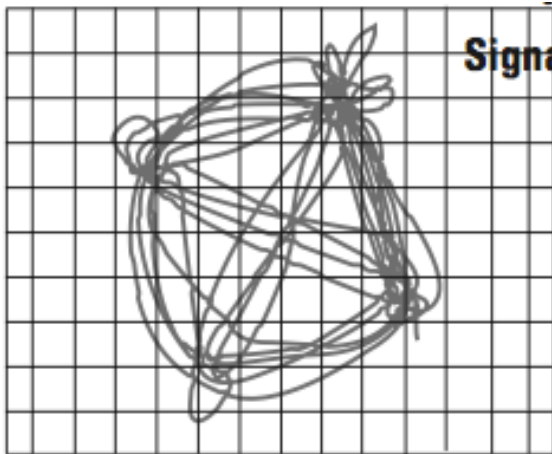


Fig. 37a

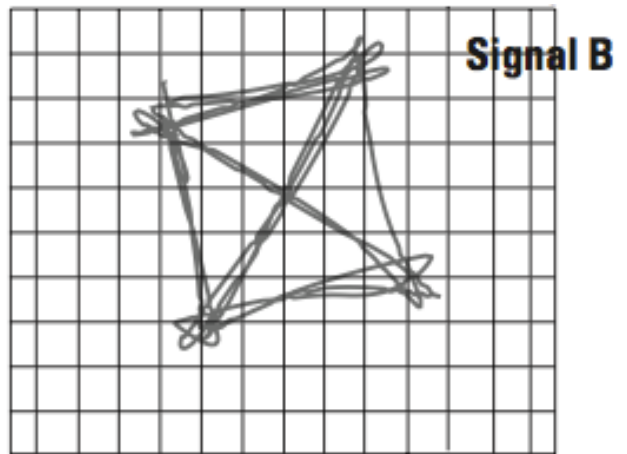
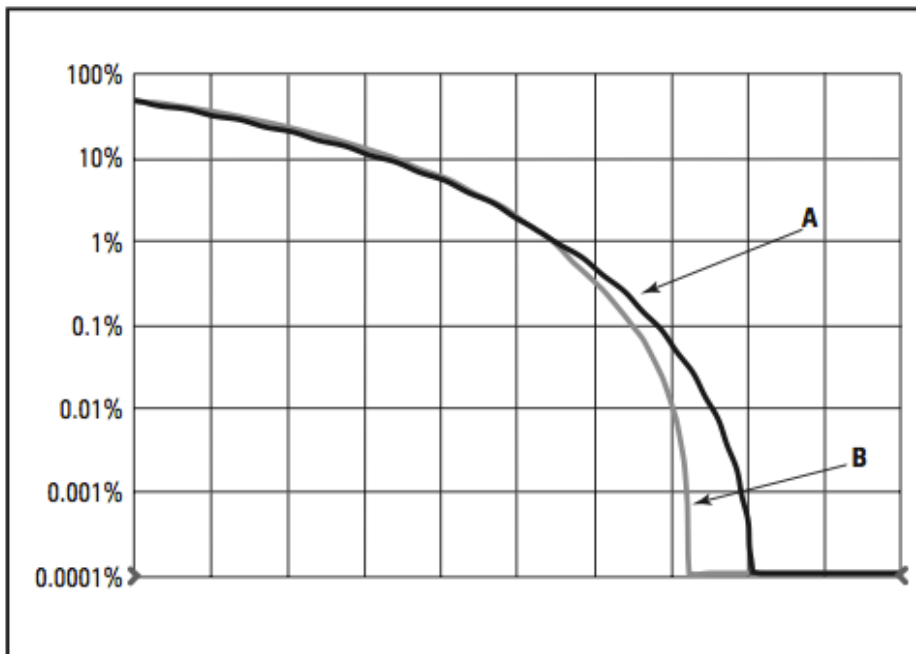


Fig. 37b



Signal A:

Root-raised-cosine filter with $\alpha = 0.22$

Signal B:

Root-raised-cosine filter with $\alpha = 0.75$

Fig. 37c

Fig. 37 CCDF curve and vector plots of high-alpha filter and low-alpha filter.

Thus, there is a need to produce spectrally efficient modulation formats which also have a low PAPR.

Multipactor Software. Modulation Filtering

In order to reduce the PAPR without degrading the system performance it is important to consider the influence of the pulse shaping filter in the modulated signal. Firstly, it is shown how to create a root-raised-cosine filter using the available Matlab toolbox. Then, the objective is to apply these filtered signals between the plates to study the effect on the trajectory of the electron.

As in previous section, the main parameter of a raised cosine filter is its roll-off factor, β , which indirectly specifies the bandwidth of the filter. The ways to code a raised cosine filter in Matlab are several, then the most intuitive one is considered here. Raised cosine filters are used for pulse shaping, where the signal is upsampled. To design a direct-form FIR filter it is necessary to define some specifications as an order for the filter. Always the filter-order + 1 represents the number of taps in the filter transfer function.

Considering a random sequence composed by ones and zeros, in next figure (Fig. 38) is easy to see how the raised cosine filter upsamples and filters the signal. The filtered signal is identical to the delayed input signal at the input sample times. This demonstrates the raised cosine filter capability to band-limit the signal while avoiding ISI.

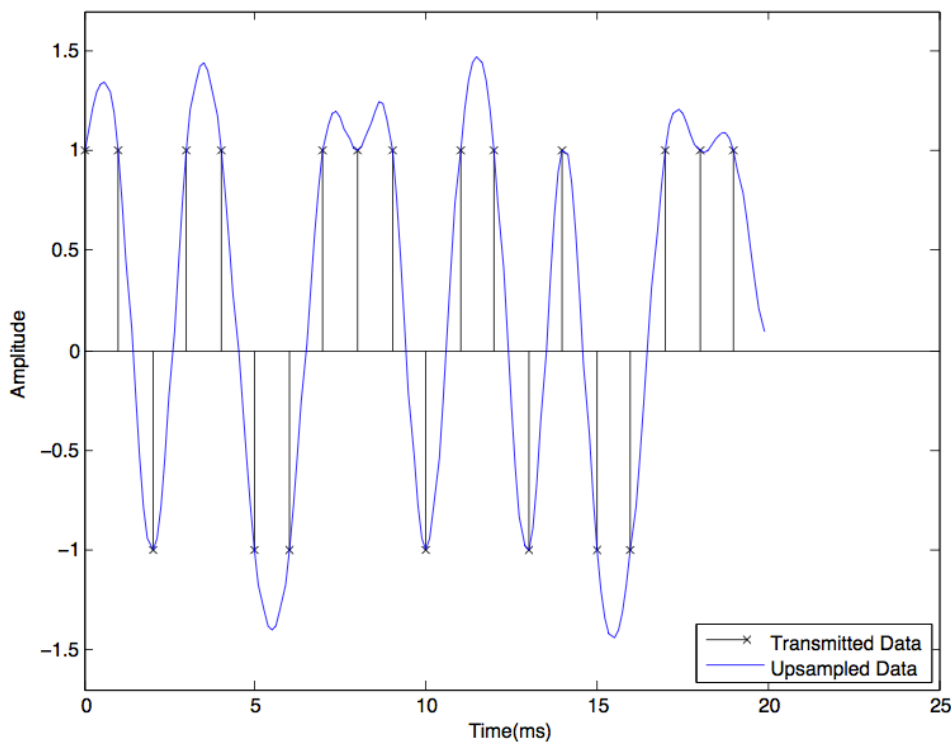


Fig. 38 Pulse Shaping with Raised Cosine Filter

Next figure (Fig. 39) tries to show the effect that changing the roll-off factor from 0.5 (blue curve) to 0.2 (red curve) has on the resulting filtered output. The lower value for roll-off causes the filter to have a narrower transition band causing the filtered signal overshoot to be greater for the red curve than for the blue curve.

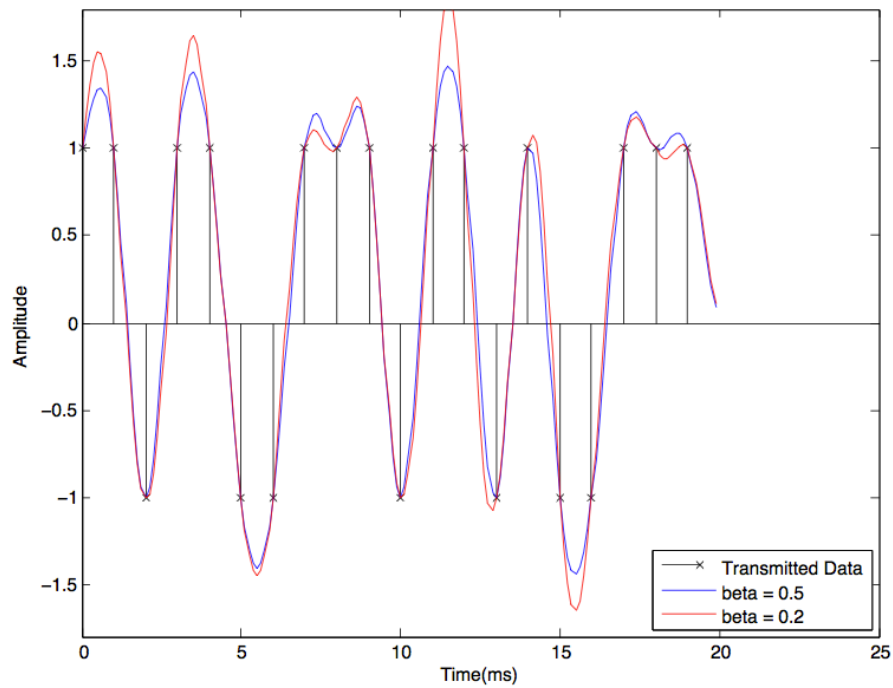


Fig. 39a Roll-off factor influence

To show better this influence, the roll-off will be taken in the extremes values, zero and one.

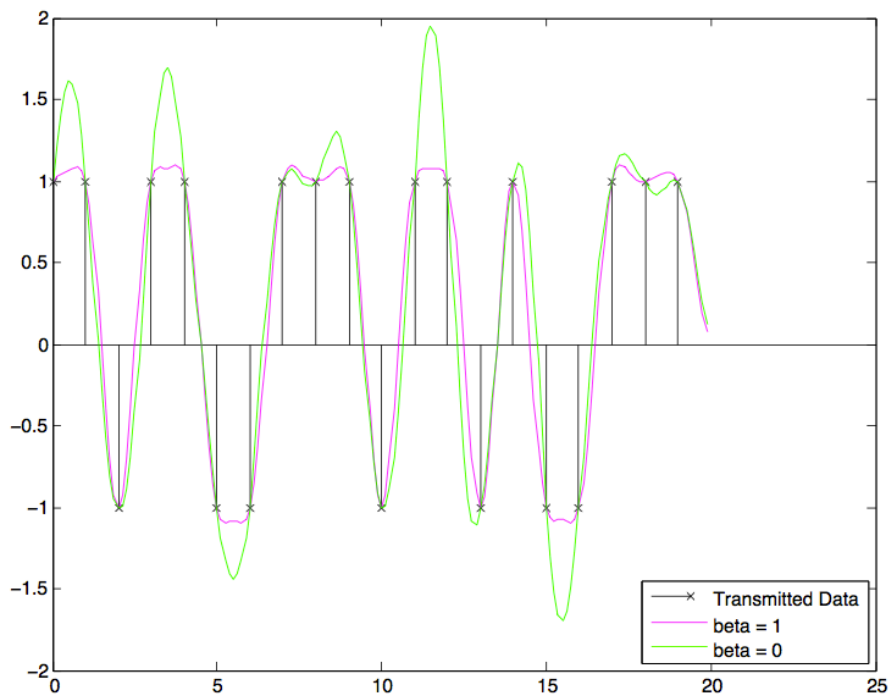


Fig. 39b Roll-off factor influence

Note that with the roll-off factor it is possible control the smoothness of the pulse shape and to determinate the signal bandwidth. According to the graph (Fig. 39) and taking a roll-off of zero, we are taking the symbol bandwidth as small as possible and this let us to confirm the theory in paper [9] about “when roll-off factor decreases the bandwidth efficiency increases. At the same time, it is clearly shown that when roll-off tends to zero PAPR tends to increase. Thus, for a particular roll-off factor the bandwidth and the PAPR tends to increase or decrease at the same time. So, it is very important to choose a roll-off factor which mediate between these two characteristic signal parameters.

In next simulations, (prior to include these effect in the Multipactor software) , a Matlab function with the name of “parameters” analyse the influence of applying a square filter, or a pulse-shaping one to the signal. Also it is possible to compare these influence in PAPR values.

Example 4

Comparison modulated and non-modulated signal with any filter.

Input Parameters:

Amplitude of the field, **Amp = 30 Volts**

Frequency, $f = 1$ GHz

Number of Symbols, $N_{sym} = 5$

Symbol Period ($T_s = n \times T$) -> $n = 2$

The sequence considered in the modulation format is next one: [1 0 1 0 1]

Non-Modulated Signal:

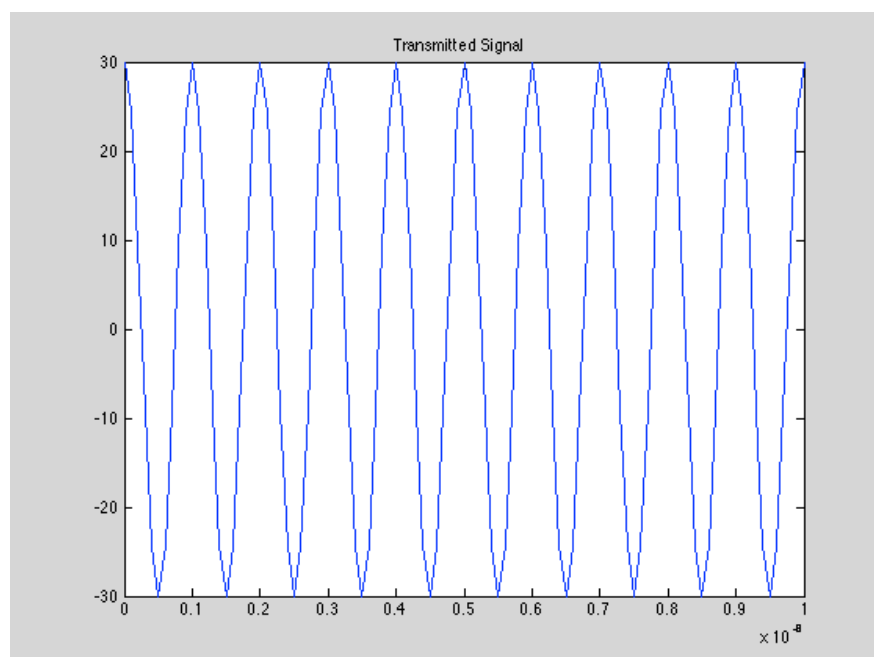


Fig 40a. Non-modulated signal without any filter

	peakpower	avgpower
W	900	454.4554
dB	29.5424	26.5749

PAPR = 2.9675 dB

BPSK Modulated Signal:

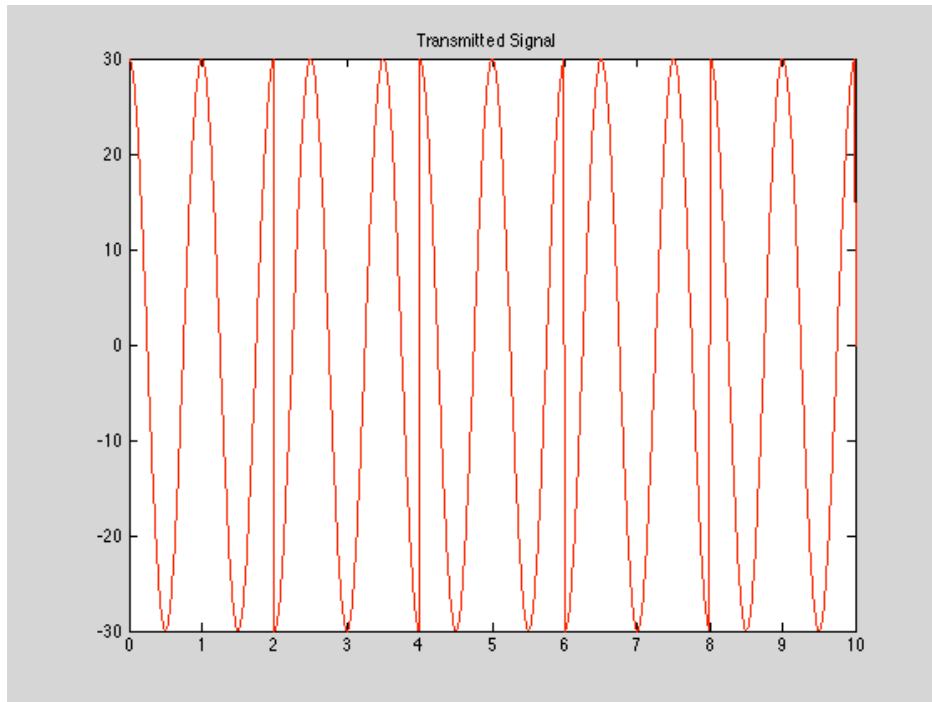


Fig 40b. BPSK modulated signal without any filter

	peakpower	avgpower
W	900	450.2260
dB	29.5424	26.5343

PAPR = 3.0081 dB

Figures 40a and 40b show the different signals considered. PAPR applying a BPSK modulation (without amplitude changes) does not change this parameter.

	Non-modulated signal	BPSK modulated signal
PAPR (dB)	2.9675	3.0081

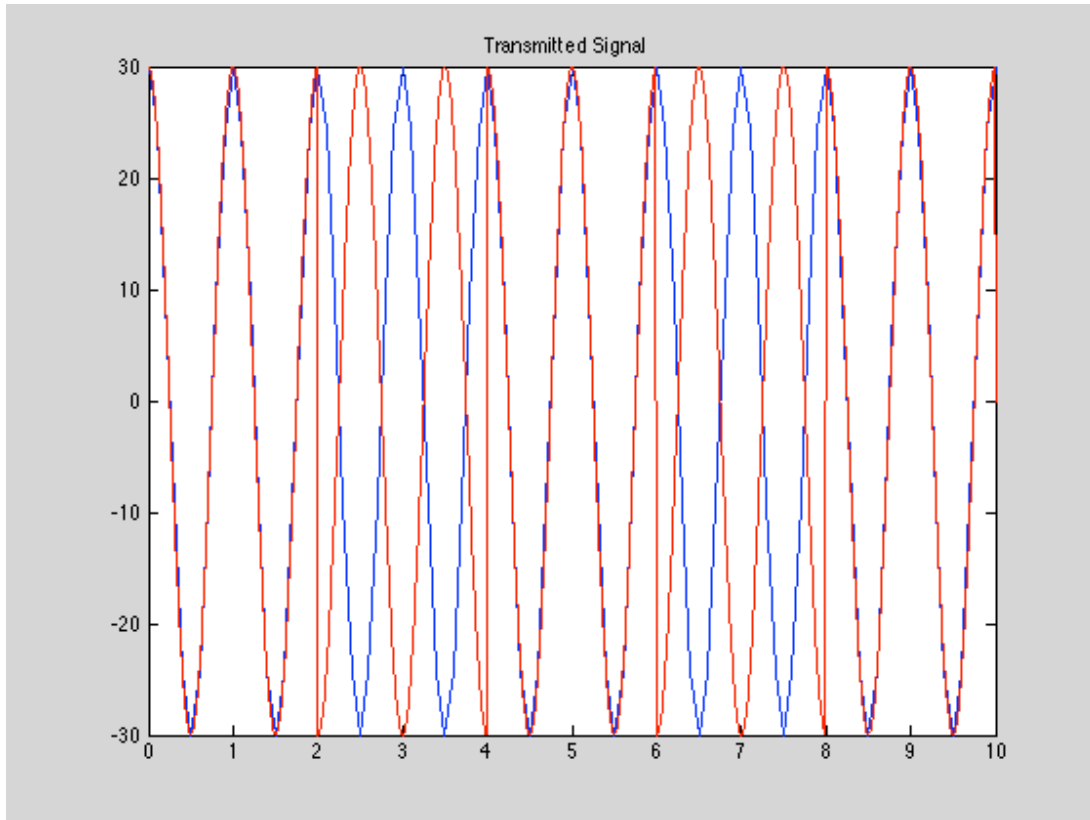


Fig. 40c Both figures (40a and 40b) together

In the above figure (Fig. 40c) no amplitude changes are represented because of applying a BPSK modulation.

Example 5

Comparison BPSK modulated signal with square and SRRC filter.

In all the examples applying different types of filter the number of samples per symbol to filter the signal is 4.

BPSK Modulated Signal with Square Filter:

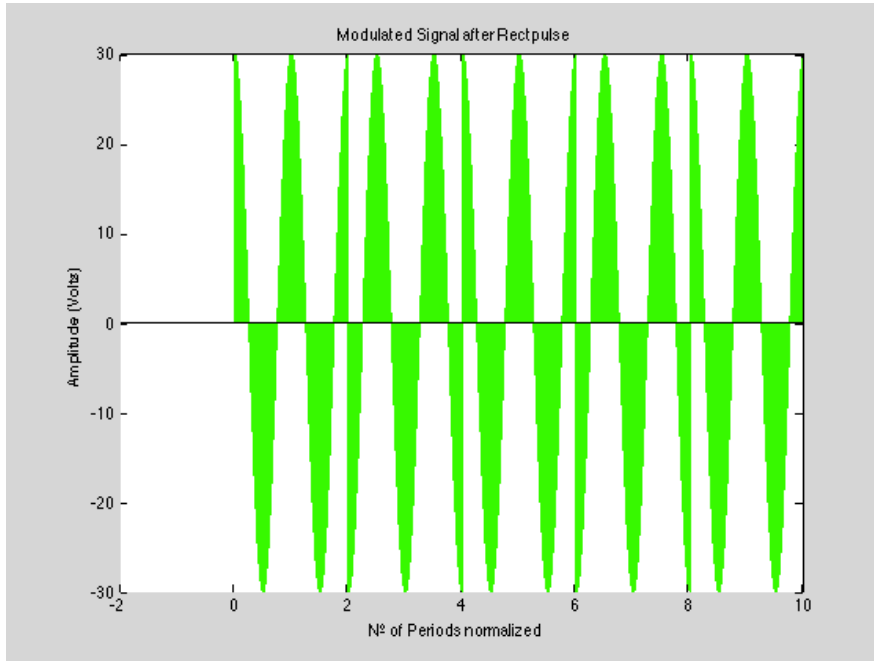


Fig. 41a BPSK with Square Filtering

	peakpower	avgpower
W	900	450.0000
dB	29.5424	26.5321

PAPR = 3.0103 dB

BPSK Modulated Signal with Pulse Shaping Filter:

The filter applied is a SRRC filter with a roll-off factor = 0.5

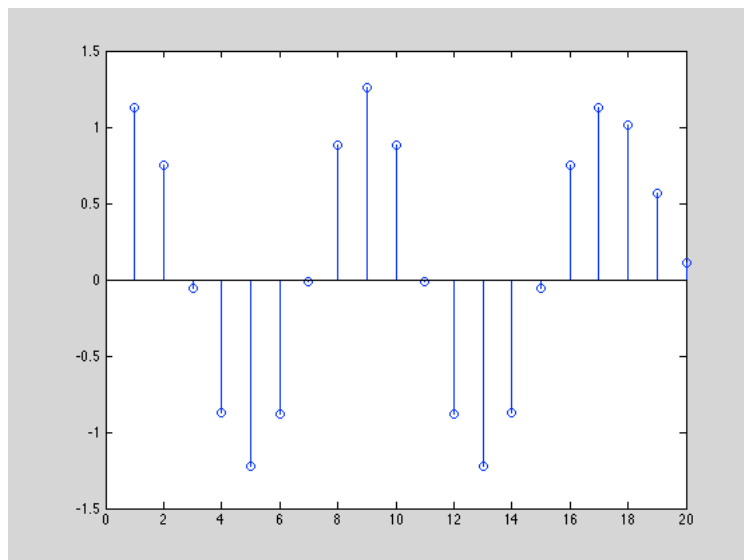


Fig. 41b SRRC with roll-off = 0.5

Figure 41b represents 5 symbols transmitted and every one takes 4 samples per symbol, the total number of samples is $4 \times 5 = 20$.

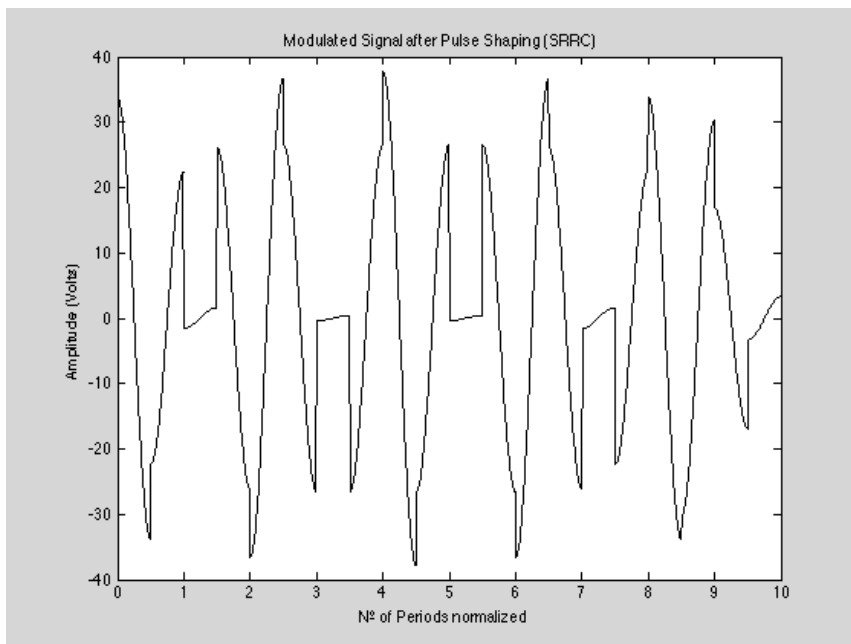


Fig. 41c BPSK with Pulse Shaping Filtering

	peakpower	avgpower
W	1.4320e+03	321.1765
dB	31.5593	25.0674

PAPR = 6.4919 dB

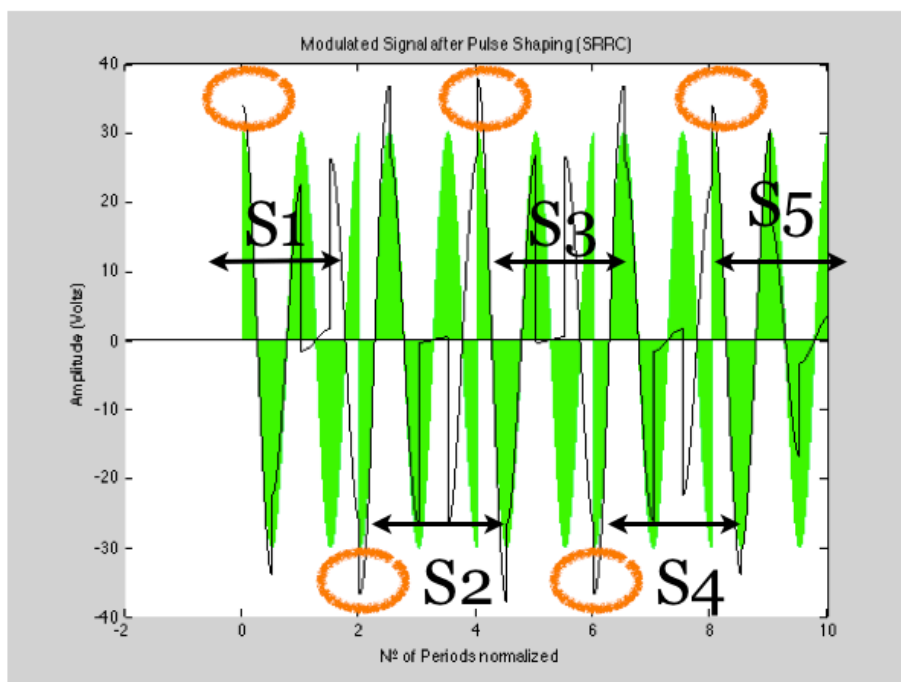


Fig. 41d
Both figures
(41a and
41c)
together

PAPR Rectpulse (dB)	PAPR SRRC (dB)
3.0103	6.4919

Clearly, when a pulse shaping like SRRC is applied to the signal the transitions followed between symbols are totally different as Fig. 41 shows. However, the most important to consider when this type of filter is used is that when every symbol starts the signal value at this exact instant is just the symbol which represents. In figure 41d is possible to check that when a symbol changes its phase because the new one is different (transitions from 1 to 0 for example) the envelope of the signal takes the extreme value (positive or negative depending on the symbol). The trajectory between symbols does not care us excepting for their influence in the PAPR value. Note that extremely high peak power levels may be attained, thus increasing the risk of a multipactor discharge.

Example 6

BPSK modulated signal with different roll-off in SRRC filter.

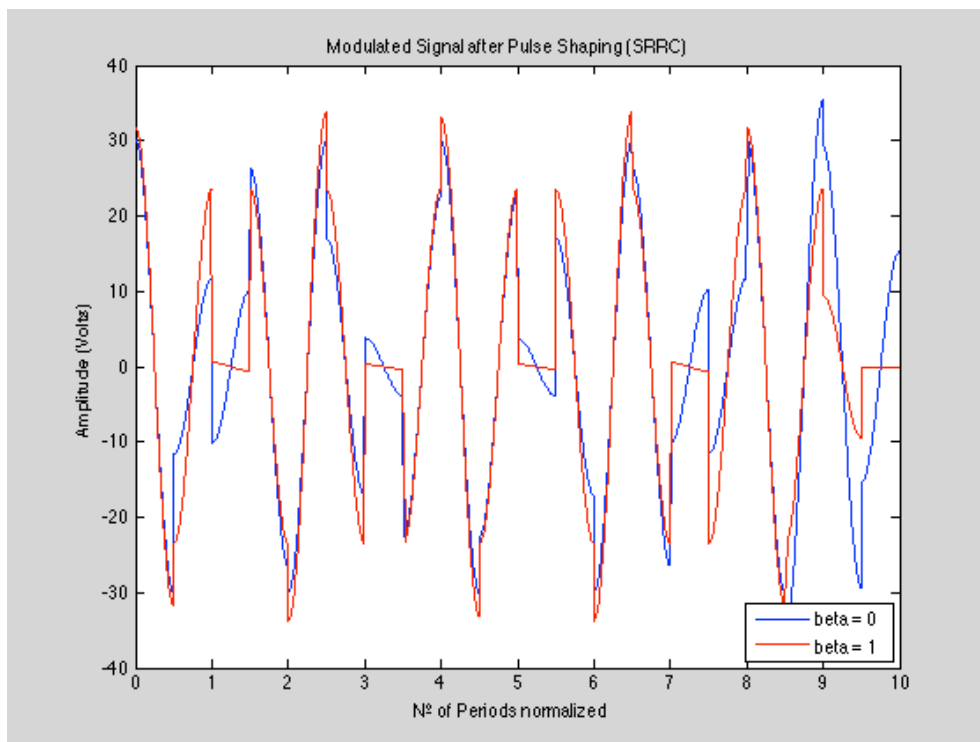


Fig. 41 Extreme Roll-off factors

PAPR using a SRRC filter with roll-off = 0:

	peakpower	avgpower
W	1.2540e+03	259.5264
dB	30.9831	24.1418

PAPR using a SRRC filter with roll-off = 1:

	peakpower	avgpower
W	1.1380e+03	262.3477
dB	30.5613	24.1888

Comparison:

PAPR roll-off = 0	PAPR roll-off = 1
6.8413	6.3725

Conclusion

The above examples try to check the theory in [9]. Analysis of the results shown in this section lead to the conclusion that the PAPR increases as the roll-off factor decreases.

The graphics presented in this section should guide to select a proper-pulse shaping filter with appropriate roll-off factor for a particular type of modulation format. Just particular examples have been shown to present the influence of PAPR in modulated signal, but these examples can be generalized using different modulation schemes.

Currently, as in next sections will be presented, the key idea is to introduce all these functions in the Multipactor Software to find out what is the possible influence in the multipactor threshold.

|5 **PRESENT RESULTS**

Finally, after having conducted an intensive analysis of the influence that the modulated signals have in the initiation of multipactor, now, we have considered to finish the work addressing the issue from a different perspective. The main objective in this section is to calculate the minimum necessary voltage to produce a multipactor discharge.

Three different aspects explained in previous sections are again taken into account:

- Single carrier (non-modulated signal)
- Modulated Signals with a square filter
- Modulated Signals with a SRRC filter

The purpose of this work is to compare which is in every context the minimum voltage to predict a discharge considering different symbol periods on the modulated signals comparing the obtained results between them and with the non-modulated signal.

In an improved final version of the software, trying to apply these different types of filters we realise an important issue explained in the next section ‘Convergence Study’ to consider in the multipactor predictions. So, previously to apply the filters and analyse the results it is time to explain the trouble found and currently satisfactorily solved.

Convergence Study

In the last Multipactor software developed version considering modulated signals it is being studied the convergence of the numerical methods used to calculate the exact position and time instant in which the electron reaches one of the device walls. The cause to start this section-work is that for particular cases, numerical methods do not present the same exact results and it is very important to study why this behaviour happens to ensure that the prediction is correct.

Several simulations shown below have concluded that the main factor that produces these not equals results can be observed when different tolerances are used. The tolerance is the time step order between two times values during a simulation. In next examples, three different steps/tolerances are considered and represented with different colours as the legend shows ($\Delta t = 1 \cdot 10^{-10}, 1 \cdot 10^{-11}, 1 \cdot 10^{-12}$).

Simulation a) and b) represent the trajectory followed by an electron between plates considering a signal like a BPSK modulated one between the plates. The numerical method used in these simulations is ode45, an adaptive method from Matlab explained in section 3.2.2 Software Development. This time we have used ode45 to solve the equation in theses represented simulations, but it is important to understand that the algorithms used in the ode solvers vary according to order of accuracy and the type of systems (stiff or nonstiff) they are designed to solve.

Simulation a)

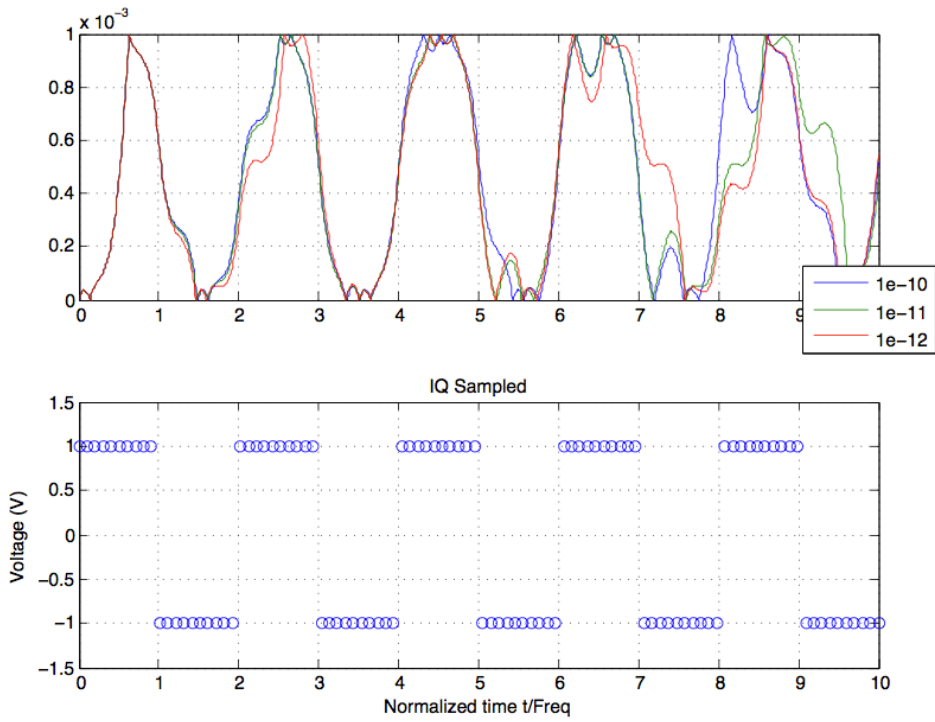


Fig. 42 Simulation using abrupt transitions between symbols

Simulation b)

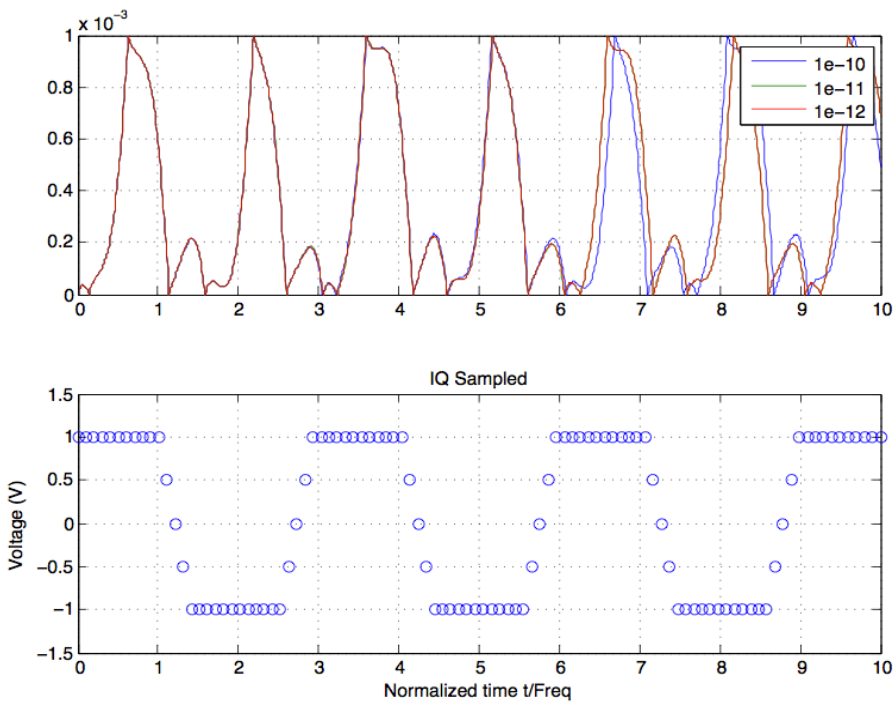


Fig. 43 Simulation using smooth transitions between symbols

In figure 42 is very easy to observe that the trajectory is not the same using different steps in the vector time. In this examples only ten RF time periods have shown, but for instance, in 'real' simulations the simulations will have an order of hundred RF time periods.

Very different is the graph shown in figure 43 where the transition from one symbol to the new one is not immediate. Five points are considered in the middle of the transitions and this makes possible that the numerical method is adapted to the new circumstances in a better way. This time, the change between phases is not so abrupt and therefore the electron trajectory is easier to control and predict accurately. Now, the transitions between symbols are not as abrupt as in simulation a) and it is possible to check that the difference using several tolerances is not as different as in the previous simulation.

These results lead us to think that if we use more points for moving from one state to another (a symbol transition between 0 and 1, or from 1 to 0) to predict the trajectory of an electron is more reliable. Therefore, it is possible to think that if we apply the above explained pulse shaping filter to make smoother transitions between symbols, the accurate results and numerical methods behave will become more stably providing us security in predicting multipactor.

When a filter is applied to the simulation, a given number of samples (normally 4 or 8, per symbol) are used to upsample the signal. The idea is to interpolate the abrupt transitions between symbols from a straight line equation that considers two known points. The interpolation performed is very easy and is shown in the following equation:

$$y = ax + b$$

$$a = \frac{y_2 - y_1}{x_2 - x_1}$$

$$b = y_1 - \frac{y_2 - y_1}{x_1 - x_2} x_1$$

being, (x_1, y_1) and (x_2, y_2) two known points on the line.

5.1 Non-Modulated Signal

Conditions:

Frequency, $f = 435$ MHz


Distance between plates, $d = 1.9747$ mm

Electron initial velocity, $v_0 = 3.68$ eV

Material between plates: $A_{g3}A$ ($E_1 = 30$ eV, $E_2 = 5000$ eV, $E_{max} = 165$ eV, $\delta_{max} = 2.22$)

Number of initial electrons introduced = 120

Max. Time = $100Trf$



$$fxd = 0.859 \text{ GHzmm}$$

According to the simulated conditions and applying the new detection algorithm, the minimum voltage required to start the multipactor discharge is about **40 Volt**.

In the figure it has been only shown 10 periods of the RF signal, however all the simulations done in this sections have a maximum simulation time of hundred time periods of the RF signal. In this case, $Trf = 1/f = 1/435MHz = 2.3 \text{ nsec}$.

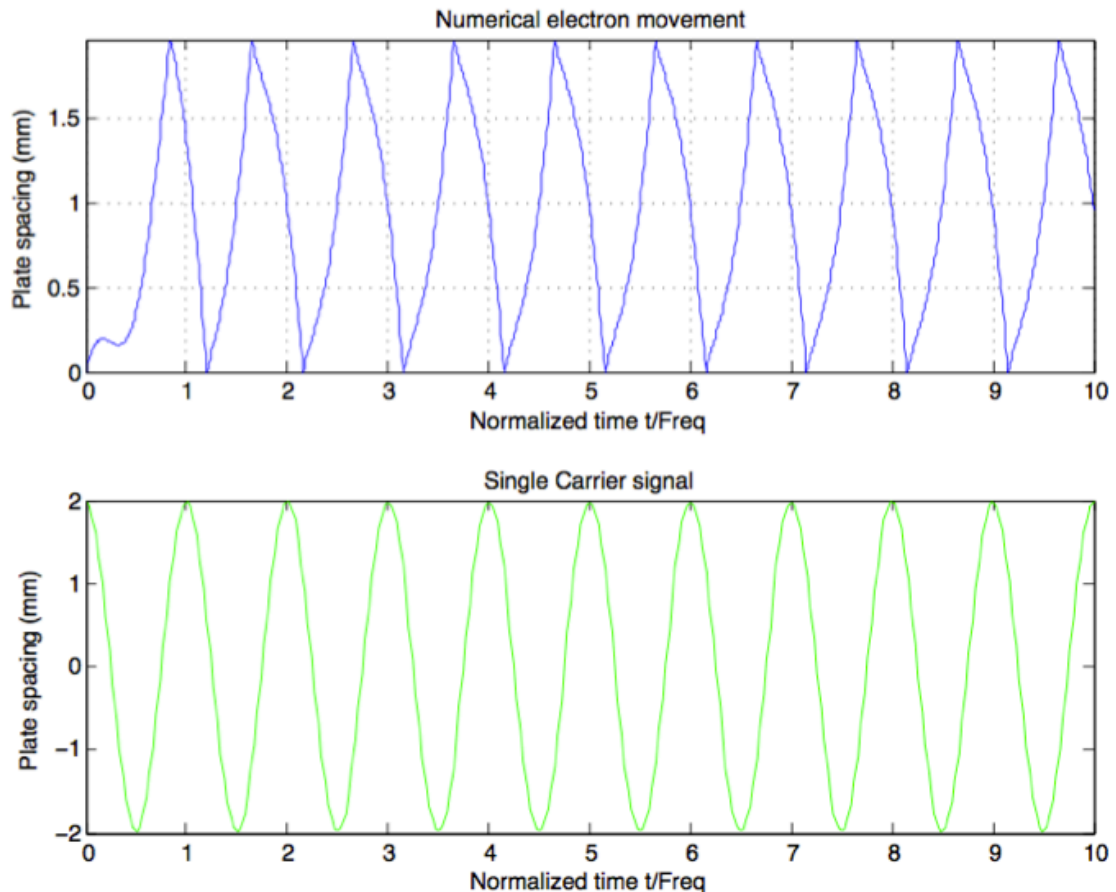


Fig. 44 Simulation using a non-modulated signal with Voltage = 39.75 Volt

5.2 BPSK-Modulated Signal with RECTPULSE FILTER

Frequency, $f = 435 \text{ MHz}$

Distance between plates, $d = 1.9747 \text{ mm}$

Electron initial velocity, $v_0 = 3.68 \text{ eV}$

Material between plates: A_{g3A} ($E_1 = 30 \text{ eV}$, $E_2 = 5000 \text{ eV}$, $E_{max} = 165 \text{ eV}$, $\delta_{max} = 2.22$)

Number of initial electrons introduced = 120

Symbol Period ($T_s = n \times T$), $n = [1 \ 2 \ 3 \ 4 \ 5 \ 6 \ 7 \ 8 \ 9 \ 10 \ 20 \ 30 \ 40 \ 50 \ 60 \ 70 \ 80 \ 90 \ 100]$

Max. Time = $100Trf$

To analyse the results, we have simulated this case using two different sequences. The first one composed only by ones [1 1 1 1...] where therefore, there is not phase changes because all the time the symbols sent are the same. In this case the behaviour must be the same (or very similar, because the filter could introduce some different characteristic in the exact simulation) as non-modulated signal was simulated.

Case 1: Seq [1 1 1 ... 1 1 1]

Tsym	minVolt
1 Trf	40.0469
2 Trf	40.0469
3 Trf	40.0469
4 Trf	40.0469
5 Trf	40.0469
6 Trf	40.0469
7 Trf	40.0469
8 Trf	40.0469
9 Trf	40.0469
10 Trf	40.0469

Tsym	minVolt
20 Trf	40.0469
30 Trf	40.0469
40 Trf	40.0469
50 Trf	40.0469
60 Trf	40.0469
70 Trf	40.0469
80 Trf	40.0469
90 Trf	40.0469
100 Trf	40.0469

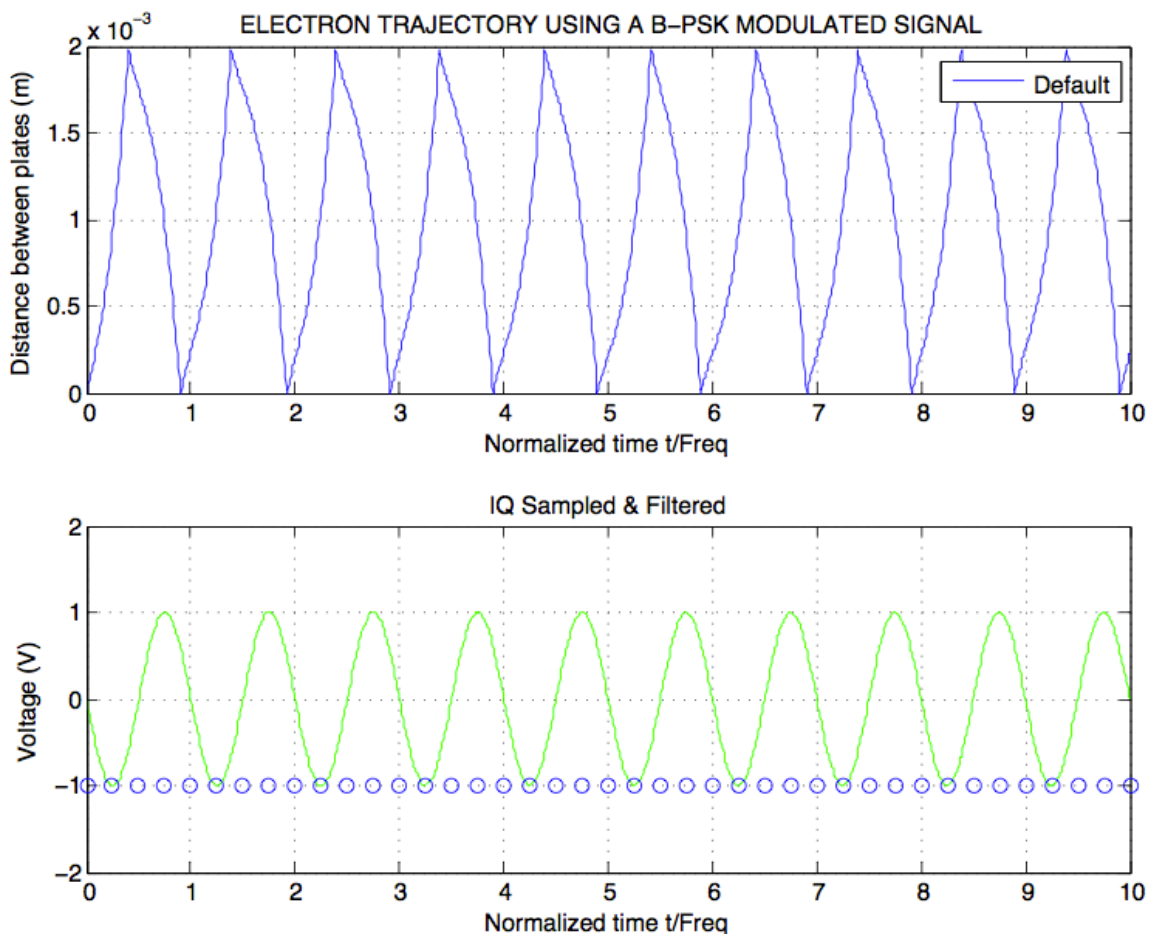


Fig. 45 Simulation using a BPSK-modulated signal with a square filter and Voltage = 40 Volt

Case 2: Seq [1 0 1 0 ... 1 0 1]

Tsym	minVolt
1 Trf	36.7930
2 Trf	62.3594
3 Trf	39.1172
4 Trf	39.1172
5 Trf	47.0195
6 Trf	44.6953
7 Trf	44.6953
8 Trf	42.8359
9 Trf	39.5820
10 Trf	39.5820

Tsym	minVolt
20 Trf	40.0469
30 Trf	40.0469
40 Trf	40.0469
50 Trf	40.0469
60 Trf	40.0469
70 Trf	40.0469
80 Trf	40.0469
90 Trf	40.0469
100 Trf	40.0469

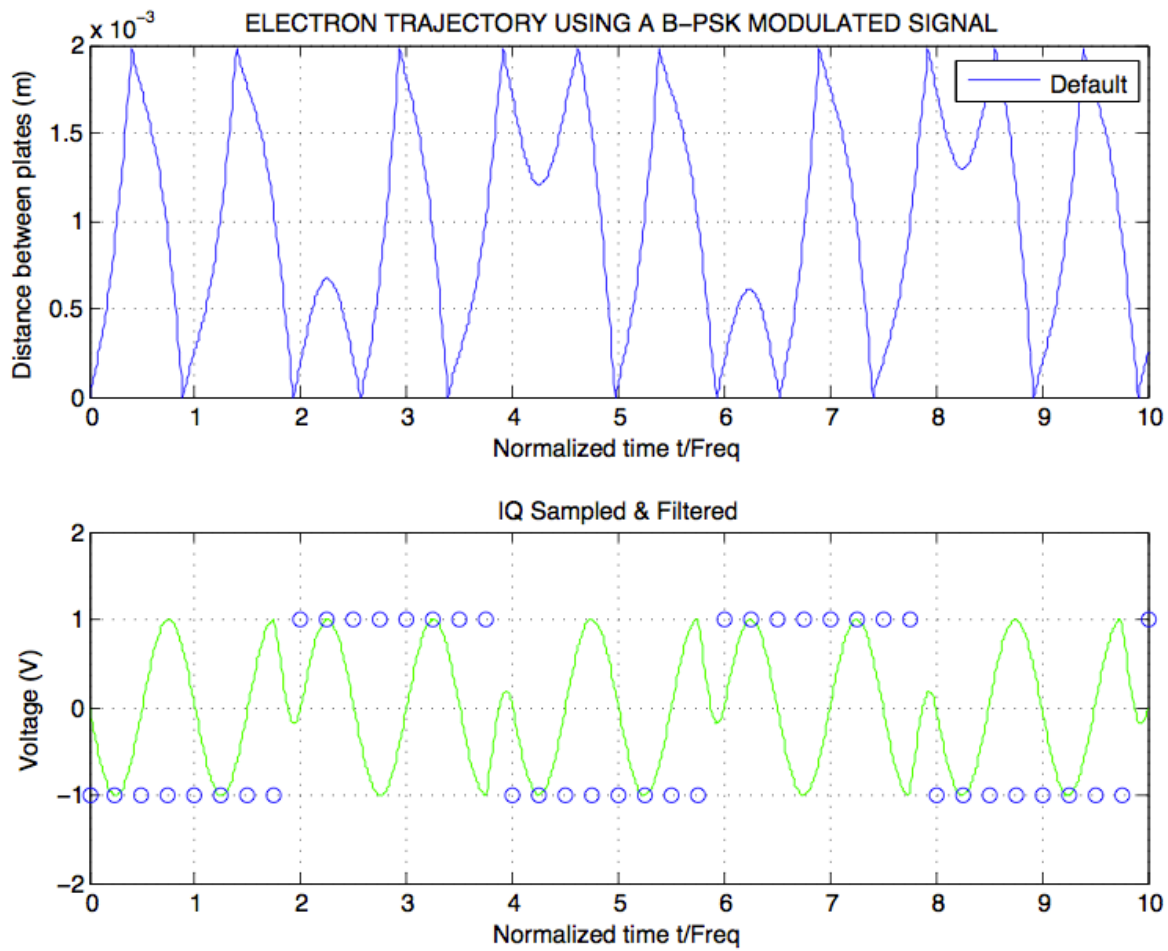


Fig. 46 Simulation using a BPSK-modulated signal with a square filter and Voltage = 40 Volt

As in Section 5.1 new tables are obtained by performing a simulation of 100 periods of the RF signal with an initial seeding of 120 electrons. However, the graph only shows the first 10 periods for a single electron with symbols with two periods of duration, to get an idea of the performance. In this case and in order to solve the convergence issue explained above, the number of samples per symbol used in the filter is eight. With eight samples per symbol the convergence of the algorithm has been validated to be correct.

If we compare the graphs 44 and 45 (obtained for an uniform sequence without any type of phase jump) obviously the solution is virtually identical regardless of the number of RF periods each symbol takes. Nevertheless, in the case that the simulation sequence presents continuous phase jump between two symbols (between 0 and 1) the trajectory of the electron is different as it is possible to observe in figure 46. Also, by applying this second sequence composed by abrupt changes between phases the value of the minimum voltage required to start a discharge is different depending on the length of the symbol.

In the case of applying symbol periods less than ten periods of RF can be observed as multipaction threshold is different and will be different in the case of applying an other binary sequence. We used the sequence of alternating ones and zeros because it is the worst case, where the phase changes are abrupt and each less time the electron trajectory could be affected by the switch of phase.

As expected when the symbol length is greater (more than about ten time periods of the RF signal) the voltage needed to initiate the discharge tends to be the same as in the case of applying an un-modulated signal.

5.3 BPSK-Modulated Signal with SRRC FILTER

Frequency, $f = 435 \text{ MHz}$

Distance between plates, $d = 1.9747 \text{ mm}$

Electron initial velocity, $v_0 = 3.68 \text{ eV}$

Material between plates: $A_{g3}A$ ($E_1 = 30 \text{ eV}$, $E_2 = 5000 \text{ eV}$, $E_{max} = 165 \text{ eV}$, $\delta_{max} = 2.22$)

Number of initial electrons introduced = 120

Symbol Period ($T_s = n \times T$), $n = [1 \ 2 \ 3 \ 4 \ 5 \ 6 \ 7 \ 8 \ 9 \ 10 \ 20 \ 30 \ 40 \ 50 \ 60 \ 70 \ 80 \ 90 \ 100]$

Max. Time = $100T_{rf}$

In the same way as in the previous section, it is going to study the effect of applying a pulse shaping filter to the signal using the same two different digital sequences as in 5.2.

Case 1: Seq [1 1 1 ... 1 1 1]

Tsym	minVolt (Volt)
1 Trf	42.8359
2 Trf	42.8359
3 Trf	42.8359
4 Trf	42.8359
5 Trf	42.3711
6 Trf	43.3008
7 Trf	42.3711
8 Trf	43.3008
9 Trf	42.3711
10 Trf	42.3711

Tsym	minVolt (Volt)
20 Trf	41.9062
30 Trf	42.3711
40 Trf	43.7656
50 Trf	40.9766
60 Trf	47.0195
70 Trf	43.3008
80 Trf	39.5820
90 Trf	37.7227
100 Trf	37.2578

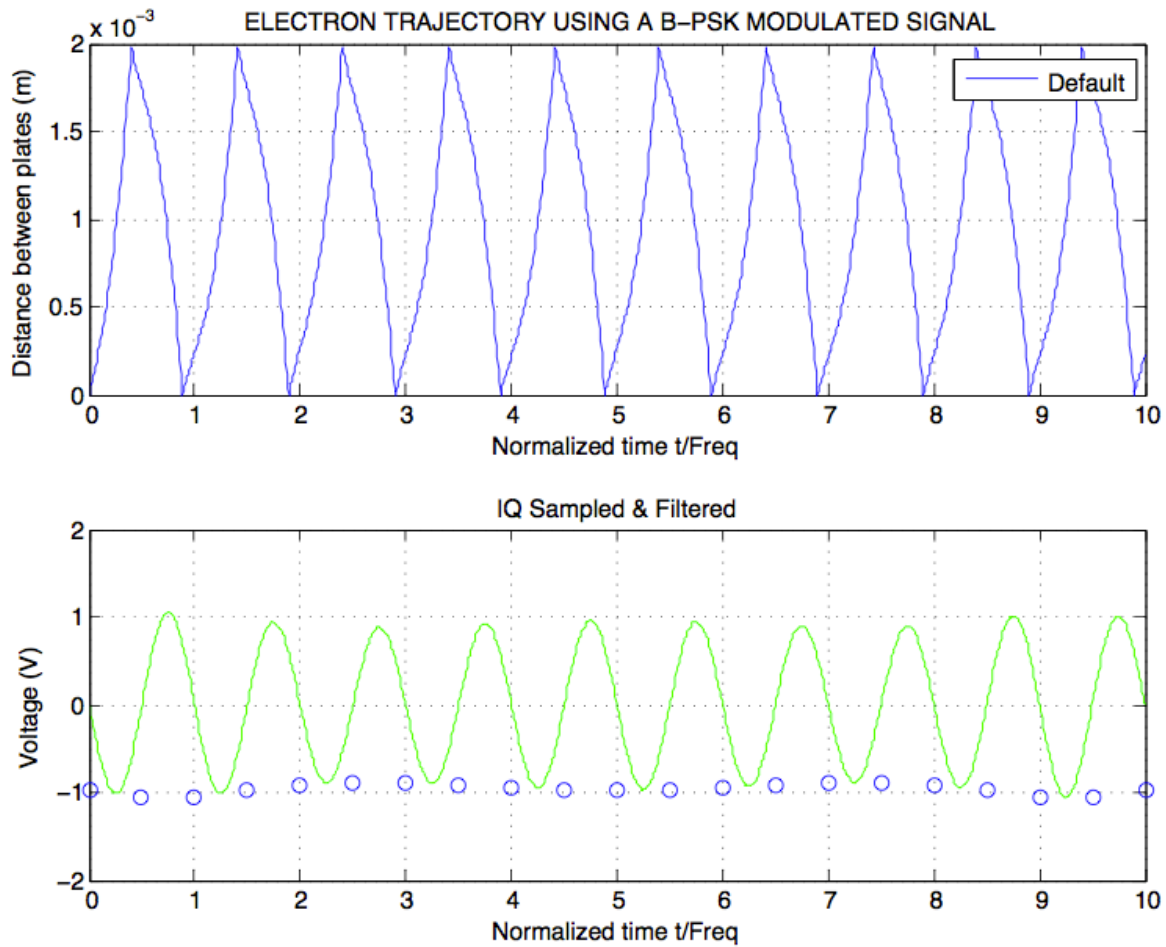


Fig. 47 Simulation using a BPSK-modulated signal with a square filter and Voltage = 40 Volt

Case 2: Seq [1 0 1 0 ... 1 0 1]

Tsym	minVolt (Volt)
1 Trf	44.2305
2 Trf	42.8359
3 Trf	46.0898
4 Trf	40.9766
5 Trf	44.2305
6 Trf	47.4844
7 Trf	42.3711
8 Trf	45.1602
9 Trf	46.0898
10 Trf	48.4141

Tsym	minVolt (Volt)
20 Trf	48.8789
30 Trf	51.2031
40 Trf	49.3438
50 Trf	58.1758
60 Trf	54.4570
70 Trf	49.3438
80 Trf	53.0625
90 Trf	57.2461
100 Trf	62.8242

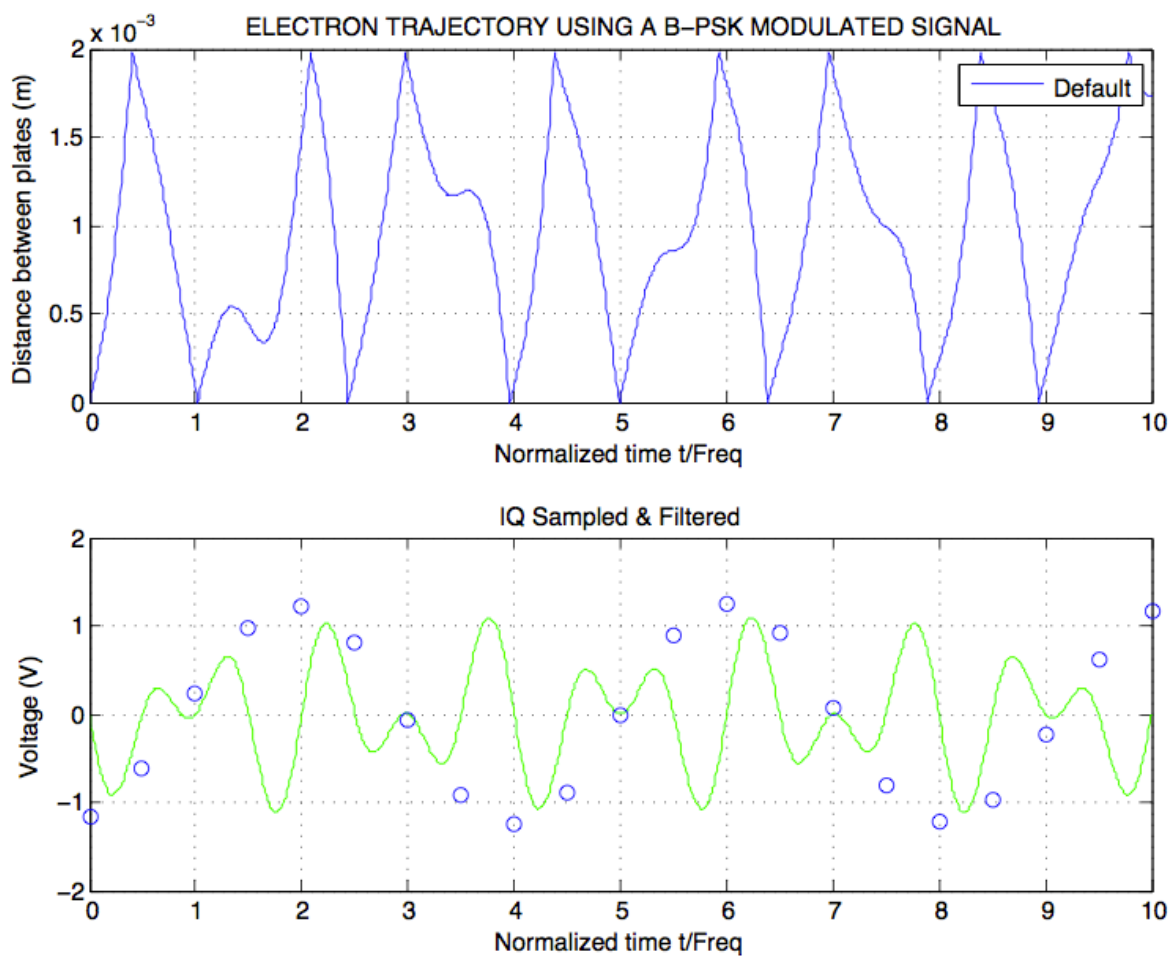


Fig. 48 Simulation using a BPSK-modulated signal with a square filter and Voltage = 40 Volt

The results of introducing the digital signal through a pulse-shaping filter are much more complex to analyse. In this case, as the theory explained in previous sections showed, these filters affect the amplitude of the signal depending on roll-off factor and the number of samples per symbol. In figure 48 is represented the signal filtered using a roll-off factor of 0.25 and 4 samples per symbol.

In the case of applying the sequence composed by only ones, it is seen that symbols with durations less than ten periods of RF the minimum voltage to initiate the multipactor effect is more or less similar as before, but when the duration of the symbols is greater than 10 RF periods, the transmitted signal in this case does not tend to behave like an unmodulated signal one. Why does it happen? In next figure it is showed the explanation that when a pulse shaping is applied the transmitted sequence takes extra-importance.

The chosen sequence to simulate influences greatly in the end results because the filter behaves in a different way depending on the rear symbol. For example, figure 49 shows how the filter samples the signal depending on the next symbol is the same (in figure 49 top, the sequence shown is [1 1...]) or is different (fig. 49 bottom shows the sampled transition between an one and a zero)

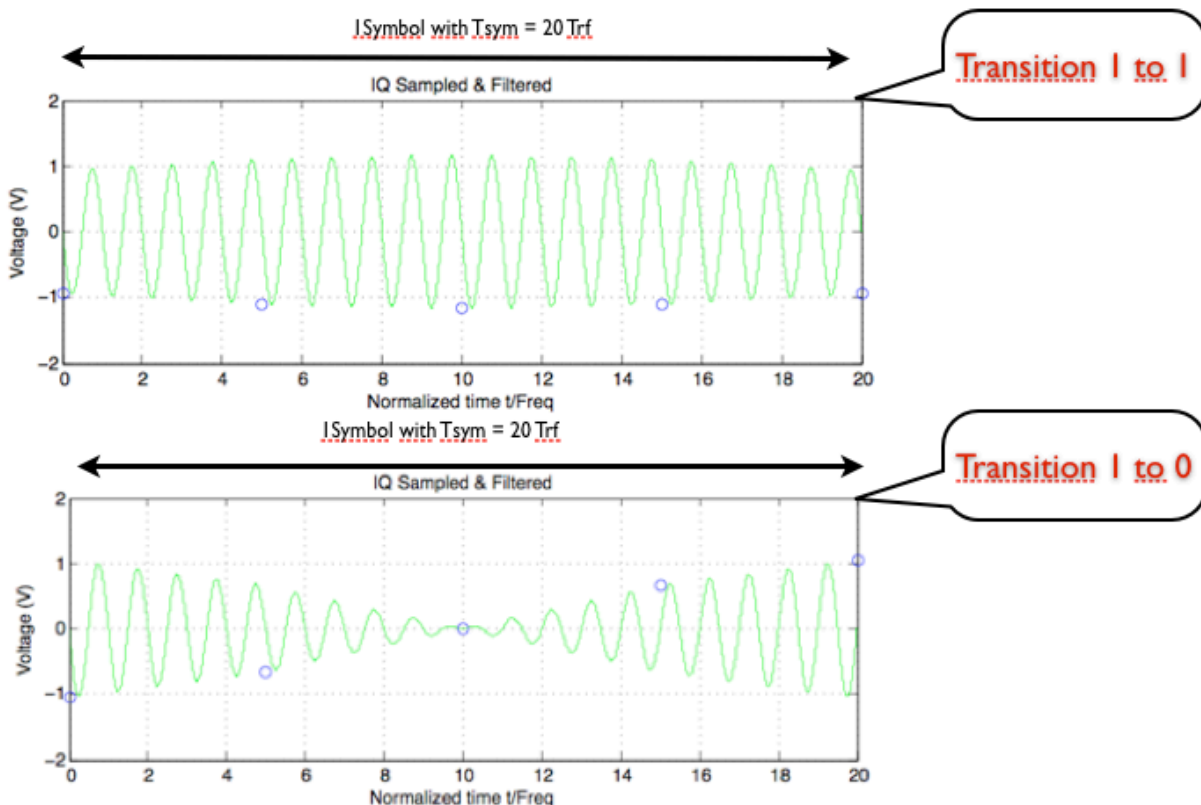


Fig. 49 Different transitions between symbols

So, in conclusion, if two consecutive symbols are different (1 and 0) but each symbol has a duration of more than ten periods of the RF signal, as can be seen in Figure 49, the behavior is not the same as in a non-modulated signal because sampling and filtering is different depending on the posterior symbol. In the case that two symbols are equal (1 and 1 or 0 and 0) and the symbol periods are long, the filter has a behaviour very similar to the result considering a non-modulated signal (compare Fig. 49 top with 44 and 45).

Nevertheless, it is strange that the MP threshold increases about 20 Volts when only one symbol is applied ($T_{sym} = 100Trf$ and Maximum Time Simulation is $100Trf$ too). So, if we repeat the simulation using a final time of $1000 * Trf$ we may validate this theory.

New conditions:

Frequency, $f = 435 \text{ MHz}$

Distance between plates, $d = 1.9747 \text{ mm}$

Electron initial velocity, $v_0 = 3.68 \text{ eV}$

Material between plates: A_{g3A} ($E_1 = 30 \text{ eV}$, $E_2 = 5000 \text{ eV}$, $E_{max} = 165 \text{ eV}$, $\delta_{max} = 2.22$)

Number of initial electrons introduced = 120

Symbol Period ($T_s = n \times T$), $n = [20 \ 30 \ 40 \ 50 \ 60 \ 70 \ 80 \ 90 \ 100 \ 200 \ 400 \ 600 \ 800]$

Max. Time = $1000Trf$

Tsym	minVolt (Volt)
10 Trf	39.5820
20 Trf	41.4414
30 Trf	41.4414
40 Trf	42.3711
50 Trf	41.4414
60 Trf	41.4414
70 Trf	41.4417
80 Trf	40.9766
90 Trf	40.5117
100 Trf	47.9492

Tsym	minVolt (Volt)
200 Trf	51.2031
400 Trf	51.6680
600 Trf	54.4570
800 Trf	54.4570

If we analyse the results again calculated changing only the length of the time vector the results have a better understanding. The difference and the main conclusion is that it is necessary to send enough symbols to predict the minimum voltage to start the discharge. In the previous simulation also using a RRC filter, the number of symbols introduced in the simulation to predict MP was not enough to synchronize the behaviour of the signals. In the same way that when non-modulated signals were applied and after a several RF time periods the electrons with different initial phases were synchronized, the same behaviour is happening for modulated signals. If the number of transmitted symbols is not enough long

(for example for $T_{\text{sym}} = 500 \text{ Trf}$, only two different symbols are considered) the minimum voltage is not real.

In conclusion, for a BPSK-modulated signal where only the phase changes according to bit which is transmitted in a time interval, the pulse shaping does not produce significant changes in the MP threshold.

In summary, the transmitted digital sequence has a great influence on the electron trajectory and it is important to consider when calculating the minimum voltage to initiate the multipactor discharge. As well, other important parameters like the roll-off factor or the number of samples per symbol may be controlled to predict the appearance of the phenomenon. This last example, using a BPSK-modulated signal with a SRRC pulse is an important case to consider and to prove experimentally because it may show new theories unknown until now.

In Section 5 have been just shown special cases using a B-PSK modulation. However, these examples can also be performed for QPSK modulation using the initial conditions given by the user.

|6 FUTURE WORK

In order to complete all investigations it will be a good idea to validate the simulation platform providing several tests to verify the behaviour of modulated signals in real testing. Firstly, the main objective shall focus on the effect of modulated single carrier signals in the multipactor breakdown. To study this effect, low power signals will be used. In section 4.3.3 with the title Results several simulations have been done with the purpose of preparing the possible tests which will take place at the ESA-VSC European High Power RF Laboratory in Valencia.

The purpose is to investigate how the modulation parameters affect the Multipactor threshold and to this aim both theoretical and experimental studies are being performed to carry out this proposal.

The device under test (DUT) is a multipactor sample of P-Band. Figure 50 shows the basic RF breakdown Test-bed configuration.

Nowadays, the intention is to perform three tests with the characteristics shown in section 4.3.3. The key idea is to analyse the multipactor discharge for a frequency value of 435 MHz (P-Band) for the sample of figure 51. This device has a gap $f \times d = 0.895 \text{ GHzmm}$ and the distance between the plates is approximately 2 mm (precisely 1.9747 mm).

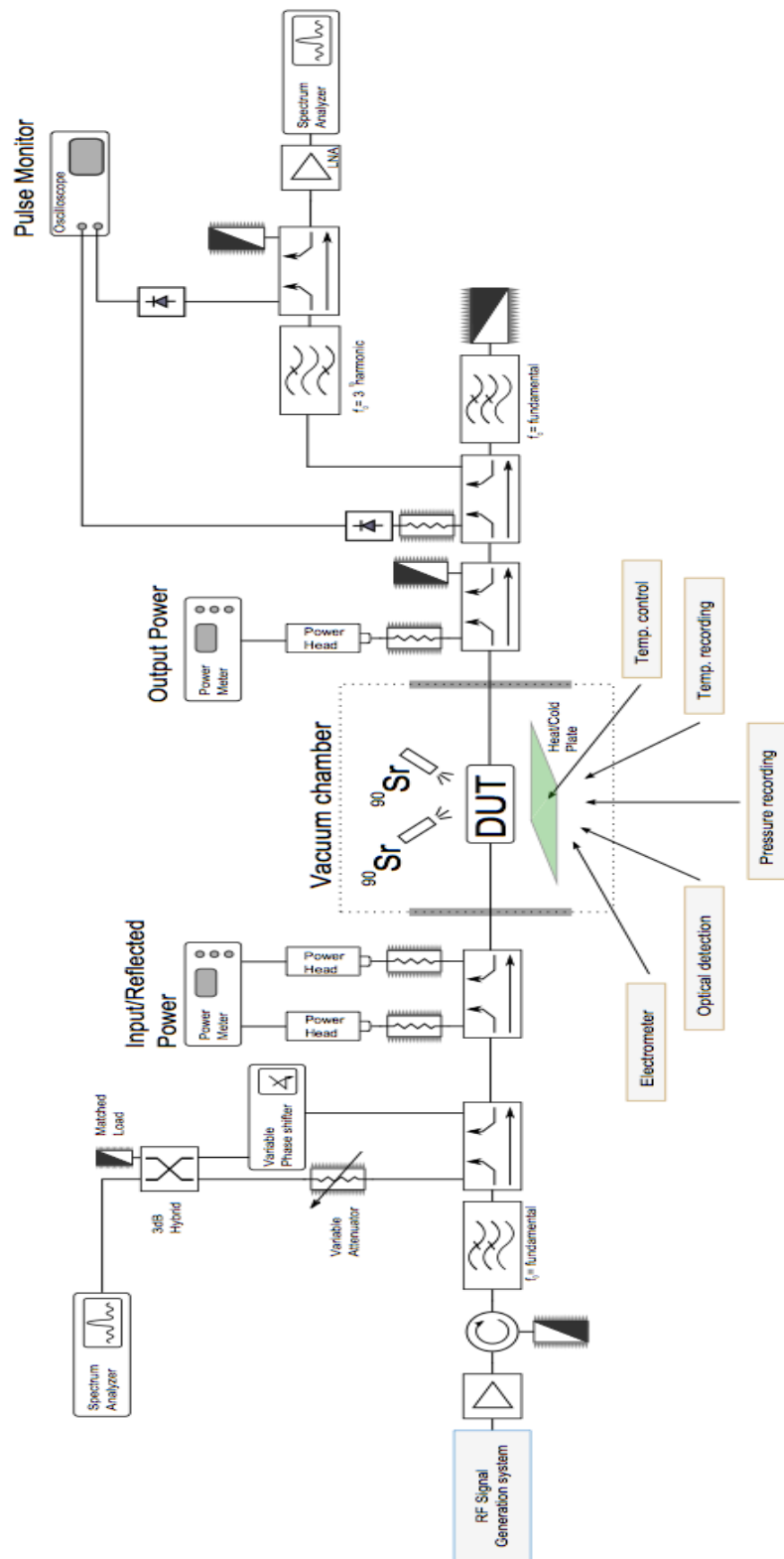


Fig. 50 Basic RF Breakdown Test Bed Configuration



Fig. 51 Sample for testing.

Every test to be performed using any modulation scheme must be compared and validated by an initial test with a non-modulated signal with the same characteristics. A brief description of the set-up is given below. The main equipment is composed by:

- a) Up: PSG Vector Signal Generator
- b) Down: PXA Signal Analyzer

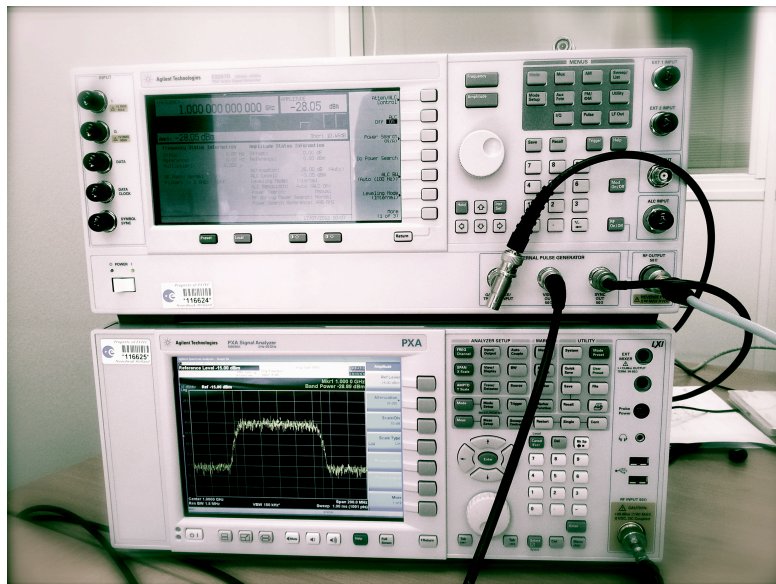


Fig. 52 Instruments Real Picture

The principal connections between both are represented in the schematic below with three different wires:

- 1) 10 MHz Reference. This wire causes the local oscillators of the instruments oscillate at the same frequency (10MHz) (Rear Panel)
- 2) Ext Trigger & Synchronization. This syncs the pulse modulator start, with the IQ samples player and triggers an acquisition from the PXA.
- 3) RF Signal. In the future this wire is replaced by Test-bed + Amplifier.

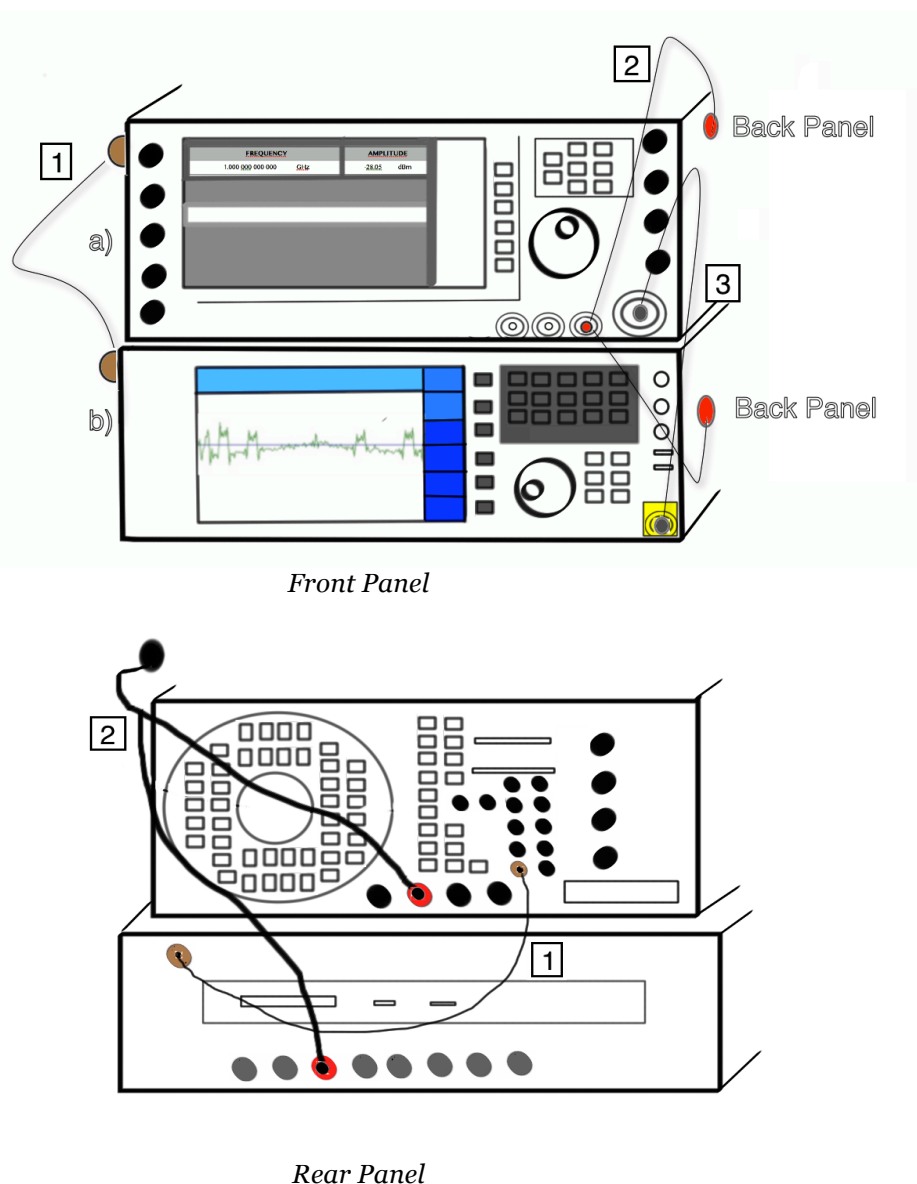


Fig. 53 Instruments schematic with the main connections

6.1 Experimental setup

For these investigations both specialized hardware and software has been procured.

Hardware

From the transmitting side an Agilent PSG up to 20GHz with 64Msample memory. Internal base band generator is constrained to 80MHz, nevertheless 1GHz base band inputs for external modulation are available.

For the receiving side an Agilent PXA up to 50GHz with a 160MHz demodulation bandwidth is available.

Software

As in previous sections, a Multipactor software in Matlab software is being developed. Using the existing license it has been feasible to implement a customize modulation-demodulation algorithm.

The software is prepared to work with pulsed signal. This constrains makes out of the shelf software as Agilent VSA not proper for this application.

Currently the software operates properly with BPSK, and QPSK with full control of the generated signal. Once the software will be fully validated a graphical user interface will be developed in order to make easy the user task.

Planning Tests

In summary, the planning tests are:

Test 1: *Using a Non-modulated Signal in the frequency of 435 MHz considering the above characteristics described.*

Test 2: *Using a BPSK-modulated Signal in the same frequency filtered with a square filter.*

The exact Symbol Period to validate and control the multipactor threshold is been investigated at this moment.

Test 3: *Using a BPSK-modulated Signal in the same frequency filtered with a pulse shaping filter (SRRC).*

Same parameters characteristics as in test 1 and 2. Also, some simulations have been doing with the objective to clarify which roll-off, number of samples per symbol are been investigated at this moment.

|7 CONCLUSIONS

In this degree thesis it is analysed the influence of different field conditions in the RF signal for the multipactor threshold.

To this end, Multipactor simulator has been developed using Matlab. This software correctly predicts under which conditions Multipactor effect occurs in a parallel-plates capacitor considering a harmonic excitation done produced by a modulated signal. The results of the software in single carrier have been validated using the ECSS Multipactor Tool.

This degree thesis has focused on the study of PSK modulations type, but the purpose of the software is to work globally with any kind of signal and modulation parameters introduced by the user.

By looking at the results in Section 5, and using all the theoretical data provided along the project, it is clear that, new aspects and perspectives have been covered by this new Multipactor simulator.

One of the main of this work has been to analyse the influence of phase modulation on multipactor discharge initiation. It has been shown that the effect of the modulation depends on the type of modulation applied, the symbol period and the filter. It is important do not forget that in RF communication, pulse shaping filtering is essential for making the signal fit in its frequency band.

According to the results, when the ratio between the phase-switching period and the RF signal period is smaller than then the interval between successive phase switches was enough to change the minimum voltage to initiate the discharge, therefore the multipactor threshold oscillates due to the fast phase switches. The trajectory followed by the electrons is not the same because the signal that excites their movements between the plates is changing due to the different modulation parameters. In this work, one of the main conclusions is that the type of filter applied (rectpulse or RRC) to a BPSK-modulated signals is not a determining factor in the multipactor threshold.

In space telecommunication applications, the ratio of the phase-switching interval to the RF period is in the range of several hundreds, which means that the phase switching interval is large enough to essentially correspond to the situation of a monochromatic RF field.

Finally and in a personal way I think this work is just the beginning of a field study to explore accurately. We found as the minimum voltage to initiate the multipactor changes when we apply different modulation parameters and filters to the same signal, but it is time to work because it is sure that there are still many theories to discover and much work to do in this extensive area.

|8 REFERENCES

[1]. Multipactor in Microwave Transmission Systems Using Quadrature Phase-Shift Keying

V. Semenov, M. Buyanova, D. Anderson, M. Lisak, R. Udiljak and J. Puech
Plasma Science, IEEE Transactions on, april , 2010. Vol. 38(4), pp. 915 -922 (2010)

[2] The significance of amplitude and time statistics of multiple carrier signals for multipactor testing.

L. Friedrichs, in Proc. Workshop Multipactor, RF, DC Corona, Passive Intermodulation Space RF hARDW., 2000, PP. 79-84

[3] Long-term multipactor discharge in multicarrier systems.

S. Anza, C. Vicente, B. Gimeno, V.E. Boria and J. Armendáriz
Physics of Plasmas, August, 2007. Vol. 14(8), pp. 082112 (2007)

[4] A new formula for Secondary Emission Yield.

J. Vaughan, IEEETrans. Electron Devices, vol. 36, p. 1963, September 1989.

[5] Multipactor breakdown prediction in rectangular waveguide based components.

C. Vicente, M. Mattes, D. Wolk, H. Hartnagel, J. Mosig and D.Raboso.

[6] Multipacting design and test.

ESTEC Document ECSS-20-01, April 2000.

[7] Surface Treatment and Coating for the Reduction of Multipactor and Passive Intermodulation (PIM) Effects in RF Components.

D. Wolk, J. Damaschke, C. Vicente, B. Mottet, H.L. Hartnagel, L. Galán, I. Montero, E. Roman, M. Alfonseca, J. de Lara, D. Raboso, AO-4025 ITT ESA

[8] Simulation of Secondary Electron Emission Based on a Phenomenological Probabilistic Model.

M. A. Furman, M. T. F. Pivi, June 2, 2003

[9] Peak to Average Power Ratio in Digital Communications.

Dov Wulich, Lev Goldfeld and Gill R. Tsouri. Ben-Gurion, University of the Negev, Department of Electrical and Computer Engineering

[10] Multipactor suppression in amplitude modulated radio frequency field

V. Semenov, A. Kryazhev, D. Anderson and M. Lisak
Physics of Plasmas, November, 2001. Vol. 8, pp. 5034-5039 (2001)

[11] **Starting potentials of high-frequency gas discharges at low pressure.**

E. W. B. Gill and A. von Engel, Proc. R. Soc. Lond. A, Math. Phys. Sci., vol. 192, no. 1030, pp. 446–463, Feb. 1948.

[12] **Multipactor.**

J. Vaughan, IEEE Trans. Electron Devices, vol. 35, no. 7, pp. 1172–1180, Jul. 1988.

[13] **Digital Phase Modulation.**

A Review of Basic Concepts *James E. Gilley Transcrypt International, Inc., August 7, 2003*

[14] **POWER RATIO DEFINITIONS AND ANALYSIS IN SINGLE CARRIER MODULATIONS.**

J. Palicot and Y. Lout, Proc. EUSIPCO 05, Antalya, Turkey, Sep. 05

[15] **Root-Raised Cosine filter influences on PAPR distribution of single carrier signals.**

Steredenn Daumont, Basel Rihawi, Yves Lout. IETR / SUPELEC

[16] **PEAK-TO-AVERAGE POWER RATIO OF SINGLE CARRIER FDMA SIGNALS WITH PULSE SHAPING.**

Hyung G. Myung Junsung Lim David J. Goodman. The 17th Annual IEEE International Symposium on Personal, Indoor and Mobile Radio Communications (PIMRC'06)